On the role of

treml6 in B-1a B cell development

And

ICOS co-stimulation in adaptive immune responses against *M. tuberculosis*

vorgelegt von

Diplom-Ingenieurin

Geraldine Nouailles

Von der Fakultät III - Prozesswissenschaften
der Technischen Universität Berlin
zur Erlangung des akademischen Grades
Doktor der Ingenieurwissenschaften
- Dr.-Ing. -

genehmigte Dissertation

Promotionsausschuss:

Vorsitzender: Prof. Dr. Ulf Stahl
Berichter: Prof. Dr. Roland Lauster
Berichter: Prof. Dr. Jens Kurreck
Berichter: Prof. Dr. Stefan Kaufmann

Tag der wissenschaftlichen Aussprache: 12.02.2010

Berlin 2010
D83

TABLE OF CONTENTS

1 INTRODUCTION

1.1 Immune System

The mammalian immune system has evolved to ensure protection against various pathogens. It is organized by an array of cells and molecules with specialized roles in the defense against infection. All cells of the immune system develop from pluripotent stem cells in the bone marrow (BM). Among these cells are lymphocyte precursors that mature to naïve cells in BM and/or thymus, the generative lymphoid organs, and respond to antigen in the peripheral secondary lymphoid organs such as spleen, lymph nodes, and mucosal and cutaneous lymphoid tissues.

Pathogens entering the organism have to overcome the surface barriers of the immune system, such as the epidermis and mucosa and are then confronted with two different types of immune responses, the innate and the adaptive immune response. Innate immune responses occur to the same extent regardless of how many times the infectious agent is encountered, whereas acquired immune responses improve on repeated exposure to a given infection. Both immune responses are tightly interconnected and function by cooperation (1-3).

1.2 Innate Immunity and its receptors

The innate immune system consists of all immune defense mechanisms that lack immunologic memory and is phylogenetically ancient. Beside various soluble antimicrobial proteins of the complement system, it comprises phagocytic cells such as monocytes, dendritic cells (DCs), neutrophils and macrophages, cells that release antimicrobial and inflammatory mediators (basophils, mast cells, and eosinophils), and cells that kill infected cells (natural killer cells). In addition to antimicrobial effector mechanisms, some of the cells of the innate immune system also play a crucial role in antigen presentation, thereby linking the innate and the adaptive immune response (4).

In contrast to the adaptive immune response (for details see 1.3), the innate immune response is mediated by germ-line encoded receptors e.g. pattern recognition receptors (PRR), with genetically predetermined specificity. The best-known class of innate immune receptors are the toll-like receptors (TLRs). Other classes include the nucleotide oligomerization domain (NOD)-

like receptors (or recently defined as nucleotide-binding domain and leucine-rich repeat containing molecules [NLRs]), RIG-I-like receptors (RLRs), and C-type lectin receptors (CLRs) (5, 6). Although more limited in their diversity, compared to adaptive immune receptors, cells equipped with PRR are able to respond faster to various microbial products, be they bacterial, viral, fungal, or parasitic (7). The replication of the invading pathogen can thus be controlled within hours. The recognized pathogen-associated molecular patterns share three aspects: a) they are produced only by pathogens, and not by the host, b) the structures are usually essential for the survival or pathogenicity of the microorganism, and c) they are usually invariant structures shared by entire classes of pathogens (e.g. lipopolysaccharides (LPS) shared by virtually all gram-negative bacteria). Recognition of these structures by the innate immune system induces expression of costimulatory molecules, secretion of cytokines and chemokines, which recruit other cells of the innate immune system and activate antigen-specific lymphocytes and initiate the adaptive immune response (8, 9).

1.2.1 Triggering receptors expressed on myeloid cells (TREM) receptor family

TREM receptors belong to a surface receptor family of NON-TLR innate immune receptors that participate in immunological processes. The TREM gene cluster is localized on human chromosome 6p21 and murine chromosome 17C3; it comprises the gene sequences of e.g. TREM1 (gene: *trem1*), TREM2 (gene: *trem2*), TREM-like transcript- (TLT-)1 (gene: *trem-like* (*treml*)*1*) and, TLT-2 (gene: *treml2*) all of which are conserved between mice and men. Genes encoding TREM or TREM-like (TREML) receptors have been identified in several species, such as chicken, pig, and cow (10-12). In these species, the number of *trem* and *trem-like* genes is weakly conserved, and for some *trem* and *trem-like* genes, it is not possible to define orthologs between mice and men (10-12). Murine *trem5*, *pdc-trem, trem3* and *treml6* have no human ortholog (Fig. 1) (10-12).

Structurally TREM and TREML receptors share an extracellular, variable (V-type) immunoglobulin (Ig) domain and a transmembrane region. TREM receptors have a short cytoplasmic tail and couple with DNAX activating protein of 12kDa (DAP-12) that carries an immunoreceptor tyrosine-based activating (ITAM) motif (green in Fig. 1). TREML or TLT

receptors have a longer cytoplasmic tail that contains, except for *treml2* (grey in Fig. 1), one or more immunoreceptor tyrosine-based inhibitory (ITIM) motifs (red in Fig. 1) (12).

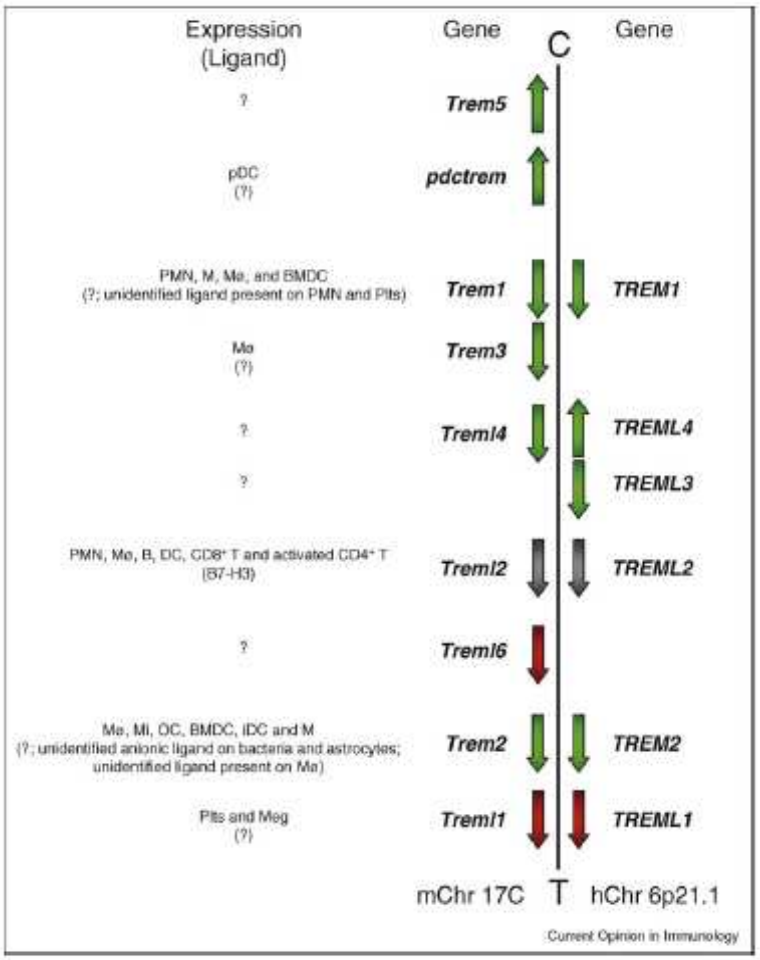

FIGURE 1. TREM family of receptors. Localization of TREM genes on mouse chromosome 17C (left) and human chromosome 6p21.1 (right). Genes shown in green are either known or predicted to associate with DAP12. Those shown in red contain an ITIM motif(s). *Treml2*, shown in gray, neither associates with DAP12 nor has an ITIM. Where known, TREM expression is indicated. pDC (plasmacytoid dendritic cells); PMN (polymorphonuclear leukocytes); M (monocytes); Mϕ (macrophages); BMDC (bone marrow-derived dendritic cells); B (B lymphocytes); DC (dendritic cells); iDC (immature dendritic cells); T (T lymphocytes); Mi (microglia); OC (osteoclasts); Plts (platelets); Meg (megakaryocytes). Ligand identity or lack thereof is listed in parentheses underneath the cell type(s) expressing TREM. Diagram is representative of TREM chromosomal location but is not drawn to scale. C and T define the centromeric and telomeric ends of the chromosome, respectively. Figure and legend taken from Ford and McVicar (12)

ITAM containing receptors induce cell activation through protein tyrosine kinase dependent signaling pathways. Ligand binding induces a phosphorylation cascade that results in cell activating processes such as actin polymerization, calcium mobilization and activation of transcription factors. Inhibitory receptors, e.g. ITIM-containing receptors (ITIM-Rs), attenuate such activation signals (13). Inhibitory receptors mediate this function normally only upon their clustering with an activating counterpart on the cell surface. When both activating and inhibitory receptors are coengaged by their respective ligands, the net outcome is determined by the relative strength of these opposing signals. In general, inhibition exerted by ITIM-Rs is only local and transient. It does not induce a cell-wide or sustained non-responsiveness but abrogates activation signals when and where they occur (13).

TREM receptors are expressed on a variety of cells, including monocytes, macrophages, DCs, T cells, B cells, microglia, thrombocytes, and osteoclasts (Fig. 1). The functions of TREM receptors are well described for a few members only and have mainly been studied by *in vitro* or blocking antibody experiments. TREM1 was the first member to be described; it functions through the ITAM-domain bearing adaptor molecule DAP12 as an amplifier of TLR signaling (14, 15). TREM2$^{-/-}$ mice are so far the only published knock-out animals within the family (16). TREM2 is primarily described as an attenuator of macrophage activation and cytokine secretion in response to TLR ligands LPS, zymosan, and CpG (16, 17). More recent data suggest an additional role in negative regulation of autoimmunity (12). PDC-TREM is expressed on murine plasmacytoid DCs (pDCs) upon stimulation with CpG and enhances type 1 interferon production (18). TLT-1 and TLT-2 also promote cellular activation, although neither couples to DAP12 for signaling. TLT-1 inhibits platelet aggregation *in vitro* and enhances FcεRI-mediated calcium signaling in platelets (19, 20). TLT-2 is expressed on peritoneal and alveolar macrophages, and neutrophils and TLT-2 is the only TREM receptor that is expressed on lymphocytes (CD8$^+$ T cells, activated CD4$^+$ T cells and B cells). It plays a role in leukocyte activation and might confer co-stimulation to T cells by binding to B7-H3. Notably, TLT-2 does not carry ITIM motifs, but contains a src homology 3 (SH3)-binding domain (21). No report has investigated functions of *treml6*, the subject of this thesis.

1.2.2 Antigen presentation

Antigen presenting cells (APCs) are capable of antigen processing, presentation and T cell activation. DCs have long been regarded to be the most potent APCs due to their enhanced ability to initiate T cell responses. Nevertheless, B cells and macrophages are also capable of antigen presentation and evidence accumulates that doubts the unique role of DCs versus macrophages in the initiation of T cell responses (22). Moreover, recent studies showed that basophils also act as APCs and are able to initiate Th2 type immune responses (23-25). Regardless which cell acts as the APC, for an antigen to be presented, proteins first have to be fragmented by proteolysis. The resulting peptides are then associated with major histocompatibility complex (MHC) molecules and the MHC-peptide complexes are expressed at the cell surface where they can be recognized by the T cell receptor (TCR) on a T cell. However, the pathway leading to the association of peptides with MHC molecules differs for MHC class I (MHCI) and MHC class II (MHCII) molecules. MHCI molecules present degradation products

derived from cytosolic (endogenous) proteins and present those to $CD8^+$ T cells. MHCII molecules present fragments derived from extracellular (exogenous) proteins that are located in an intracellular compartment and present those to $CD4^+$ T cells (26, 27).

1.3 Adaptive Immunity

Defense against microbes is mediated by early reactions of the innate immune system and subsequently by the responses of the adaptive immune system. Adaptive immunity is characterized by specificity for distinct molecular entities and the ability to "remember" and thus to respond faster and more vigorously upon repeated exposure to the same pathogen.

It is based on the activation and clonal expansion of B and T lymphocytes following antigen recognition through the TCR or B cell receptor (BCR) (2, 3). The lymphocyte receptors are responsible for the great diversity and specificity of antigen recognition. In contrast to the receptors of the innate immune system, they are not genetically predetermined but are generated through somatic rearrangement of germ-line encoded gene segments. This rearrangement results in 10^8 to 10^{15} possible BCRs and TCRs even though the human genome consists of only 75,000 to 100,000 genes (28).

The adaptive immune response can be divided into humoral and cell-mediated immunity. The first is accomplished by B cells and helper T cells type 2 (Th2 cells) and is directed against extracellular bacteria, viruses, parasites and their toxins. Cell-mediated immunity is mediated by helper T cells type 1 (Th1 cells) directed against viruses and intracellular bacteria, e.g. *Mycobacterium tuberculosis* (Mtb) (2, 3, 29). B lymphocytes are antibody-producing cells. After recognizing extracellular antigens through the BCR, a membrane-bound form of an antibody, B cells differentiate into antibody-secreting effector cells, called plasma cells. A subset of the activated B cells differentiates into memory B cells (2, 3).

1.3.1 T cell activation and co-stimulation

The classical activation of naïve T lymphocytes is the result of a two-cell interaction between the T cell and an APC during which the T cell receives two signals from the APC. Signal one is the

recognition of antigenic peptides presented by MHC molecules by the TCR (for details see 1.2.2). Signal two is e.g. provided by the triggering of CD28 on the T cell by CD80 (B7-1) and CD86 (B7-2) molecules on the APC (30). Notably, CD28 is only one member of the CD28 family of co-stimulatory molecules (30, 31). The latter family consists of several members which differ with regard to their expression profiles, their ligands, and consequently their immunological functions. CD28-coreceptors bind to their respective ligands of the diverse B7-family of molecules and either amplify, such as CD28 and ICOS, or hinder, such as PD-1 and CTLA-4, signals of the TCR complex (30-34). Together with distinct cytokines that provide signal three these signals can lead to the activation and proliferation of the T cells resulting in the generation of antigen specific effector T cells that act during the acute phase of infection. In addition activation of lymphocytes also leads to the generation of memory cells. In contrast to effector cells, memory cells require fewer signals for activation and proliferation and therefore act faster upon re-infection. Memory T cells can be divided into central memory T cells (T_{CM}), which reside preferentially inside secondary lymphoid organs and have the ability to proliferate upon activation to become effector cells, and effector memory T cells (T_{EM}), which reside within the periphery and quickly produce effector cytokines upon TCR trigger without having the ability to proliferate (35, 36).

1.3.2 Effector T cells

The differentiation of $CD4^+$ effector T cells initiated by the interaction with APCs in the presence of cytokines secreted from pathogen-activated cells of the innate immune system is a hallmark of adaptive immunity. Dependent on the cytokine milieu in which the APC T-cell interaction takes place, $CD4^+$ effector T cells can differentiate into different types of effector cells, such as regulatory T cells (Treg), Th1 cells, Th2 cells, and helper T cells type 17 (Th17 cells). These lineages differ in their cytokine expression profile and immune-regulatory functions (29).

The generation of Th1 effector cells is coupled to the sequential actions of interleukin-12 (IL-12) produced by innate immune cells and interferon-gamma (IFN-γ) secreted by NK cells and possibly the binding of Notch receptor ligands of the DLL family. Transcription factors involved in the polarization towards the Th1 cell differentiation are signal transducer and activator of transcription (STAT) 4, STAT1 and T box transcription factor (T-bet) (37, 38). The differentiated

Th1 cells are characterized by their production of IFN-γ and are involved in cellular immunity against intracellular pathogens. They exert their effector function through IFN-γ which induces the classical activation of macrophages, comprising the up-regulation of MHC-II, secretion of pro-inflammatory cytokines IL-6, tumor necrosis factor (TNF), and IL-1, as well as nitric oxide (NO) production and respiratory burst, and thereby they improve the killing of intracellular microbes by macrophages (39, 40). $CD4^+$ Th1 cells also provide help to $CD8^+$ T cells, by promoting both their activation through APCs and their proliferation (41-43).

The development of Th2 cells depends on the presence of IL-4, possibly as well on the binding of Notch receptor ligands of the Jagged family, and the sequential activation of STAT6 and GATA3 transcription factors (38, 44). Th2 cells produce IL-4, IL-5 and IL-13 and are required for humoral immunity to control parasites and other extracellular pathogens. Their main effector function is to provide B cell help. The secretion of typical type 2 cytokines such as IL-4, IL-5 and IL-13 promotes antibody secretion and antibody class switching by B cells (40, 45). The antibodies secreted into the blood and body fluids by B cell can in turn target extracellular pathogens. Th2 type response can also induce alternative activation of macrophages, including upregulation of mannose receptor, up-regulation of MHCII, and expression of arginase. Alternatively activated macrophages contribute to clearance, presentation of antigens and parasite-induced granuloma formation in Th2 type immunity (39, 40).

Recently, Th17 cells have been described as a distinct lineage of $CD4^+$ effector T cells characterised by IL-17A and IL-17F production and the expression of the transcription factor retinoic acid-related orphan receptor γ expressed in T cells (RORγt) (46-48). Their development from naïve $CD4^+$ T cells depends on CD28/ICOS co-stimulation (48) and is driven by transforming growth factor-beta (TGF-β) and IL-6 (49, 50). Although initially thought to be the inducing cytokine, it is now evident that IL-23 is necessary for long-term survival of Th17 cells (47, 50). The role Th17 cells play during infection is not yet fully clarified. Mangan et al. showed that Th17 cells are required for host protection against the extracellular bacterium *Citrobacter rodentium*. However, Th17 cells were discovered in the context of autoimmune diseases, where they induce tissue inflammation through IL-17 secretion (48, 51). In particular, IL-17 has been linked to neutrophil recruitment into tissue sites through the induction of granulocyte colony-stimulating factor and IL-8 (52, 53). Therefore, Th17 cells are thought to regulate tissue inflammation (54).

In contrast, Treg inhibit autoimmunity and protect against tissue injury. The developmental pathways of Treg and Th17 cells have been described to be reciprocal. The peripheral development of Treg depends on TGF-β while the presence of IL-6 inhibits the differentiation into Treg (49, 50). Treg can be classified into two major populations, naturally occurring Treg (nTreg) and induced Treg (iTreg). Both express the forkhead-box transcription factor P3 (FoxP3). The nTreg mature in the thymus while the iTreg derive from $CD4^+$ T cells that acquired their suppressive activity upon TCR stimulation in the periphery (55, 56). Initially characterized by their ability to control autoimmune disease in mice (57), Treg have now been shown to influence immune responses in a wide variety of microbial infections (58-60), e.g. *Leishmania major* (61), *Listeria monocytogenes* (62), Plasmodium falciparum (63) and Mtb (64-66).

Noteworthy, the differentiation of naïve $CD4^+$ T cells into the different effector lineages is no longer considered to be necessarily irreversible. With the discovery of Treg and Th17 cells and the investigation of their development, data accumulates that suggest that at least iTreg and Th17 remain more plastic than expected, and that under specific circumstances they can acquire another effector phenotype (67).

The signals that stimulate differentiation of naïve $CD8^+$ T cells into $CD8^+$ effector T cells (also named cytotoxic T lymphocytes (CTLs)) are antigens presented by MHCI, co-stimulatory molecules, and Th cells secreting IFN-γ and IL-2. Activated CTLs are effector T cells that recognize and kill target cells expressing MHCI-antigen complexes, e.g. infected host cells containing bacteria or viruses. The killing occurs through release of granules with perforin and granzymes. Cytotoxic T lymphocytes (CTL), like $CD4^+$ T cells of Th1 type ($CD4^+$ Th1 cells), are capable of secreting cytokines, predominantly IFN-γ, and TNF-α (36).

1.3.2.1 Role of ICOS co-stimulation in immune responses

A prominent member of the CD28 receptor family and object of this thesis is ICOS (33). ICOS expression is restricted to activated T cells, and ICOS binds to ICOS-ligand (ICOS-L) (33, 68-70) a member of the B7 protein family. ICOS-L is highly expressed on professional APCs; however, endothelial and epithelial cells have also been shown to express ICOS-L (71, 72). *In vitro*, ICOS co-stimulation increases T cell proliferation, and production of both Th1 and Th2 type cytokines, but it only induces marginal IL-2 secretion (33, 68). T cells from ICOS-deficient mice exhibit reduced IL-4 and IL-5 production, but normal or increased IFN-γ production (73-75).

Consequently the biological role of ICOS was studied in Th1 and Th2 type autoimmune and infection models (76-84). During infection with *Listeria monocytogenes*, the inhibition of ICOS signaling impaired both listeria-specific $CD4^+$, as well as $CD8^+$ T cell responses, and resulted in higher susceptibility of mice (76). A reduction of $CD4^+$ T cell responses was observed after infection of mice with other intracellular pathogens (e.g. *Leishmania mexicana*, *Nippostrongylus brasiliensis, Toxoplasma gondii* and vesicular stomatitis virus (77, 79, 81)). In contrast, genital tract infection with *Chlamydia trachomatis* resulted in an increased $CD4^+$ Th1 response in $ICOS^{-/-}$ mice (78). Although phenotypes varied with the specific model employed, in general, the absence or blockage of ICOS led to either unaffected or reduced effector $CD4^+$ or $CD8^+$ T cell responses (76-84). Moreover, a recent study observed that ICOS regulates the expansion and pool size of effector T cells, T_{EM}, and regulatory T cells (Treg) in steady state (85). These results suggest a biological role of ICOS as a co-stimulatory molecule that confers survival signals to a variety of T cells (85).

1.3.3 Development of peripheral B cell subsets

In the mouse, B cells are generated from pluripotent hematopoietic stem cells (HSCs) in the liver during mid-to-late phase fetal development and in the bone marrow after birth. Different nomenclatures for the developmental stages of B cells exist and the two major ones shall be introduced here, namely those of Hardy (86) and Melchers-Rolink (87). The classifications of the differentiation stages are based on cell surface markers and recombination events. Both classifications use CD45R/B220 to identify B-lineage cells, and IgM and IgD to identify immature and mature B cells. CD19 was described later and then integrated into these classifications. It was found to be the most specific marker of B cell commitment because it is regulated by the B-cell exclusive transcription factor Pax5 (88). Melchers-Rolink proposed the expression of the cytokine receptors CD25 and c-kit (CD117) to subdivide B cell precursors.

The following description refers to the stages of B-2 B cell development from HSCs in adult BM (Melchers-Rolink nomenclature). Common lymphoid progenitors (CLPs) emerge from HSCs. They still retain some T-cell developmental potential, but they express recombination-activating gene (Rag) proteins. Their immediate downstream progeny are referred to as pro-B cells in which immunoglobulin heavy chain rearrangements have begun. Pro-B cells in turn generate

pre-B1 cells. These two populations express B220 and c-kit, but differ in CD19 expression: pro-B cells ($CD19^-$) and pre-B1 cells ($CD19^+$). Pre-B1 cells in which immunoglobulin heavy chain gene rearrangement was successful mature into pre-B2 cells that express μ heavy chain protein in their cytoplasm. CD25 is a specific marker for pre-B2 cells within the B lineage (87). Following the productive rearrangements of immunoglobulin light chain genes and the expression of light chain proteins, pre-B 2 cells mature into B-2 cells distinguished by the expression of surface IgM.

In this thesis developing B cells were named and identified according to the Melchers-Rolink classification, pro-B ($B220^+CD19^-$c-Kit^+CD25^-), pre-B1 ($B220^+CD19^+$c-$Kit^{dim}CD25^-$), pre-B2 ($B220^+CD19^+$c-Kit^-CD25^+), immature ($CD19^+$IgM(μ-chain)$^+$kappa-light-chain$^+$$IgD^-$) and mature B cells ($CD19^+$IgM(μ chain)$^+$kappa-light-chain$^+$$IgD^+$). The pro-B cells in this thesis correspond to Hardy fraction A, and some of Hardy fraction B. Pre-B1 cells correspond to Hardy fraction B and C (pro-B). Pre-B2 cells correspond to Hardy fraction C' and D (large and small pre-B cells). Immature and mature B cells correspond to Hardy fractions E and F, respectively (Fig. 2).

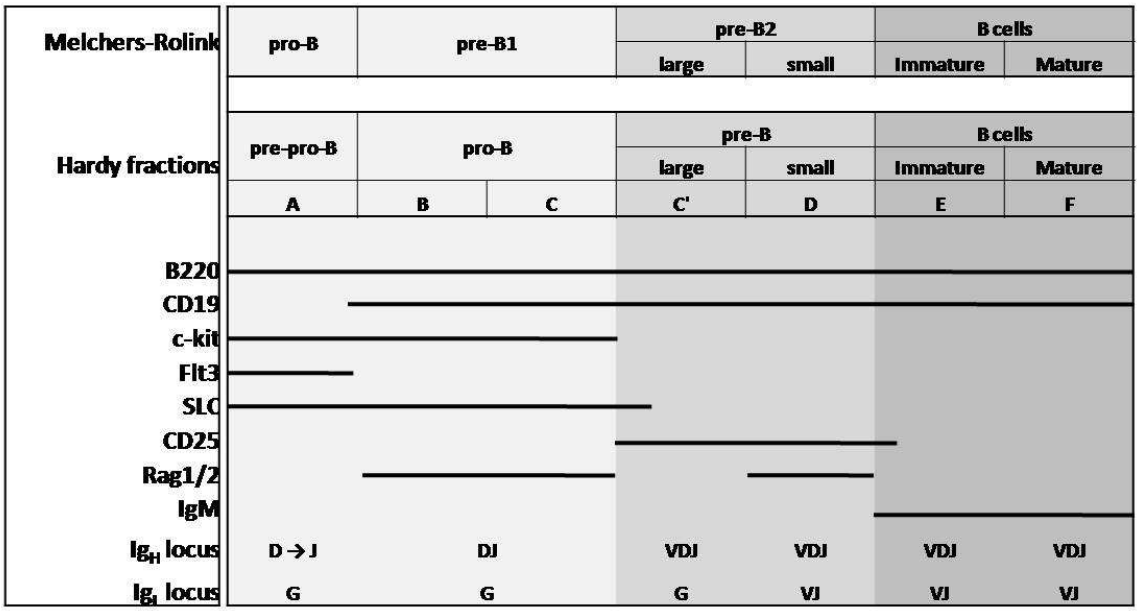

FIGURE 2. Nomenclature of stages in B cell development and expression of differentiation markers according to Melchers-Rolink classification and corresponding fractions and nomenclature by Hardy classification. Marker expression is indicated by lines.

Immature B cells that have escaped negative selection leave the bone marrow and migrate as transitional B cells to secondary lymphoid organs. Only a minority of transitional B cells will survive and be selected into one of the three long-lived mature B cell subsets, namely B-1,

follicular (FO) or marginal zone (MZ) B cells (89). FO and MZ B cells are the most abundant B cell populations found in the spleen and are also referred to as B-2 B cells.

FO B cells are re-circulating small resting cells with an average life span in excess of several months (90). Naïve FO B cells reside in the 'follicular niche' of spleen, lymph nodes or Peyer's Patches. They generate Thymus-dependent immune response to protein antigens and are mediators of adaptive immunity. TLR ligation induces the proliferation of FO B cells, but in contrast to MZ and B-1 B cells they lack the intrinsic ability to differentiate into antibody-secreting cells if stimulated only by TLR ligands (91).

MZ B cells are a rather sessile population, in mice they preferentially reside in the vicinity of the marginal sinus. They have a lower threshold for TLR activation and respond without priming to blood-borne pathogens. MZ B cells bear BCR biased toward bacterial components (92, 93). In addition to their important role in Thymus-independent (TI) immune responses, MZ B cells may also participate in Thymus-dependent immune responses to protein antigen, as well as in responses to lipid antigens (94).

The main habitats of murine B-1 B cells are pleural and peritoneal cavities, but B-1 B cells can also be found at lower numbers in the spleen and intestine. B-1 B cells are a persistent, self-renewing population. They have a less diverse immunoglobulin repertoire than B-2 B cells and their BCR specificities are biased toward microbial components, as well as self-antigens (95). B-1 B cells can be further subdivided into B-1a and B-1b B cells, which show functional differences during the immune response. B-1a B cells participate in innate immune responses by spontaneously secreting IgM and thereby providing a first line of defense against certain encapsulated bacteria, such as *Streptococcus pneumoniae*, whereas antibody production by B-1b B cells is induced and has a role in the ultimate clearance of the pathogen and in providing long-term protection (96).

The mechanisms of selection of newly formed B cells into B-1, FO or MZ B cell compartments are not completely unraveled yet as well as the developmental differences between B-2 and B-1 B cells. Two main models are under debate, the 'lineage model' was proposed by Hayakawa, Hardy, and Herzenberg and claims that the B-1 phenotype is genetically predetermined (97, 98). This model was based on the observation that B-1 B cells possess unique features, such as the disposition to express self-reactive autoantibodies, their self-replenishment capacity, the

expression of CD5 and their preferential occurrence in pleural and peritoneal cavities that distinguish them phenotypically and functionally from B-2 B cells. In addition, cell transfer studies showed that fetal liver progenitors are more effective in giving rise to B-1 B cells than bone marrow progenitors in irradiated recipient mice (86, 99). It was thus concluded that two types of B cell developmental pathways exist, one being fetal and generating B-1 B cells and one being adult and generating B-2 B cells (97).

The 'induced differentiation model' was propagated first by Wortis and Clarke and suggests that all B cells are derived from a common progenitor called B-0 cell. In their model the instruction in the B-1 lineage is driven by the encounter of B-0 cells with naturally occurring TI-2-like antigens and depends on BCR signaling strength (100, 101). This model was based on the observation that B-1 phenotype - CD5 expression - can be induced in B-2 B cells after BCR cross-linking with αIgM in the presence of IL-6, notably this conversion was independent of innate antigen, T cell help, and CD40L (102). Further experimental evidence for the importance of BCR specificity for B-1 B cells fate came from different studies showing that transgenic mice expressing genes for autoantibodies generate preferentially B-1 B cells, e.g. mice expressing transgenic autoantibodies specific for red blood cells (103) and transgenic mice expressing antiphosphatidylcholine autoantibodies (104-106). The correlation that BCR signaling per se is necessary for B-1 B cell development came from studies with mice that carried mutations or transgenes inhibiting BCR signaling strength, these mice had reduced numbers of B-1 B cells (107-109), while mice carrying mutations or transgenes that enhanced BCR signaling, had increased numbers of B-1 B cells (110-115).

Obviously, both models aim to convert certain arguments brought by the other camp. Followers of the 'induced differentiation model' claim that the different capacities of fetal versus adult precursors to generate B-1 B cells simply origin in differences of the BCR repertoire in the fetal or adult mice, the fetal BCR repertoire is skewed towards TI-2 specificities, while the adult BCR repertoire seldom generates such specificities (100). Supporters of the 'lineage model' suggest that the observed differences in the BCR repertoire between mature B-1 and B-2 B cells are caused by antigen-driven positive selection for survival of B-1 B cells and not by the acquisition of B-1 B cell phenotype by B-0 cells with such BCR specificities (116).

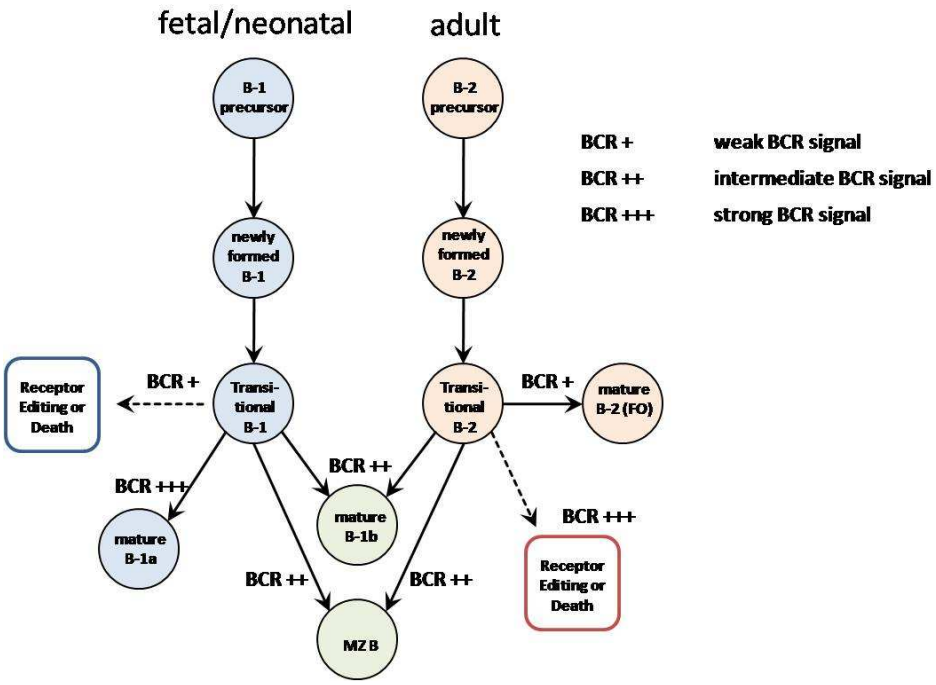

FIGURE 3. Unified model for B cell development adapted from Hardy (95) and Casola (117)

The recent identification of a B-1 B cell progenitor (B-1P) in fetal and adult bone marrow and studies showing that cytokine requirements for B-1 B cell and B-2 B cell development differ, provided new evidence for the lineage model (118, 119). In an attempt to combine all findings of the past years two recent reviews proposed a 'unified model' that comprises both, distinct B-1 and B-2 progenitors and different requirements of immature B cells in BCR signaling strength to be positively selected into the mature B cell pool (95, 117). In this model BCR signal strength is not driving the lineage type of the B cells, but influencing the positive or negative selection of the immature B cells into the different B cell subsets, strong BCR signal drives the cells in the B-1 lineage, while cells receiving weak BCR signals become B-2 B cells. Intermediate BCR signals favor the development of B cells along the MZ fate (117).

1.4 Tuberculosis

1.4.1 Epidemiology and disease

Mycobacterium tuberculosis (Mtb), the causative agent of tuberculosis (TB), is one of the most threatening human pathogens worldwide with the highest prevalence in developing countries

(Fig. 4). It was first described on March 24, 1882 by Robert Koch who received the Nobel Prize in physiology or medicine for the discovery in 1905 (120). The bacterium is a slowly growing obligate aerobe. *Mycobacterium* species are classified as acid-fast bacteria due to their cell wall impermeability to certain dyes. The composition of its cell wall is dominated by mycolic acids that make up more than 50% of its dry weight (121). The genome of Mtb was sequenced in 1998. It has a size of 4.41Mb and consists of about 4000 protein-coding genes of which 52% have a known function (122, 123).

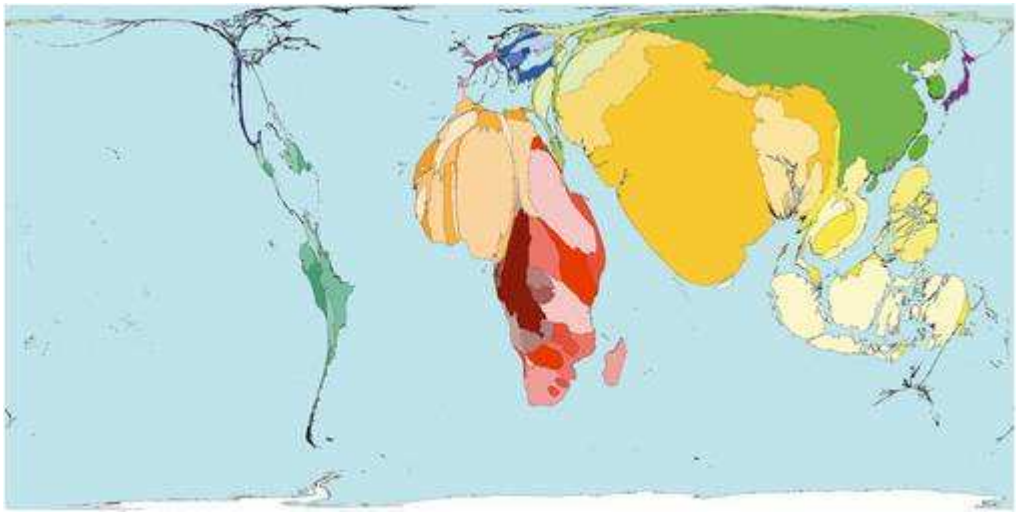

FIGURE 4. Territories are sized in proportion to the absolute number of people who died from tuberculosis in one year. © Copyright 2006 SASI Group (University of Sheffield) and Mark Newman (University of Michigan).

The World Health Organization (WHO) estimates that up to one third of the world population is infected with Mtb. Annually 9 million people develop TB of whom 2 million die (124-126). However, morbidity and mortality figures are only one facet of TB. Ninety percent of infected individuals will never develop active TB disease, indicating that the human immune system controls Mtb infection effectively, even though sterile eradication of Mtb is normally not achieved.

Infection with Mtb generally occurs via inhalation of Mtb-containing droplets expelled by a patient with pulmonary TB. The lung is the typical site of infection although all organs can be affected. Within the lung alveolar space, bacilli are engulfed by alveolar macrophages and transported into the lung parenchyma where they are contained by tissue macrophages within granulomatous lesions (125, 127-129). A chronic infection develops and a balance between pathogen replication and immune response is maintained, with the inherent risk of reactivation

at a later times (124, 125, 127). Notably, the risk of reactivation especially upon immune suppression, e.g. during human immunodeficiency virus (HIV) infection increases 100-fold (128, 130).

The Bacille Calmette-Guérin (BCG) vaccine only protects from severe forms of pediatric TB, but not from pulmonary TB in adults. Moreover, the available therapeutic options are poor. Antimycobacterial drug treatment is lengthy and expensive leading to poor regimen compliance. Another alarming observation is the rise of multi-drug resistant strains e.g. the genotype family Beijiing/W and extensively drug-resistant (XDR) TB. For these strains, the treatment costs are 100-fold higher if drug treatment is possible at all (129, 131).

1.4.2 Murine immune response to Mtb infection

Mouse models aided profoundly to understand the immune response against Mtb. To mimic the natural infection route mice are usually infected with low doses (100-200 colony forming units (CFU)) Mtb via aerosol.

After aerosol infection the invading bacilli are phagocytosed by alveolar macrophages and probably interstitial DCs. Phagocytosed mycobacteria are able to block their delivery to the lysosome and can therefore escape lysosomal destruction (132). The surviving bacteria are then either transported to the draining lymph nodes where antigen-specific T cells are primed or reach deeper lung tissues where they reside within macrophages. Infected macrophages initiate an inflammatory response that results in the recruitment of different cells to the sites of infection, beginning with monocytes, neutrophils, DCs, and later lymphocytes (133).

Notably, Mtb can first be detected in lung draining lymph nodes at 8 to 9 days post infection (p.i.) (134, 135) and only then T cell activation occurs (134, 136). The mechanisms that restrict a faster migration of infected DCs to the lymph nodes are incompletely understood. In consequence, murine T cell response following a low-dose Mtb aerosol infection are relatively slow, when compared with responses to viral or other bacterial infections (127). By day 9 p.i. T cell priming occurs in the draining lymph nodes and IL-12 secretion by activated macrophages and DCs drives the generation of Th1 type effector cells (137, 138). Since Mtb resides in endosomes, antigen-specific T cell priming in the draining lymph node is mainly MHCII

restricted. However, MHCI priming also occurs. It is likely that crosspriming plays a role in $CD8^+$ T cell activation. Mycobacteria induce apoptosis in macrophages causing the release of apoptotic vesicles that carry mycobacterial antigens to APC which in turn present them through CD1 (glycolipids) or MHCI (peptides) (139).

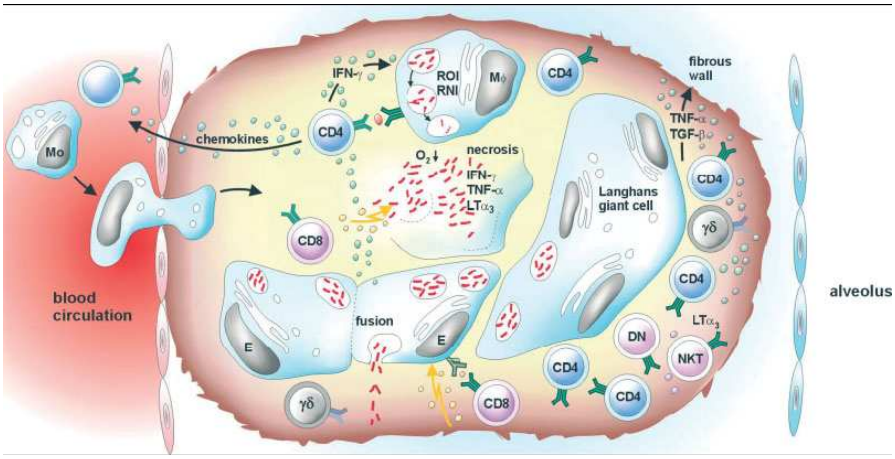

FIGURE 5. Scheme of classical granuloma structures and proposed local immune responses; reprinted from Ulrichs & Kaufmann (137)

Activated effector Th1 $CD4^+$ and $CD8^+$ T cells reach the lung by 3 weeks p.i.. T cells, notably $CD4^+$ Th1 cells, dominate in protective immunity against Mtb (125, 127-129). Upon activation, $CD4^+$ T cells secrete multiple cytokines including IFN-γ and TNF-α, which in turn activate anti-mycobacterial mechanisms in mononuclear phagocytes (124, 125, 127). Besides $CD4^+$ T cells, other T cell subsets, such as $CD8^+$ T cells, gamma delta (γδ) T cells, CD1-restricted T cells and Treg, participate in the immune response against Mtb and consequently influence disease outcome (64, 66, 124, 127, 140-142).

Only with the arrival of effector Th1 $CD4^+$ and $CD8^+$ T cells, the so far steady growth of mycobacteria in lungs and spleen of infected mice will be halted. Subsequent to this acute infection phase, a chronic phase ensues where bacterial numbers remain stable at a level of approximately 10^6 CFU in C57BL/6 mice for many months until progressive pathology results in death.

During the chronic phase of infection structures resembling human tuberculous granuloma form in the lungs of infected mice. As for humans, murine 'granuloma' are thought to ensure the containment of mycobacteria and to focus the immune response to the site of infection. The morphology of human solid granuloma is characterized by a necrotic center surrounded by

concentric layers of macrophages, epitheloid cells, multinucleated Langerhans giant cells, and lymphocytes (Fig. 5). In contrast, murine 'granuloma' consist of loosely aggregated cells and usually lack necrosis. Development of the granuloma is mediated by chemokines and cytokines produced by local tissue cells and infiltrating leukocytes. $CD4^+$ T cells and macrophages produce TNF-α and lymphotoxin alpha 3, which are required for the formation of the wall surrounding the granuloma (121, 129, 130, 137, 138, 143)(Fig. 5).

2 AIMS OF THIS STUDY

This thesis has two independent aims. The first aim is to gain knowledge about the function of a so far uncharacterized receptor that was predicted to be part of the innate immune system, namely murine TLT-6 (gene: *treml6*), an ITIM-containing receptor of the TREM protein family. The second aim is to investigate the role of ICOS, a well described co-stimulatory molecule known to participate in adaptive immune responses, in the context of murine Mtb infection.

Immunological characterization of *treml6* via the analysis of *treml6*$^{-/-}$ mice

TREM receptors form a newly identified family of NON-TLR surface receptors (12). Some of their members have already been characterized, while the functions of others are still undefined (12). TREM are of great interest in infection immunology since most characterized members have been described to participate in inflammatory immune responses by either amplifying or dampening TLR-derived signals (14, 17, 18, 144). In this context, *treml6* was predicted to carry an ITIM motif and was therefore proposed to be of inhibitory nature (12). Since nothing was known about *treml6*, the first aim was to determine the expression profile of *treml6* in WT mice. The second aim was to phenotype our in-house generated *treml6*$^{-/-}$ mice with the focus on the immune system. As the result of an initial analysis, I discovered that *treml6* influences the frequencies of B-1a B cells and their precursors. B-1 B cells were discovered in the early 1980's (145-147), and since then both their role in the immune system and their development have been under debate (86, 148-150). Since *treml6* appeared to be an important player in this context, I further expanded the aim of this project and investigated the impact of *treml6* on the development, function and, maintenance of B cells.

Analysis of the influence of ICOS signaling on T cell responses against Mtb

The World Health Organization (WHO) estimates that up to one third of the world population is infected with Mtb and annually 9 million people develop TB of whom 2 million die (124-126). These numbers make Mtb, the causative agent of TB, one of the top three microbial killers (126). The primary goal of this research was to expand the current knowledge about the host response during Mtb infection. Protective immunity to tuberculosis depends on $CD4^+$ Th1 cells

in humans and in mice (151-154), but the adaptive immune response fails to eradicate Mtb and to achieve sterile immunity. Nevertheless, a prerequisite for successful vaccine or drug design is the understanding of this immune response and especially its weaknesses.

In the search of putative immune modulators, I analyzed Th1 responses against Mtb during my diploma project and observed that ICOS expression correlated with Th1 effector phenotype. In line with our observation, other groups reported that the amount of IFN-γ secretion by T cells from patients with active TB disease correlates with their ICOS surface expression, and that ICOS signaling can increase IFN-γ secretion (155). Moreover, Urdahl and colleagues showed that pulmonary Treg express elevated levels of ICOS during murine Mtb infection (66). These data pointed to ICOS as an important player in the formation of any kind of T cell response against Mtb. Therefore, I aimed clarifying the role of ICOS co-stimulation in the generation and maintenance of T cell responses against Mtb.

3 MATERIALS AND METHODS

3.1 Mice

Abbreviation	Full strain Designation	Notes
wild-type (B6 or WT)	C57BL/6NCrl	Charles River Laboratories
ICOS$^{-/-}$	C57BL/6.ICOS$^{-/-}$	
Rag1$^{-/-}$	C57BL/6J-*Irf2*^{tm1}*Rag1*^{tm1}	
Treml6$^{-/-}$	C57BL/6.treml6$^{-/-}$	
WT	C57BL/6.treml6$^{+/+}$	

3.2 Materials

See APPENDIX 1: MATERIALS

3.3 Methods

3.3.1 Animal work

3.3.1.1 Breeding of mice

Mice were bred and maintained under special pathogen free conditions with a 12 hour light cycle; food and water were provided ad libidum. B6 mice were purchased from Charles River Labs (Germany). ICOS$^{-/-}$ mice were a gift from Andreas Hutloff (RKI, Berlin). Rag1$^{-/-}$, *treml6*$^{-/-}$ and wild-type (WT) control mice were bred at the Max Planck Institute for Infection Biology animal breeding facility (Berlin-Marienfelde, Germany). Infected mice were kept in a biosafety level 3 facility and non-infected ones in a biosafety level 2 facility. Mice were sacrificed by cervical dislocation. The experiments were conducted according to the German animal protection law.

3.3.1.2 Construction of gene-deficient mice

Treml6 deficient mice were generated by Dr. M. Kursar in the laboratory of Bernard Malissen at the Centre d'Immunologie de Marseille-Luminy, France. In the targeting construct depicted in Fig. 6A, a deoxyribonucleic acid (DNA) fragment that includes exon 1 (starting from the ATG translational start codon), 2, 3 and 4 of the *treml6* gene was replaced by a *beta-galactosidase* (lacZ) gene followed by a self-excising ACN-cassette (156) bearing a locus of X-ing over (loxP)-

sequence flanked neomycin resistant gene and a testes-specific promoter from the angiotensin-converting enzyme gene (tACE)-promotor driven *cre*-gene. Briefly, the C57BL/6 BAC-DNA clone RP23-32N6 – containing TREM-genes *trem1, trem3, treml4, treml2, treml6, trem2,* and *treml1*- was purchased from RZPD Deutsches Ressourcenzentrum für Genomforschung GmbH. BAC-DNA was used as template to poly chain reaction (PCR)-amplify a 5`-homology arm (HA-5`) and a 3`-homology arm (HA-3`) using primers P1 (5'-**ttggcgcgcc**gggaacagcctgtagctattga-3') and P2 (5'-**acgcgtcgac**cactggggagagcaggtatg-3'), and P3 (5'-**acgcgtcgac**gaggagaccactgtaagtaaaaatgac-3') and P4 (5'-**ataagaatgcggccgctaaactat**tatttctgtgtaaaacataaggcagga-3'). In addition to sequence homologous to the BAC-DNA, P1 contains a *AscI*-site, P2 and P3 a *SalI*-site, and P4 a *NotI*-site (bold sequences). The lacZ-ACN sequence was excised by *SalI* digestion from vector pTK-lacZ-Neo-Cre, which was engineered and kindly provided by Dr. Markus Koch. HA-5`, lacZ-ACN, and HA-3` were cloned into the thymidine-kinase (TK) containing vector pTK_MK (engineered and kindly provided by Dr. Markus Koch). The resulting targeting vector was *ScaI*-linearized and electroporated into *Bruce4* mouse embryonic stem (ES) cells (origin B6). Colonies resistant both to G418 (300 mg/mL) and to gancyclovir (2 mM) were screened by PCR for homologous recombination using primers P5 (5'-tgcctggttttctccttactt-3') and P6 (5'-aatgggataggttacgttggtgtag-3') – for homologous recombination of HA-5`, and P7 (5'-atcgatgagttgcttcaaaaatc-3') and P8 (5'-tccttctccttctccttcttgtt-3') – for homologous recombination of HA-3`. One recombinant ES clone (M1_E1) was found positive for both screening PCRs (Fig. 6B).

Production of Mutant Mice Mutant embryonic stem cells (ES cells) were injected into (white) B6 blastocysts and were capable of germline transmission. The ACN cassette was self-excised during male germline transmission.

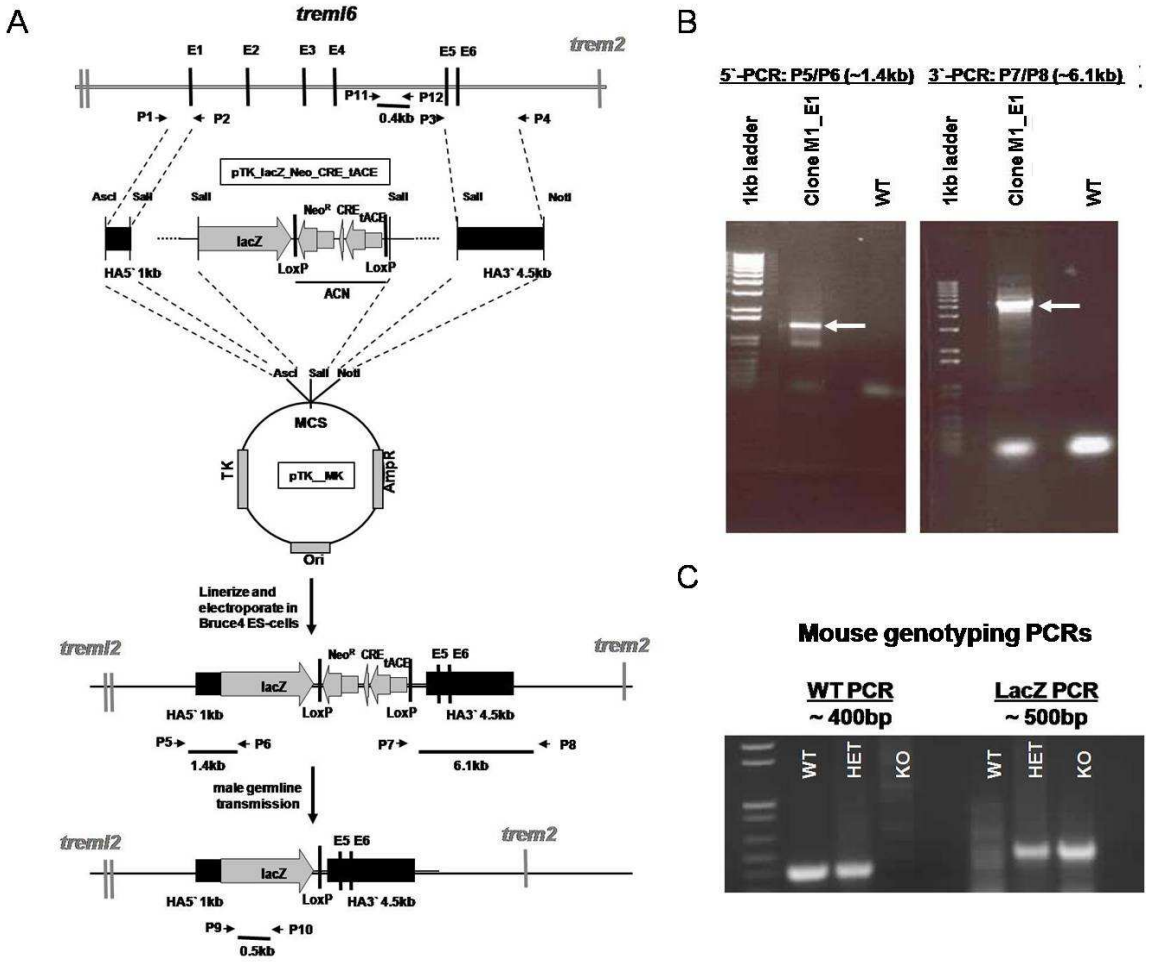

FIGURE 6. Generation of *treml6*$^{-/-}$ mice. ***A,*** Cloning strategy. ***B,*** Screening PCRs of 5' and 3' homology arms on Bruce4-B6 (WT) ES cells and mutated ES clone M1_E1. ***C,*** Mouse genotyping; WT PCR (primer P11 and P12 in Fig. 6A), LacZ PCR (primer P9 and P10 in Fig. 6A). In white, tail DNA from WT mice (WT), *treml6*$^{+/-}$ (HET), and treml6$^{-/-}$ (knockout (KO)) mice.

3.3.1.3 Genotyping of *treml6*$^{+/+}$ (WT) and *treml6*$^{-/-}$ mice

Genomic DNA isolation from tail biopsies Five mm tail biopsies were kept in 1.5-ml microcentrifuge tubes at -20°C until genomic DNA isolation. Tails were lysed overnight with 500 µl tail buffer supplemented with 0.2 mg/ml Proteinase K under shaking at 55°C and 900 rpm. Next day samples were centrifuged for 10 min at 20,000x g and 4°C. Supernatants contained DNA, and were collected in fresh 1.5-ml microcentrifuge tubes. DNA was precipitated by adding 500 µl isopropyl alcohol, shaking of the mixture and centrifugation for 10 min at 20,000x g and 4°C. Supernatants were discarded and DNA pellets washed with 500 µl 70% ethanol. To re-sediment the DNA pellets, they were centrifuged for 5 min at 20,000x g and 4°C. Ethanol supernatants were removed and DNA pellets were allowed to dry before resuspending them in

500 µl double distilled (dd) H_2O. To improve dissolving, DNA-water samples were shaked for 15 min at 60°C and 600 rpm.

PCR amplification and analysis of wildtype and LacZ gene PCR products PCRs were performed on tail DNA amplifying either the wild-type gene (WT PCR product ~400 bp; with primer B4 Tail WT fw1 (P11) and B4 Tail WT rev1 (P12)) or the inserted LacZ gene (KO PCR product ~500 bp; primer TP_B4_KO-sHA_ fw (P9) and TP_B4_KO-lacZ-rv (P10)). PCR mix contained 5 µl tail DNA, 16.9 µl dH_2O, 0.2 µl dNTP's (10 mM each), 0.1 µl forward primer (100 pmol/µl), 0.1 µl reverse primer (100 pmol/µl), 0.2 µl Taq polymerase and 2.5 µl BioTherm buffer (10x). PCR cycles comprised 3 min of initial denaturation at 94°C, followed by 30 cycles of 1) 40 sec at 94°C, 2) 40 sec at 60°C and, 3) 1 min at 72°C and a final elongation step for 5 min at 72°C. PCR samples were stored at 4°C. 5 µl of DNA loading buffer were added to 25 µl PCR products and samples were run for 40 min on a 1% agarose gel. Gels were photographed with a UV-light photometer and resulting bands were analyzed to determine the genotype (Fig. 6C).

3.3.1.4 Infection of mice with Mtb

Mtb strain H37Rv NY was grown in Middlebrook 7H9-broth at 37°C with shaking until bacterial growth reached an OD_{600}=0.7, corresponding to an approximate cell density of 10^8 cells/ml. These mid-logarithmic cultures were harvested by centrifugation, washed with 1x phosphate buffered saline (PBS), re-suspended in 10% glycerol, aliquoted and stored at -80°C until use. All mycobacteria stocks were titrated prior to use by plating serial dilutions onto 7H11-agar plates and counting the CFU after three weeks of incubation at 37^oC. Aliquots were homogenized prior to use by repeated transfer through a syringe with a 26G needle. Infection of mice was performed using a Glas-Col inhalation exposure system. An aliquot of frozen Mtb stock culture was thawed and diluted (as determined in titration experiments performed for every infection stock) with water. The next day, five mice were sacrificed, their lungs removed, homogenized and plated onto 7H11-agar to verify the initial infection dose.

Determination of bacterial titers Mice were sacrificed at distinct time points after infection by cervical dislocation. Lungs and spleens were transferred into sterile sample bags containing 1 ml PBS/Tween solution (PBST). For experiments in which T cell analysis was performed simultaneously with CFU determination, the small lower right lung lobe was used for CFU and estimated to represent 1/5 of the total lung for CFU calculations. Similarly, half of the spleen

was used for CFU determination. Organs were homogenized in the sample bags by smashing and after serial dilution in PBST, 50 µl were plated on 7H11-agar plates containing ampicillin and cyclohexamide which were sealed with PARAFILM® and wrapped in aluminum foil. After 3-4 weeks of incubation at 37°C, CFU were counted. Statistical significance was determined using the Mann-Whitney test.

Histology Tissues were fixed in 4% paraformaldehyde (PFA) in 1x PBS for 24 h at 4°C, transferred into 1x PBS and stored at 4°C until embedding. Histology samples were dehydrated, embedded in paraffin blocks and allowed to harden. Five µm sections were cut, mounted on glass slides and dried overnight at 37°C. Sections were re-hydrated and stained with Hematoxylin and Eosin Y (H&E). Re-hydration was performed as follows: 2x 10 min xylene, 2x 10 min 95% ethanol, 2x 10 min 80% ethanol, 10 min 70% ethanol and finally 10 min de-ionized water. For H&E staining, slides were incubated for 1 min in concentrated Hematoxylin solution, dipped in acid ethanol (1% HCL in 95% ethanol), rinsed with tap water for 10 min, rinsed with de-ionized water, and followed by Eosin Y staining for 20 sec. Slides were subsequently rinsed with water and dehydrated for 3 min in 95% ethanol followed by 2 min in xylene. Samples were mounted using cover slip slides and Mercor glass and were photographed at 2.5, 10, 20, and 40x magnification. For experiments in which T cell analysis was performed simultaneously with histological analysis, the entire large left lobe of lungs was used.

3.3.1.5 Tissue and organ isolation

Peritoneal Cavity Peritoneal cavities were flushed twice with each 5 ml 1x PBS using a 1.20 x 40 mm needle and 10-ml syringe, the resulting cell suspension was collected in 15-ml tubes.

Mesenteric lymph nodes (*MLN*) Abdomen was opened with an incision made with surgical tweezers. MLN were removed carefully from mesenteric tissues and collected in 5 ml PBS/BSA (bovine serum albumin) solution in a 15-ml tube.

Spleen A small incision at the left of the peritoneal wall was made with surgical scissors. The spleen was grasped with tweezers and pulled free of the peritoneum and the connective tissues. It was placed in 5 ml PBS/BSA solution in a 15-ml tube.

Liver Livers were removed from the abdomen by disconnecting them from the diaphragm. They were placed in 5 ml PBS/BSA in 50-ml tubes.

Peyer's Patches The small intestine was isolated from the peritoneal cavity and carefully searched for white-shimmering Peyer's Patches. Peyer's Patches were removed from the small intestine with surgical scissors and tweezers.

Lungs Lungs were isolated by an incision in the chest, beginning at the xiphoid and extending to the neck with surgical scissors. The ribs were cracked left and right of the ribcage and lifted. To diminish the numbers of blood lymphocytes lungs were perfused through the right heart ventricle with cold 1x PBS. Excised lungs were placed in 5 ml PBS/BSA in 50-ml tubes.

Thymus Once lungs were removed, thymi could be isolated by grasping them with tweezers.

BM To isolate BM, first the skin of mice was removed around the leg and ankles. Then flesh and tissues were cut away from femur and tibia. Femur was cut above the hip joint and tibia at foot joint. Femur and tibia were separated and cut open on both ends. BM was extracted by flushing the bones with 20 ml complete Roswell Park Memorial Institute (cRPMI) media using a 0.55-mm needle and 20-ml syringe. BM cell suspensions were collected in 50-ml tubes.

Bones Remaining bones after BM isolation were used as bone samples.

3.3.1.6 Isolation of leukocytes from tissues and organs

Lung Individual lungs were placed in Petri dishes and cut into 5 mm sized pieces with scissors. Typically, the right lung lobes were used for lymphocyte analysis. Lungs from 1-2 mice were pooled in order to obtain enough cells. Freshly prepared Collagenase medium (10 ml) was added to the diced lungs and incubated for 30 min at 37°C, 7% carbon dioxide (CO_2). The digested lung pieces were pressed through iron mesh sieves into the lids of the Petri dishes using plungers of 10-ml syringes. The cell suspensions were collected in 50-ml tubes. The sieves and Petri dishes were washed twice with 10 ml PBS/BSA added to the 50-ml tubes and centrifuged for 6min in a Heraeus centrifuge at 400x g. The pellets were re-suspended in 10 ml 40% Percoll/RPMI solution at room temperature (RT). Five ml of this cell suspension were layered over 3 ml 70% Percoll/RPMI in a 15-ml tube. The resulting gradients were centrifuged for 25 min at 600x g without brake at RT. The cells from the interface were transferred to new 50-ml tubes and washed with 30 ml RPMI. The pellets were re-suspended in red blood cell lysis buffer and incubated for 2 min to remove remaining erythrocytes. After an additional washing

with PBS/BSA, cells were filtered through 70-µm filters and re-suspended in RPMI complete media and kept on ice.

Spleen, MLN and thymus Freshly removed organs were placed in 5 ml PBS/BSA solution in 15-ml tubes. Normally, half of the spleen was used for lymphocyte analysis. Spleens from 2 mice were pooled, in order to be consistent with lung cell preparations. Spleens or MLN or thymus were pressed through 70-µm filters with plungers of 10-ml syringes into Petri dishes. The suspensions were collected in 15-ml tubes. The filters and Petri dishes were washed with 10 ml PBS/BSA solution and the washes were added to the 15-ml tubes. Next the suspensions were centrifuged for 6 min in a Heraeus centrifuge at 400x g. To remove erythrocytes, the pellets were re-suspended in 2 ml red blood cell lysis buffer and incubated for 2-3 min with occasional shaking. 10 ml PBS/BSA solution were added and the tubes were centrifuged. The resulting pellets were re-suspended in RPMI-10 complete medium and filtered through 70-µm filters.

Peritoneal Cavity Cell suspensions were centrifuged for 6 min in a Heraeus centrifuge at 400x g. Pellets contaminated with erythrocytes were excluded from analysis. Pellets were then re-suspended in RPMI-10 complete medium and filtered through 70-µm filters.

BM Tibia and femur from dissected mice were cut and flushed with RPMI-10 complete medium to remove leukocytes from the bones. Cell suspensions were collected in 50-ml tubes. To remove erythrocytes, the pellets were re-suspended in 2 ml red blood cell lysis buffer and incubated for 2-3 min with occasional shaking. 10 ml PBS/BSA solution were added and the tubes were centrifuged. The resulting pellets were re-suspended in RPMI-10 complete medium and filtered through 70-µm filters.

The viability of the cells was determined by Trypan blue exclusion. Twenty µl of each cell suspension were diluted in 180 µl 1x Trypan blue solution and counted in a haemocytometer. Cell numbers were calculated with the following formula: cell number from 16 quadrants x chamber factor (10^4) x dilution factor x volume of cell suspension = total cell number. Cells were re-suspended in RPMI complete medium at 10-40x 10^6 cells/ml.

3.3.1.7 Blood samples

Blood samples were taken from the tail vein. The blood was directly collected in serum separator tubes, let stand for a minimum of 30 min at RT, followed by centrifugation at 12,000x g for 3 min and finally the serum was stored at -20°C until analysis.

3.3.1.8 In vivo cytotoxicity assay

Splenocytes target cell suspensions from naive B6 mice were prepared as described above and evenly split into two fractions. One fraction was pulsed with 10^{-4} M Mtb32A-derived peptide (PepA: GAPINSATAM) for 1 h at 37°C and then labeled with a high concentration (2 µg/ml) of Carboxy-fluorescein diacetate succinimidyl ester (CFSE) ($CFSE_{high}$ population), and the other fraction was incubated for 1 h at 37°C with 10^{-5} M listeriolysin$_{91-99}$ (LLO_{91-99}: GYKDGNEYI) control peptide and labeled with a low concentration (0.2 µg/ml) of CFSE ($CFSE_{low}$ population). $CFSE_{low}$- and $CFSE_{high}$-labeled cells (2x 10^7 cells in total) were mixed at a 1:1 ratio and adoptively transferred in 200 µl 1x PBS into Mtb-infected B6 and $ICOS^{-/-}$ mice via tail vein injection. Twenty hours later, recipient spleen cells were analyzed by flow cytometry. Percent specific lysis was determined by loss of the peptide-pulsed $CFSE_{high}$ population compared to the control $CFSE_{low}$ population in infected mice relative to loss of the peptide-pulsed $CFSE_{high}$ population compared to the control $CFSE_{low}$ population in naïve mice using the formula $(1 – (AVG\ r_{naive}/r_{infected}) \times 100)$, r: % $CFSE_{low}$/ % $CFSE_{high}$.

3.3.1.9 Irradiation of mice and cell transplantation

$Rag1^{-/-}$ recipient mice were sublethally γ-irradiated (400 rad) 24 h before transplantation. For transplantation either donor mouse BM cells, or *in vitro* cultivated pre-B I cells kept on IL-7/stromal cells (OP9) were used. The harvested cells were washed twice in cell culture-tested 1x PBS and were concentrated to 5x 10^7 cells/ml. The remaining cell clumps were removed by straining the cell suspension through a MACS® Pre-Separation Filter with 30-µm mesh. For intravenous (i.v.) transplantation mice were warmed by infrared irradiation for vasodilatation of the tail veins. 100 µl with 5x 10^6 cells were injected into the lateral tail vein. The condition of transplanted mice was controlled regularly.

3.3.1.10 Bromodeoxyuridine (BrdU) *in vivo* proliferation assay

Mice received drinking water supplemented with 0.8 mg/ml BrdU and 1% (wt/vl) Sucrose for 4, 8 or 12 days. BrdU drinking water was protected from light with aluminum foil. At day 4, 8 or 12 of treatment mice were sacrificed and *in vivo* B cell proliferation was analyzed as described in 3.3.3.7.

3.3.1.11 Thymus independent-type-2 (TI-2) immunizations with trinitrophenol (TNP)-Ficoll

Mice were immunized with TNP-Ficoll by intraperitoneal (i.p.) injection of 10µg TNP-Ficoll in 100µl 1x PBS. At days 0, 5, 8 and 14 serum samples were taken and analyzed for TNP-specific antibodies via enzyme-linked immuno sorbent assay (ELISA).

3.3.2 mRNA expression profile of *treml6*

3.3.2.1 Preparation of ribonucleic acid (RNA) from isolated tissues or cell suspensions

Tissue isolation B6 mice were sacrificed and tissues (BM, bones, spleen, MLN, peritoneal cavity, Peyer's patches, thymus, lung, liver, fetal liver) were removed. Fetal liver was obtained by mating the mice overnight and intercepting the pregnancy at day 18. RNA was isolated by the Trizol Reagent RNA preparation method. Briefly, about 100 mg tissue was homogenized in 1 ml of Trizol Reagent with an Ultra Turrax T8 tissue homogenizer. Cell samples were collected in 1.5-ml microcentrifuge tubes in 1 ml Trizol and homogenized by pipeting. Trizol samples were stored at -80°C until RNA extraction.

RNA extraction RNA was extracted as recommended by the manufacturer. Homogenized tissue samples were centrifuged at 500x g for 5 min to remove insoluble material. The cleared homogenate solution was transferred into a fresh 1.5-ml microcentrifuge tube. All samples were incubated for 5 min at RT, before 0.2 ml chloroform were added and mixed vigorously for 15 sec. Following 2-3 min incubation at RT, the suspensions were centrifuged for 20 min at 14,000x g and 4°C to allow phase separation. The upper colorless phase, containing the RNA, was removed and transferred into fresh microcentrifuge tubes. To precipitate the RNA 0.5 ml

isopropyl alcohol were added to the samples, mixed and incubated for 10 min at RT. After 20 min centrifugation at 14,000x g and 4°C the RNA precipitate formed gel-like pellets. Supernatants were removed and pellets were washed with 1 ml 75% ethanol, vortexed and centrifuged for 5 min at 7,500x g at 4°C. Again, supernatants were removed and pellets were allowed to dry briefly before resuspending them in 20 µl RNase free water. Purified RNA samples were stored at -80°C.

3.3.2.2 Reverse transcription of RNA and qRT-PCR

Reverse transcription of purified RNA 10 µl of the initially purified RNA samples (maximum 5 µg) were used for reverse transcription. For that 1 µl random hexamer primers (200 µg/ml) were added, the mixture was incubated for 10 min at 65°C and then placed on ice. After 5 min on ice, a reaction mix containing 4 µl 5x first strand buffer, 1 µl 10 mM dNTPs and 2 µl 0.1 M DTT were added and after 10 min incubation at RT 1 µl of superscript reverse transcriptase was added. This mixture was immediately incubated for 50 min at 42°C and finally incubated for 15 min at 70°C in order to inactivate the reverse transcriptase and to stop the reaction.

qRT-PCR on complementary DNA (cDNA) To compare the amount of cDNA used in each reaction, beta-actin (*ß-actin*) and *glyceraldehyde-3-phosphate dehydrogenase* (*gapdh*) primers were included. PCRs were either run in standard mode for 40 cycles with 20 sec 95°C and 60 sec 60°C in the ABI Prism 7000 Sequence Detection System (*Applied Biosystems*) using ABI PRISM optical 96-well plates (*Applied Biosystems*) or in FAST mode for 40 cycles with 1 sec 95°C and 15 sec 60°C with MicroAmp™ Fast Optical 96-Well Reaction Plates (*Applied Biosystems*). To control specificity of primers, in both standard and FAST mode, dissociation stages with 15 sec 95°C, 15 sec 60°c and 15 sec 95°C were added to the runs.

3.3.2.3 RT-PCR analysis

Amplifying primers were designed to span exon-exon junctions (EEJ) to avoid amplification of genomic DNA and to generate products of 100 – 300 bp size. Reaction mixtures were set up in 30 µl final volume using 15 pmol of each primer, 5 µl template cDNA and 15 µl 2x (Fast) SYBR-Green PCR Master mix (Applied Biosystems). Quantifications were performed at least twice with independent cDNA samples and in triplicates for each cDNA and primer pair. Data analysis was performed using the ABI Prism 7000 SDS Software, REST-MCS© beta (Pfaffl &Horgan) and

Microsoft Excel. The threshold cycle (c_t) was determined for each sample and fold differences relative to the expression level in one of the analyzed cDNA samples or a virtual value (for *treml6* expression in naïve organs or cells) was calculated for each cDNA sample and primer pair (fold-difference=$2^{-\Delta Ct}$). Differences in amount of transcribed cDNA were normalized to the expression of housekeeping genes *gapdh* and *β-actin*.

3.3.3 Flow cytometry

Single and multicolour stainings were analysed on a LSR-II flow cytometer equipped with a (L1) argon laser (488 nm), a (L2) Helium neon laser (633 nm), a (L3) UV laser (355 nm) and a (L4) violet laser (405 nm) or in the biosafety level 3 facility on a FACS Canto II equipped with a (L1) argon laser (488 nm), a (L2) HeNe laser (633 nm), and a (L4) violet laser (405 nm). If necessary, fluorescence minus one (FMO) staining was performed to adjust photo multiplier tubes (PMT) voltages and to compensate manually between the channels.

3.3.3.1 Standard staining protocol and MHCI tetramer staining

Standard staining protocol All stainings were carried out in U-bottom 96-well-plates, which were kept on ice or at 4°C during the whole procedure. Unnecessary light exposure was avoided. The centrifugation was done for 3 min at 300x g and 4°C. Generally, 2-4x 10^6 cells were incubated in 100 µl PBS/BSA solution with rat serum, anti (α)CD16/αCD32 monoclonal antibodies (mAbs) to block non-specific antibody binding. After 5 min primary antibodies were added at a previously titrated optimal dilution and cells were incubated for 15 min at 4°C. Cells were then centrifuged, washed with 180 µl PBS/BSA, re-centrifuged, and re-suspended in 100 µl of PBS/BSA solution. If a primary antibody was biotin-conjugated, the staining procedure was repeated with streptavidin conjugates. Stained cells were kept at 4°C protected from light until measurement by flow cytometry the same day.

PepA tetramer staining Identification of PepA specific $CD8^+$ T cells in organs of Mtb infected mice was performed using MHCI tetramers constructed with peptide from the Mtb-derived antigen PepA and labeled with the fluorochrome PE. About 2-4x 10^6 cells were incubated in 100 µl PBS/BSA solution with rat serum, αCD16/αCD32 mAb and streptavidine to block non-specific tetramer and antibody binding. After 5 to 10 min, cells were stained with

PepA tetramers as well as several T cell surface antigens including αCD8, αCD4, αCD62L, αCD69, αCD44, and αCD27 mAb. After 45 min at 4°C, stained cells were washed with PBS/BSA and re-suspended in 100 µl of PBS/BSA solution. Stained cells were kept at 4°C protected from light until measurement by flow cytometry the same day.

3.3.3.2 Immunological characterization of immune cell types

Leukocytes from peritoneal cavity, spleen, MLN, thymus and BM were isolated and numbers determined as described in 3.3.1.6. Frequencies and absolute numbers of a) T cells, b) B cells, c) APCs, and d) neutrophils were determined by flow cytometric analysis as described in 3.3.3.1. T cells were identified as helper T cells by the surface expression of $CD4^+$ and CTLs were identified by the surface expression of CD8α and absence of CD11c or CD11b expression. B cells were defined as B220 expressing cells and representative for APCs were DCs defined by the surface expression of CD11c and macrophages defined by the intermediate expression of CD11b. Neutrophils were defined as high GR-1 and CD11b surface expressing leukocytes.

3.3.3.3 *In vitro* re-stimulation and intracellular cytokine staining (ICS)

Mtb-protein-derived peptides used for restimulation Antigen 85A (Ag85A) and Antigen 85B (Ag85B) The MHCII presented peptides Ag85A (QDAYNAGGGHNGVFDFPDSG) and Ag85B (FQDAYNAAGGHNAVFNFPPNG) are derived from proteins Ag85A and Ag85B, respectively which are secreted by Mtb in early infection stages and which are encoded by the respective genes are *fbpA* and *fbpB*.

Six Kilodalton Early Secretory Antigenic Target (ESAT6) The MHCII presented ESAT6 peptide (MTEQQWNFAGIEAAASAIQG) is derived from the ESAT6 protein and encoded by the gene *esxA*. ESAT6, together with culture filtrate protein 10 (CFP10) are exported through an alternative secretion pathway encoded by genes of the region of deletion-1 locus. ESAT6 and CFP-10 are important antigens in diagnosis of TB, where they are used to detect the presence of Mtb specific T cells in patients.

Mtb32A-derived Peptide (PepA) The MHCI presented peptide PepA (GAPINSATAM) is derived from Mtb32A protein which was isolated from Mtb culture filtrate and was identified as a putative serine protease. The open reading frame of Mtb32A corresponds to “pepA” Rv0125. Mtb32A is rapidly processed and exported from the bacilli after synthesis.

In vitro restimulation To measure antigen-specific cells by intracellular cytokine staining, 2-4x 10^6 cells were cultured for 6 h in a total volume of 200 µl of RPMI-10 complete medium containing 10 µg/ml of Brefeldin A, and the following Mtb derived peptide antigens at 10^{-4} M concentrations: $Ag85A_{241-260}$, $Ag85B_{240-260}$, $ESAT6_{1-20}$, and PepA peptides. As a control, 2-4x 10^6 cells were also incubated in parallel in a total volume of 200 µl of RPMI-10 complete medium containing 10 µg/ml of Brefeldin A and no peptides.

Intercellular cytokine staining To determine frequencies of cytokine producing cells intracellular cytokine staining was performed. The restimulated cells (see above) were washed with PBS/BSA and blocking solution containing rat serum and αCD16/αCD32 mAb were added and incubated on ice for 10 min. Surface marker antibody solutions containing fluorochrome conjugated αCD4 and αCD8 mAb were then added and cells were incubated on ice for 20 min. Cells were then washed with 1x PBS and fixed for 15 min at RT with 2% PFA in 1x PBS. Cells were washed with PBS/BSA solution, permeabilized with saponin buffer and incubated in this buffer with rat serum and αCD16/αCD32 mAb for 10 min. Intracellular antigen antibody solutions containing αIFN-γ, αTNF-α, αIL-2, and αIL-17 mAb conjugated to different fluorochromes (see materials table) were added and incubated for 20 min on ice. After washing in 1x PBS, cells were re-suspended in 200 µl 1% PFA in 1x PBS and were kept protected from light at 4°C overnight. The next day, cells were washed with PBS/BSA and kept protected from light at 4°C at until analysis by flow cytometry.

3.3.3.4 Fluorescence activated cell sorting (FACS)

Cells were isolated and stained as described in 3.3.1.6 and 3.3.3.1, respectively. Cells were concentrated to 2x 10^7 /ml and passed through a 30-µm MACS® Pre-Separation Filter directly before sorting. Prior to sorting BD FACS tubes used to collect the sorted cells were incubated for 2-3 h with cRPMI to avoid unspecific binding of single cells to the plastic surface and contained 500 µl cRPMI to aid in collecting the sorted cells. Sorting was conducted by members of the FACS facility of the DRFZ/MPIIB, Berlin using a FACSAria™ cell sorter. After sorting, cells were centrifuged at 300x g for 6 min and cell pellets were re-suspended in 300 µl to 500 µl cRPMI and let rest for 2-4 h in a humidified incubator at 37°C and 5% CO_2 before cell counting and further manipulations.

3.3.3.5 *In vitro* B cell stimulation and proliferation assay

Peritoneal B-1a and B-2 B cells from WT and *treml6*$^{-/-}$ mice were stained with αB220 mAb and αCD5 mAb as described in 3.3.3.1 and cells were sorted as B-1a B cells (B220^{dim}CD5^{dim}) and B-2 B cells (B220^{hi}CD5^{lo}) as described in 3.3.3.4.

CFSE staining of sorted B cell populations Sorted cells were re-suspended at a concentration of 1x 10^6 /ml in prewarmed PBS/0.1% BSA. CellTrace™ CFSE (5 mM in dimethyl sulfoxide (DMSO)) was added to a final concentration of 5 µM and samples were vortexed immediately after addition and incubated in a humidified incubator at 37°C, 5% CO_2 for 10 min. The staining was quenched by adding 5 volumes of ice-cold cRPMI and incubation to the cells on ice for 5 min. Cells were pelleted by centrifugation at 300x g for 5 min and washed with cRPMI. Pelleting and washing was repeated two times. Cells were resuspend at 1x 10^6 /ml (B-2 B cells) and 5x 10^5 /ml B-1a B cell cells in cRPMI.

In vitro stimulation of CFSE-labelled B cell populations Triplicates of 1x 10^5 B-2 B cells and 5x 10^4 - 1x 10^5 B-1a B cells from WT and *treml6*$^{-/-}$ mice were cultured for 2.5 days in the presence of a) 10 ng/ml IL-4, b) 10 ng/ml IL-4 and 3 µg/ml αCD40, c) 10 ng/ml IL-4 and 15 µg/ml F(ab')$_2$ fragment goat anti-mouse IgM (F(ab')$_2$αIgM), d) 10 ng/ml IL-4 and 1.5 µg/ml F(ab')$_2$αIgM, e) 10 ng/ml IL-4 and 2 µg/ml LPS, and f) 10 ng/ml IL-4 and 1 µM CpG ODN (Oligodinucleotides containing CpG motifs) and conditions a) to f) without IL-4 supplementation.

Measurement of proliferating CFSE-labeled B cell populations At day 0, CFSE labeling was controlled. After 2.5 days plates were spun down and triplicates re-suspended in 50 µl cold PBS/BSA each. 10 min prior to measurement 2.5 µl 7-amino-actinomycin D (7-AAD) were added and CFSE and 7-AAD intensity were measured on the LSRII.

3.3.3.6 Calcium (Ca^{2+})- Signaling in B-2 and B-1a B cells

Leukocytes from spleen and peritoneal cavity cells were isolated as described in 3.3.1.6, surface-stained with αB220 mAb and αCD5 mAb as described in 3.3.3.1 and 'loaded' with Indo-1. Isolation, staining and loading was conducted at RT. Calcium movement was assessed after stimulation of cells with F(ab')$_2$αIgM. Peritoneal B-1a B cells were gated as B220^{lo}CD5^{dim} and splenic B-2 B cells were gated as B220^{hi}CD5^{lo} cells. Unstained cells were used as a control to exclude the influence of extracellular antibody binding on calcium flux.

Indo- 1 loading of cells All samples were protected from light throughout Indo-1 loading and measurement of cells. Indo-1 staining solution was prepared by adding 1 µl 10% Pluronic F127 and 0.7 µl 1 mM Indo-1 to 200 µl 5% fetal calf serum (FCS)-RPMI, followed by vortexing for 5 sec. Stained and unstained (control) leukocytes from spleen or peritoneal cavity were re-suspended at 2x 10^6 cells in 500 µl 5% FCS-RPMI, 200 µl of Indo-1 staining solution were added, samples were vortexed and incubated at 30°C under mild agitation (~300 rpm) for 25 min. Cells were centrifuged for 5 min at 300x g at RT and washed twice in 800 µl Krebs-Ringer solution + $CaCl_2$. After the final centrifugation, cells were re-suspended in 1 ml Krebs-Ringer solution and kept under mild agitation at 20°C until measurements.

Setting up the flow cytometer Increases in free intracellular calcium in gated B cell populations were measured as changes in ratio of Indo-violet (bound Ca^{2+}) to Indo-blue (unbound Ca^{2+}) signals in real time. Indo-signals were detected with the UV (L3) of the LSRII. Indo-blue peaks at 450-500nm and Indo-violet at 405nm. A violet bandpass filter (BP) centered at 405 +/- 20nm BP and a blue bandpass filter centered at 530 +/- 30nm and 505LP as long bandpass (LP) filter were used, the violet laser was turned off. Light scatter gates were set and photomultiplier tube gain settings were optimized by placing the mean blue fluorescence in the upper half of the histogram channels and the violet fluorescence in the lower half of the histogram channels. Linear amplification was used. The instrument setup and cellular loading was controlled by treating 1x 10^5 Indo-1 loaded cells with ionomycin at 1 µg/ml final concentration. If an immediate response in 100% of cells occurred, loading and set-up were successful. Remaining ionomycin was carefully removed by flushing the lines 2 min with FACS Clean, then 2 min with FACS Rinse and 2 min with dH_2O.

Measurement of Indo-1 loaded samples Samples were acquired at a flow rate of 200-500 events/sec and with linear amplification. First unstimulated samples were measured for 30 sec to determine the baseline, tubes were removed without stopping the acquisition, quickly the stimulating agent (10µg/ml or 1µg/ml $F(ab')_2$ αIgM) was added, samples were vortex and re-placed into the sample injection port for a total of 7 min. Raw data files were transferred to FlowJo software, analyzed and are presented as a median and in comparative overlay analyses using Graph Pad Prism software.

3.3.3.7 Intranuclear BrdU staining

WT and *treml6*$^{-/-}$ mice were fed BrdU as described in 3.3.1.10 and spleen and peritoneal cavity leukocytes isolated as described in 3.3.1.6. Isolated cells were surface stained with B-2, B-1a and B-1b B cell markers as described in 3.3.3.1. Surface stained cell were washed with 1x PBS and fixed for 20 min at RT in 170 µl Cytofix/Cytoperm buffer (BD Pharmingen). Fixed cells were centrifuged, washed with 170 µl BD Perm/Wash buffer, re-suspended in 170 µl BD Cytoperm Plus buffer, and incubated on ice for 10 min. Permeabilized cells were then centrifuged and washed twice with 170 µl Cytofix/Cytoperm buffer and re-suspended in 170 µl Cytofix/Cytoperm buffer and incubated for 5 min at RT. Re-fixed cells were centrifuged, washed with 170 µl 1x BD Perm/Wash buffer and re-suspended in 100 µl of diluted DNase (300µg/ml in 1xPBS) and incubated for 1 h at 37°C. Cells were then washed twice in 1x BD Perm/Wash buffer.

BrdU staining Washed cells were re-suspended in 50 µl 1x BD Perm/Wash buffer containing 1 µl BrdU-APC antibody. Cells were stained for 20 min at RT, centrifuged, washed with 170 µl 1x BD Perm/Wash buffer and re-suspended in 100 µl PBS/BSA. Cells were stored at 4°C until analysis by flow cytometry.

3.3.3.8 Measuring early apoptosis by AnnexinV stain

Leukocytes from spleen and peritoneal cavity cells were isolated as described in 3.3.1.6, surface-stained with αB220 mAb, αCD19 mAb, αCD43 mAb and αCD5 mAb as described in 3.3.3.1. Stained cells were washed twice with cold 1x PBS and resuspended in 1x AnnexinV Binding Buffer (BD) at a concentration of 1x 10^6 cells/ml. Cy^{TM}5 AnnexinV and 7-AAD were added (1:20) and samples incubated at RT for 15 min. Staining was stopped by adding 400 µl 1x AnnexinV Binding Buffer to 100µl sample. Samples were analysed within 1 h by flow cytometry. Viable cells were defined as AnnexinV$^-$ and 7-AAD$^-$, early apoptotic cells were defined as AnnexinV$^+$ and 7-AAD$^-$ and, end stage apoptotic or dead cells as AnnexinV$^+$ and 7-AAD$^+$ cells.

3.3.3.9 Flow cytometric data analysis

Data were exported as FCS 3.0 files and analyzed with FlowJo or as experiments and analyzed with BD FACSDiva software in combination with FACS-Analyser v0.9.9.

3.3.4 Cell culture

3.3.4.1 Cell culture of stromal cell lines and preB-I B cells

Cell culture of stromal cell lines The adherent stromal cell line Puromycine-Hygromycine-resistant OP9 cells (OP9-PH) were cultured in minimum essential medium (MEM) alpha medium supplemented with 2% FCS in a humidified incubator at 37°C, 10% CO_2. The stromal cell lines were passaged every 3-4 days after reaching a density of approximately 1,6x 10^6 cells/145 cm^2 dish, with 10 ml trypsin/ethylenediaminetetraacetic acid (EDTA) (0.5%) per dish to detach the cells from the plastic (5-10 min incubation at 37°C). OP9-PH cells were replated at 1x 10^5 cells/75 cm^2-flask for the co-culture with lymphocyte progenitors and at 1-2x 10^5 cells/145 cm^2-dish for the maintenance of the stromal cell lines. After three to four days of culture at 37°C, 10% CO_2, in 75 cm^2 flasks the semi-confluent stromal cell layer could be γ-irradiated with 3000 rad, which prevents further cell division during co-culture with pre-B I cells.

Cell culture of stromal cell/IL-7 dependent pre-B cell lines Fetal liver derived Pre-B I cells were grown on a 70%-80% confluent layer of 3000 rad γ-irradiated stromal cells in Iscove's modified Dulbecco's medium (IMDM)-based SF medium supplemented with 2% FCS. Additionally the medium contained about 50-100 U/ml mouse recombinant (r)IL-7 which was added as a culture supernatant from IL-7 cDNA transfected J558L cells (a kind gift from Szandor Simmons). Pre-B I cells were removed from the adherent stromal cell layer by gentle clapping of tissue culture flasks with a flat palm or by aspirating the medium several times up and down. The pre-B I cell cultures were removed every 3-4 days and replated on a new 3000 rad γ-irradiated stromal cell layer with 2-5x1 0^5 cells/T75 flasks depending on the growth behaviour of each cell line.

Establishment of pre-B cell lines Cell suspensions from fetal liver (day 18 of gestation) of WT or *treml6*$^{-/-}$ mice were plated as mass cultures on a semi-confluent layer of γ-irradiated (3000 rad) OP9 stromal cells in the presence of IL-7. The IL-7-containing medium consisted of IMDM supplemented with 2% fetal calf serum, 0.03% (wt/vol) primatone RL, 50 µM 2-mercaptoethanol, 1 mM glutamine, and 1% conditioned supernatant of rIL-7-producing J558L cells. After 1 week of *in vitro* culture, the growing pre-B I cells were further propagated as polyclonal or clonal cell lines.

Freezing and thawing of tissue culture cells Cells which were intended for storage were re-suspended in freezing medium (90% FCS, 10% DMSO) at a density of about 2-5x 10^6 cells/ml. Aliquots of 1 ml were transferred into 1.5 ml freezing vials and were frozen slowly in styrofoam boxes at -80°C (approximate cooldown -1°C/min) for at least 24 h before transferring them into a liquid nitrogen storage tank. Thawing of frozen cells was accomplished by incubating the vials in a 37°C water bath. The cell suspension was immediately diluted in 10 ml medium and washed once to remove traces of DMSO. Thereafter, cells were transferred into appropriate culture medium and grown in a humidified CO_2-incubator at 37°C, with 5% or 10% CO_2.

3.3.5 Enzyme-linked immuno sorbent assay (ELISA) and Multiplex analysis

3.3.5.1 TNP-specific ELISA

To detect TNP-specific antibodies 96-well Nunc Maxisorb plates were coated in a humid chamber either 2 h at 37°C or overnight at 4°C with 50µl 10 µg/ml TNP-BSA coating solution. Plates were then blocked with 200µl ELISA blocking solution and incubated in a humid chamber either for 2 h at 37°C or overnight at 4°C. Plates were washed 3 times with 1x PBS. Meanwhile sera dilutions were prepared in ELISA dilution buffer. Starting dilution was 1:20, the following dilutions were prepared as 1:3 dilutions from the previous, 8 dilutions were made from 1 serum. As standard, pooled sera from day 8 were used. The same samples were used as standard on all analyzed plates to allow comparison. 50µl of serum dilution were added per well and incubated in a humid chamber either for 2 h at 37°C or overnight at 4°C. Plates were washed 3-times with 1x PBS. IgG3-alkaline phosphatase (AP) and IgM-AP antibodies were diluted 1:1000 in ELISA dilution buffer, 50µl were added to each well and plates were incubated in a humid chamber either for 2 h at 37°C or overnight at 4°C. Plates were washed 3-times with 1x PBS. 100µl of 1mg/ml p-Nitrophenylphosphate substrate in Tris buffer (Sigma) were added to each well and OD was measured at 405nm on an ELISA reader. Standard curves were plotted on a semilogarithmic scale, and arbitrary concentrations of samples were determined.

3.3.5.2 Multiplex analysis of antibody isotypes in sera

Antibody isotype composition in naïve WT and *treml6*$^{-/-}$ mice was determined with the Millipore Mouse Immunoglobulin Isotyping Kit, according to the manufacturer`s instructions.

4 RESULTS

4.1 Generation and immunological analysis of *treml6* deficient mice

TREM and TLT proteins form a novel surface receptor family of NON-TLR innate immune receptors. Members of this family are thought to be either of activating (DAP12/ITAM)) or inhibitory (ITIM) nature and participate in various cell processes (10-12). We were interested in putative inhibitory regulators of inflammation. In 2003 one inhibitory ITIM carrying receptor was predicted within the family and named *treml1* (TLT-1), a second unnamed receptor (RIKEN cDNA B430306N03 gene) was also predicted to be of inhibitory nature (10). In 2009, it was named *treml6* and its cytoplasmic ITIM motif was described (12, 19).

4.1.1 *Treml6* protein product TLT-6 is a predicted ITIM-carrying receptor

Until today, *treml6* protein (TLT-6) existence is only evidenced by mRNA expression. In order to obtain deeper insights into the putative structure of TLT-6, we first performed *in silico* analyses (Fig. 7A). Different programs and databases predicted a) a signal peptide at amino acid (aa)-position 1-23 (Program Signal P), b) an extracellular region at aa-position 1-154, c) transmembrane helices at aa-position 155-177, d) an intracellular tail at aa-position 178-289 (b to d TMHMM v2.0 software), and e) an Immunoglobulin domain (position 26-122) (SMART domain database) or f) a V-set domain at aa-position 20-122 (Pfam 24.0). ScanProsite software was used to scan the C-terminal intracellular domain for canonical (…[ILV]-x-Y-x-x-[LV]…) and non-canonical/permissive (…[ILVST]-x-Y-x-x-[VLI]…) ITIM motifs (13) and identified one canonical at aa-position 222-227 and one non-canonical at aa-position 257-262 (Fig. 7A). We next performed a protein blast on the C-terminal part to identify potential orthologs in other species and analyzed whether the previously predicted ITIM motifs are conserved. Proteins from *Equus cabalus* (XP_001496610), *Canis lupus familiaris* (XP_851243 similar to triggering receptor expressed on myeloid cells-like 4), and *Gallus gallus* (NP_001074339 triggering receptor expressed on myeloid cells-like 2 and NP_001074337 triggering receptor expressed on myeloid cells) showed high sequence similarity. Amino acid sequences of these proteins and TREML6 were aligned using the CLUSTAL multiple sequence alignment program and the boxshade program. Both ITIM motifs were conserved in all analyzed proteins (Fig. 7B).

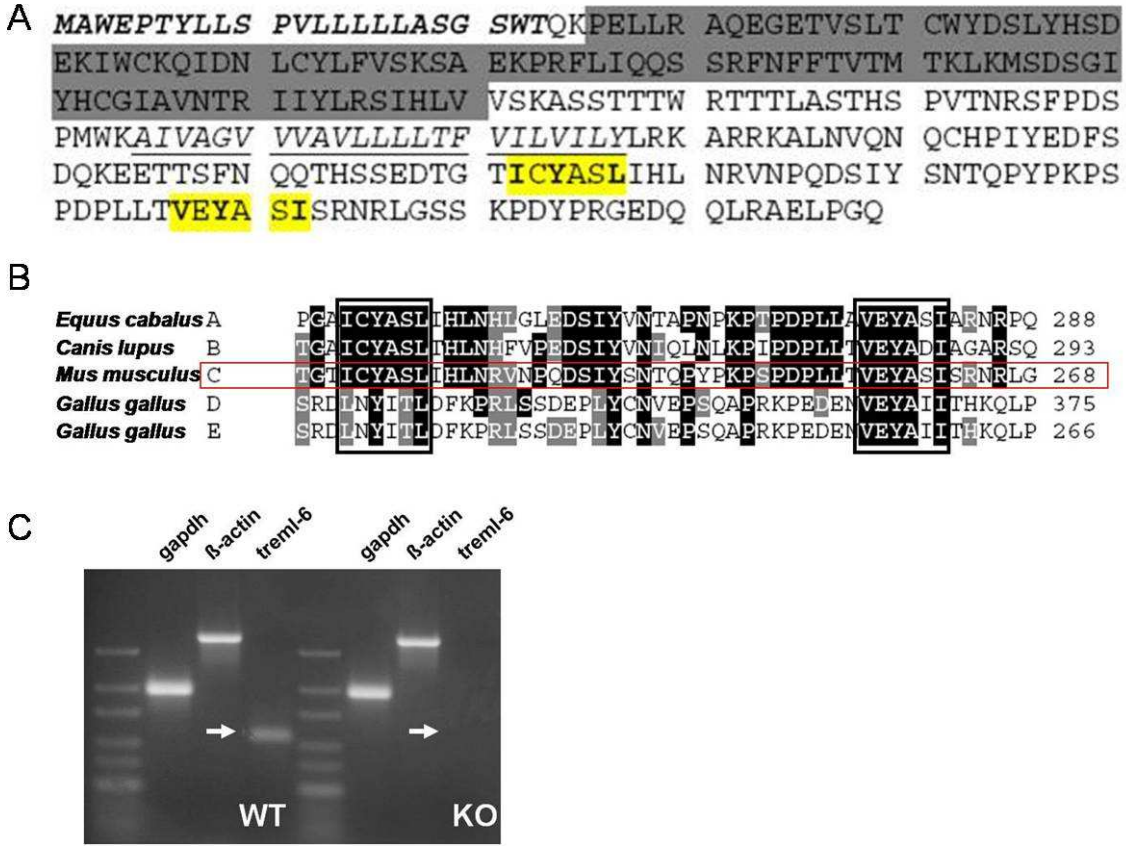

FIGURE 7. ***In silico*** **analysis of putative TLT6 protein structure.** ***A,*** Predicted amino acid sequence of *treml6*. Italics, predicted signal peptide sequence; grey-boxes, predicted V-set Ig domain; underlines, predicted transmembrane helix; yellow boxes and bold, ITIM motifs. ***B,*** Blast and alignment of C-terminal parts revealed conserved ITIM motifs (boxed). ***C,*** RT-PCR (gapdh, β-actin, and *treml6* EEJ5 primers) on WT (WT) and *treml6*$^{-/-}$ (KO) BM cells.

In silico analysis suggested TLT6 to be a functional receptor (13, 157), with a signal peptide, an extracellular V-set immunoglobulin-domain, a transmembrane region and an intracellular tail, potentially transmitting inhibitory signals via two conserved ITIM motifs. In order to investigate the biological function of TLT6, *treml6* gene deficient mice were generated by Dr. Mischo Kursar as described in 3.3.1.2. The gene targeting strategy is depicted in Fig. 6A. RT-PCR on WT and *treml6*$^{-/-}$ BM cells showed no presence of *treml6* mRNA in *treml6*$^{-/-}$ mice (Fig. 7C) and confirmed successful deletion of *treml6*.

4.1.2 *Treml6* mRNA expression pattern and initial immunological characterization of *treml6* deficient mice

Treml6$^{-/-}$ mice were viable and fertile and showed no abnormalities or growth retardation. As initial step, we studied consequences of *treml6* deficiency on immune cell composition in different organs.

TABLE 1: Absolute cell numbers

Absolute numbers of different immune cell populations in various organs of WT and *treml6*$^{-/-}$ mice. Leukocytes were isolated from depicted organs and cell subsets phenotyped by flow cytometry. Cell numbers were calculated from frequencies among total leukocytes. Results are means of 2 independent experiments with 3 mice per group and experiment. Plus-minus indicates the standard errors of the mean. Significance was calculated with Student's t test ($p>0.05$ non-significant).

	wild-type	treml-6 $^{-/-}$
thymus		
CD4$^+$ T cells	4.22±0.92	3.59±0.41
CD8$^+$ T cells	1.97±0.53	1.92±0.2
DP T cells (CD4$^+$CD8$^+$)	64.79±13.57	63.56±6.24
B cells (B220$^+$)	0.59±0.16	0.81±0.14
Dendritic cells (CD11c$^+$)	0.09±0.02	0.08±0.02
Macrophages (CD11b$^+$)	0.15±0.03	0.13±0.02
mesenteric lymph nodes		
CD4$^+$ T cells	1.92±0.35	1.92±0.43
CD8$^+$ T cells	1.3±0.26	1.3±0.29
B cells (B220$^+$)	1.88±0.35	1.74±0.4
Dendritic cells (CD11c$^+$)	0.04±0.01	0.04±0.01
Macrophages (CD11b$^+$)	0.04±0.01	0.04±0.01
spleen		
CD4$^+$ T cells	8.77±0.81	8.69±0.65
CD8$^+$ T cells	4.98±0.55	5.32±0.39
B cells (B220$^+$)	34.78±4	33.05±1.3
Dendritic cells (CD11c$^+$)	1.09±0.11	1.09±0.21
Macrophages (CD11b$^+$)	4.82±0.96	3.71±0.3
bone marrow		
CD4$^+$ T cells	0.46±0.07	0.29±0.03
CD8$^+$ T cells	0.33±0.06	0.31±0.04
B cells (B220$^+$)	11.39±1.54	9.84±1.06
Dendritic cells (CD11c$^+$)	0.22±0.06	0.15±0.02
Macrophages (CD11b$^+$)	27.97±8.26	24.05±3.5
peritoneal cavity		
CD4$^+$ T cells	0.29±0.06	0.24±0.04
CD8$^+$ T cells	0.1±0.02	0.08±0.02
B cells (B220$^+$)	0.95±0.14	1.03±0.21
Dendritic cells (CD11c$^+$)	0.08±0.03	0.08±0.01
Macrophages (CD11b$^+$)	0.18±0.04	0.19±0.05

We isolated leukocytes from thymi, MLN, spleens, BM and peritoneal cavities and stained for T cell (CD4 and CD8), B cell (B220), DCs (CD11c) and macrophage (CD11b) surface markers. Flow

cytometric analysis revealed no significant differences in frequencies (data not shown) or numbers of $CD4^+$ T cells, $CD8^+$ T cells, DP ($CD4^+CD8^+$) T cells, B cells, DCs and macrophages between the analyzed tissues of WT and *treml6*$^{-/-}$ mice (Tab. 1).

In parallel to flow cytometric analysis of treml6$^{-/-}$ mice, we measured the expression pattern of *treml6* mRNA in various tissues and cell subsets of C57BL/6. To this end, we performed RT-PCR on housekeeping-genes (*gapdh* and *β-actin*) and *treml6*. *Treml6* mRNA expression in organs or cells was normalized to expression of *gapdh* and *β-actin* and fold differences were calculated relative to a virtual tissue/cell (gapdh and β-actin c_t: 12; treml6 c_t: 30). *Treml6* mRNA expression was found preferentially in immune-related organs such as fetal liver, BM, spleen, and MLN, but also in peritoneal cavities (Fig. 8A). We further analyzed FACS-sorted cell subsets from peritoneal cavities, spleen and BM and found broad *treml6* mRNA expression in all analyzed leukocytes (Fig. 8B). Only in leukocytes from BM, (B cells ($CD19^+$), NK cells ($NK1.1^+$), and myeloid cells ($CD11b^+$)), *treml6* mRNA expression was higher (~$2^{(12\text{-}14)}$) than general *treml6* mRNA expression in the corresponding organ (BM (~$2^{(10)}$)) (Fig. 8A and 8B).

4.1.3 Lack of *treml6* reduces numbers of B-1 B cell precursors in BM and fetal liver

In adult mice, the BM is the origin of all circulating blood cells. Moreover, it is the site of B cell maturation (158). Since our initial broad immunological analysis did not reveal any differences in composition and numbers of BM leukocyte populations (Tab. 1), we decided to study B cell development in more detail.

We did not detect differences in frequencies (data not shown) or absolute numbers of pro-B ($B220^+CD19^-$c-Kit^+CD25^-), pre-B1 ($B220^+CD19^+$c-$Kit^{dim}CD25^-$), pre-B2 ($B220^+CD19^+$c-Kit^-CD25^+), immature ($CD19^+IgM(\mu\text{-chain})^+$kappa-light-$chain^+IgD^-$) and mature B cells ($CD19^+IgM(\mu$ $chain)^+$kappa-light-$chain^+IgD^+$) between BM of WT and *treml6*$^{-/-}$ mice according to Melchers-Rolink definition of B cell developmental stages (87) (Fig. 8C), indicating normal B cell maturation in *treml6*$^{-/-}$ mice. In contrast, frequencies and numbers of a newly described B-1P ($B220^-CD19^+$) (118) were reduced by half in *treml6*$^{-/-}$ mice (Fig. 8D and 8E). B-1 B cells represent a B cell subset that differs from conventional B cells (namely B-2 B cells) by phenotype, anatomic location, and immunological function. During embryonic development, B-1 B cells are the main B cell population produced in the fetal liver (116).

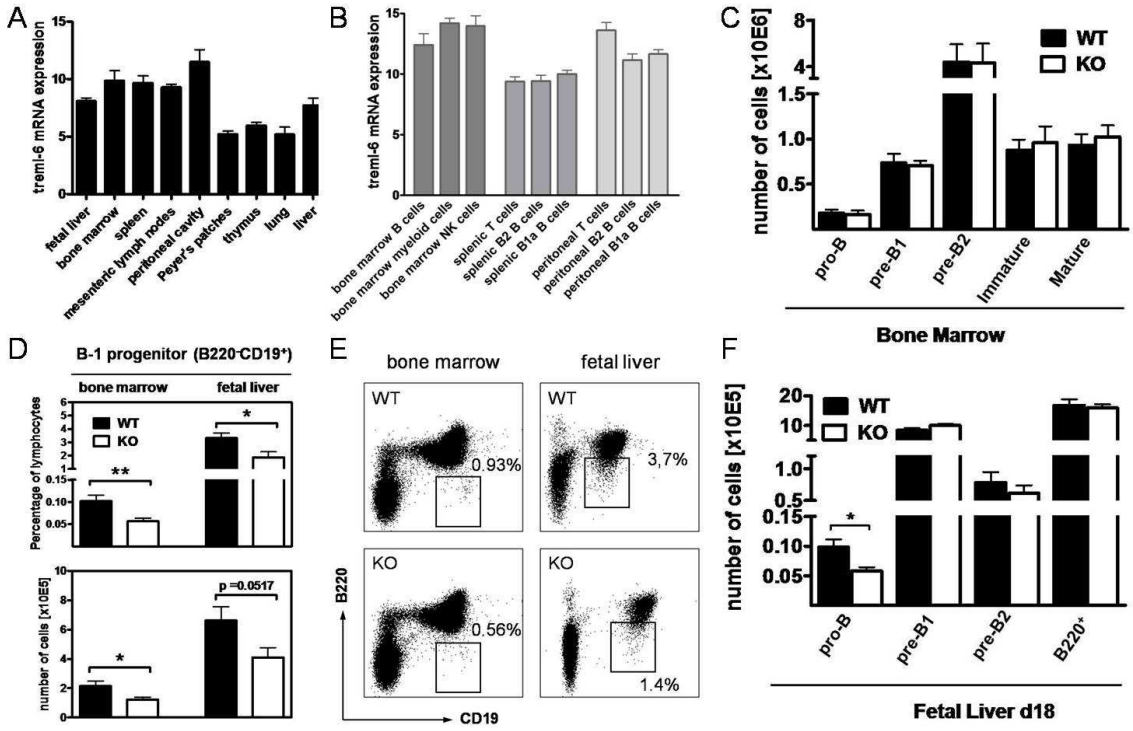

FIGURE 8. ***Treml6*** **mRNA expression in WT mice and B cell development in** ***treml6***$^{-/-}$ **mice.** ***A,*** Relative levels of *treml6* mRNA expression in indicated tissues ***B,*** relative *treml6* mRNA expression in B cells, myeloid cells and NK cells in BM and T and B cells from spleens and peritoneal cavities. WT cells were sorted by FACS (B cells (BM): CD19^{+}; myeloid cells (CD11b^{+}); NK cells (NK1.1^{+}); T cells: CD5^{hi}B220^{-}; B-2 B cells: CD5^{-}B220^{+}; B-1a B cells: CD5^{dim}B220$^{-/dim}$). Relative mRNA quantification was performed by real-time RT-PCR using primers for *gapdh* and *β-actin* as internal controls and intron-spanning *treml6* specific primers (EEJ5) for quantification. *Treml6* mRNA levels in C57BL/6 mice are represented as fold differences (log2) relative to virtual values (gapdh/β-actin c_t: 12; treml6 c_t: 30). Error-bars represent standard error of triplicates. One representative experiment of at least two is shown. ***C,*** Numbers of B cell precursor cells in BM of WT and *treml6*$^{-/-}$ (KO) mice and ***D,*** Frequencies and numbers of B-1 B cell progenitors in BM and fetal liver of WT and *treml6*$^{-/-}$ (KO) mice. ***E,*** Dot blots show FSC/SSC gated lymphocytes and demonstrate gating of B-1 B cell progenitors in BM and fetal liver of WT and *treml6*$^{-/-}$ (KO) mice. ***E,*** Numbers of B cell precursor cells in fetal livers of WT and *treml6*$^{-/-}$ (KO) mice. Leukocytes were isolated from depicted organs and cell subsets phenotyped by flow cytometry. Cell numbers were calculated from frequencies among total leukocytes. Results are means of at least 2 independent experiments with 5 mice or more per group and experiment. Error-bars represent the standard errors of the mean. Significant differences between 2 groups are indicated by asterisks (Student's *t* test: *, $p < 0.05$, **, $p < 0.01$ and ***, $p < 0.001$).

Therefore, we extended our studies on B cell development to fetal livers (day 18 of gestation). As in BM, we found B-1P to be reduced in fetal livers of *treml6*$^{-/-}$ mice (Fig. 8D and 8E). Moreover, in fetal livers of *treml6*$^{-/-}$ mice, numbers of pro-B cells were reduced by half, while numbers of pre-B1, pre-B2, or total B220^{+} B cells were similar to WT numbers (Fig. 8F).

4.1.4 *Treml6* deficiency results in B cell subset changes in peritoneal cavities

Since our data pointed to a defect in B-1 B cell development in *treml6*$^{-/-}$ mice, we next analyzed whether B-1 B cells occur at normal rate in peripheral organs of adult mice. The B-1 B cell population is mainly present in pleural and peritoneal cavities, but can also be found at lower frequencies in the spleen (94). Conventional B-2 B cells express CD19 and B220, while B-1 B cells are CD19^{+}B220$^{dim/-}$, and can be sub-divided further into B-1a B cells expressing CD5 and CD43 and into B-1b B cells which are CD5 negative, but CD43^{+} ((94) and Fig. 9A). Frequencies of B-1a B cells - among peritoneal lymphocytes - were reduced by 50% in 9-11 week old *treml6*$^{-/-}$ mice compared to WT controls and frequencies of B-2 B cells were increased by a factor of 1.3. Similar differences were observed in numbers of peritoneal B-1a and B-2 B cells. In contrast, no differences in frequencies and numbers of peritoneal B-1b, splenic B-2, and splenic B-1a B cell populations could be detected between WT and *treml6*$^{-/-}$ mice (Fig. 9B). We also analyzed other splenic B cell populations and found no differences in immature or mature, namely FO and MZ B cell populations (data not shown).

B-1 B cells are the prominent B cell subset in neonatal mice, and remain as a self-renewing population in peritoneal cavities of adult mice (100). To address the issue of whether the defect in peritoneal B-1a B cells appears already early in life or whether the population is lost over age, we performed a kinetic analysis on B-1a and B-2 B cells in peritoneal cavities and spleens (data not shown) of WT and *treml6*$^{-/-}$ mice. *Treml6*$^{-/-}$ mice showed reduced frequencies and numbers of peritoneal B-1a B cells at the age of 4-5 weeks, B-2 B cell frequencies and numbers were increased from the age of 7-8 weeks. At the age of 17-23 weeks these differences in B-1a and B-2 B cells almost normalized to WT levels, at least in terms of numbers (Fig. 9C). In spleens no differences were detected (data not shown).

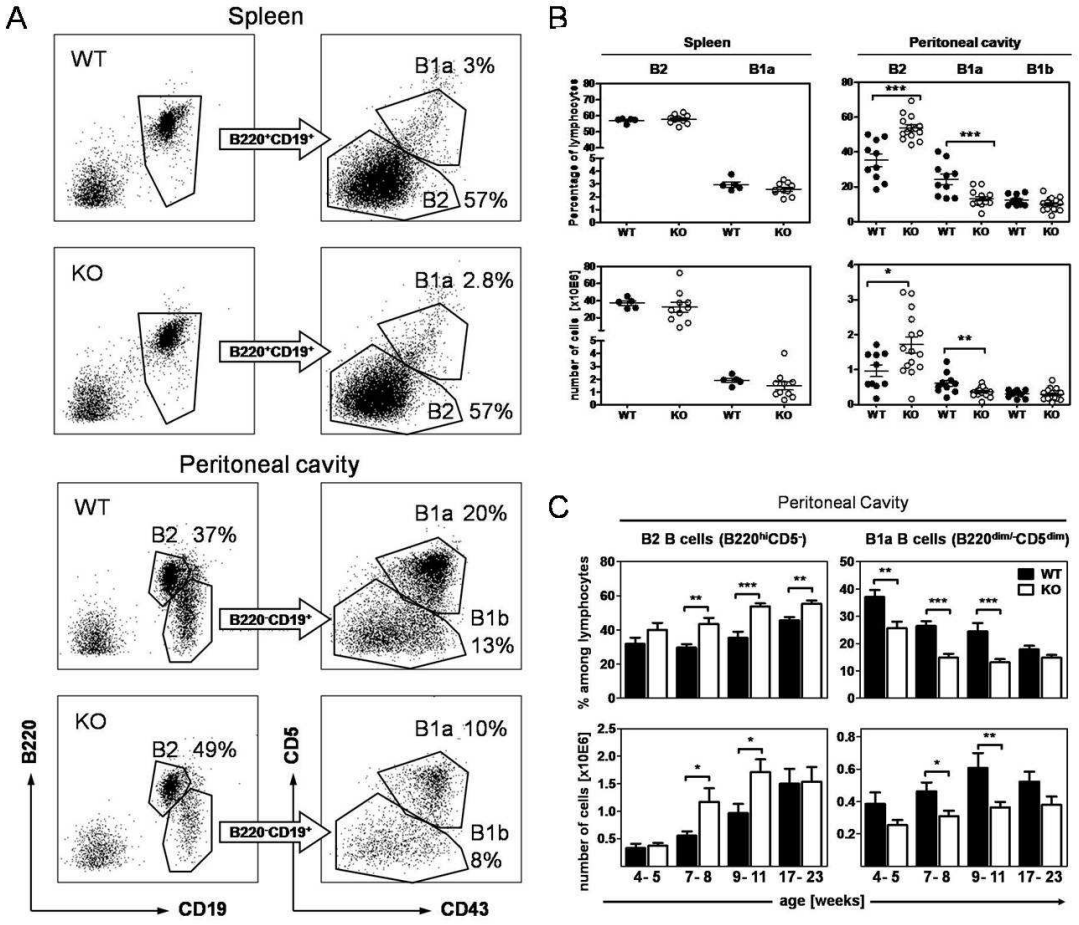

FIGURE 9. **Age dependent impact of *treml6* deficiency on B-2 and B-1a B cell populations**. ***A,*** Dot blots represent B cell staining and gating of isolated leukocytes from spleens and peritoneal cavities. Left dot blots show FSC/SSC gated lymphocytes. ***B,*** Frequencies and numbers of B-2 and B-1a B cells in spleen and B-2, B-1a and B-1b B cells in peritoneal cavities of 9 to 11-weeks old WT and *treml6*$^{-/-}$ (KO) mice. ***C,*** Frequencies and numbers of B-2 and B-1a B cells in peritoneal cavities of 4-5 weeks, 7-8 weeks, 9-11 weeks, and 17-23 weeks old mice. Leukocytes were isolated from depicted organs and cell subsets phenotyped by flow cytometry. Cell numbers were calculated from frequencies among total leukocytes. Results are means of at least 2 independent experiments with a minimum of 5 mice per group and experiment. Error-bars represent the standard errors of the mean. Significant differences between 2 groups are indicated by asterisks (Student's *t* test: *, $p < 0.05$,**, $p < 0.01$ and ***, $p < 0.001$).

4.1.5 Functional analysis of B-2 and B-1a B cells from *treml6* deficient mice

To characterize the functional properties of peripheral *treml6*$^{-/-}$ B-2 and B-1a B cells and to find further indications explaining the observed paucity in peritoneal B-1a B cells, we analyzed their proliferation capacity, their ability to mount BCR-triggered Ca^{2+} responses, their viability status, and their homing capacities.

4.1.5.1 IL-4 evoked *in vitro* proliferation is enhanced in *treml6* deficient mice

In contrast to conventional B-2 B cells which are generated throughout life in the BM, B-1 B cells are thought to be self-renewing once they reside in pleural or peritoneal cavities (100). To analyze their turnover, WT and *treml6*$^{-/-}$ mice were fed BrdU via the drinking water for a period of 12 days. At days 4, 8 and 12 the amount of incorporated BrdU was measured in B-2 and B-1a B cell populations and served as indicator of proliferation. Both, splenic B-1a and B-2 B cells from *treml6*$^{-/-}$ mice showed higher turnover rates compared to their WT counterparts after 12 days of BrdU treatment. In peritoneal cavities of *treml6*$^{-/-}$ mice B-2 B cells showed significantly reduced turnover at day 8 compared to WT B-2 B cells. In contrast, more BrdU was incorporated by peritoneal B-1a B cells of *treml6*$^{-/-}$ mice than by WT B-1a B cells. Notably, peritoneal B cells showed strong differences in BrdU incorporation between single mice of one group, impeding the interpretation of results (Fig. 10A).

Next, we sorted WT and *treml6*$^{-/-}$ peritoneal B-2 and B-1a B cells by FACS to investigate their ability to proliferate *in vitro* upon various stimuli. We observed no major differences in proliferation of peritoneal B-2 B cells of WT or *treml6*$^{-/-}$ mice. Although differences in basal proliferation and proliferation upon stimulation with 15µg/ml F(ab')$_2$αIgM and CpG were statistically significant, they were rather minor in actual numbers (e.g. WT B-2 B cells + CpG: 93%; *treml6*$^{-/-}$ B-2 B cells + CpG: 95%).

Generally, stimulated B-2 B cells from WT or *treml6*$^{-/-}$ mice proliferated stronger than B-1a B cells, except when stimulated with IL-4. Addition of IL-4 did not increase the proliferation of WT or *treml6*$^{-/-}$ B-2 B cells; however it did for B-1a B cells. The effect of IL-4 on B-1a B cells differed in strength between WT and *treml6*$^{-/-}$ cells. Compared to WT, *treml6*$^{-/-}$ peritoneal B-1a B cells proliferated significantly stronger in the presence of IL-4 (WT B-1a: 19%; *treml6*$^{-/-}$ B-1a: 31%). Moreover, increased proliferative stimulation by IL-4 on *treml6*$^{-/-}$ B-1a B cells remained in the presence of αCD40 and F(ab')$_2$αIgM stimulation, while LPS or CpG treatment outweighed the IL-4-dependent effect on *treml6*$^{-/-}$ B-1a B cells. Notably, *treml6*$^{-/-}$ B-1a like *treml6*$^{-/-}$ B-2 B cells showed stronger basal proliferation than their corresponding WT cells (Fig. 10B).

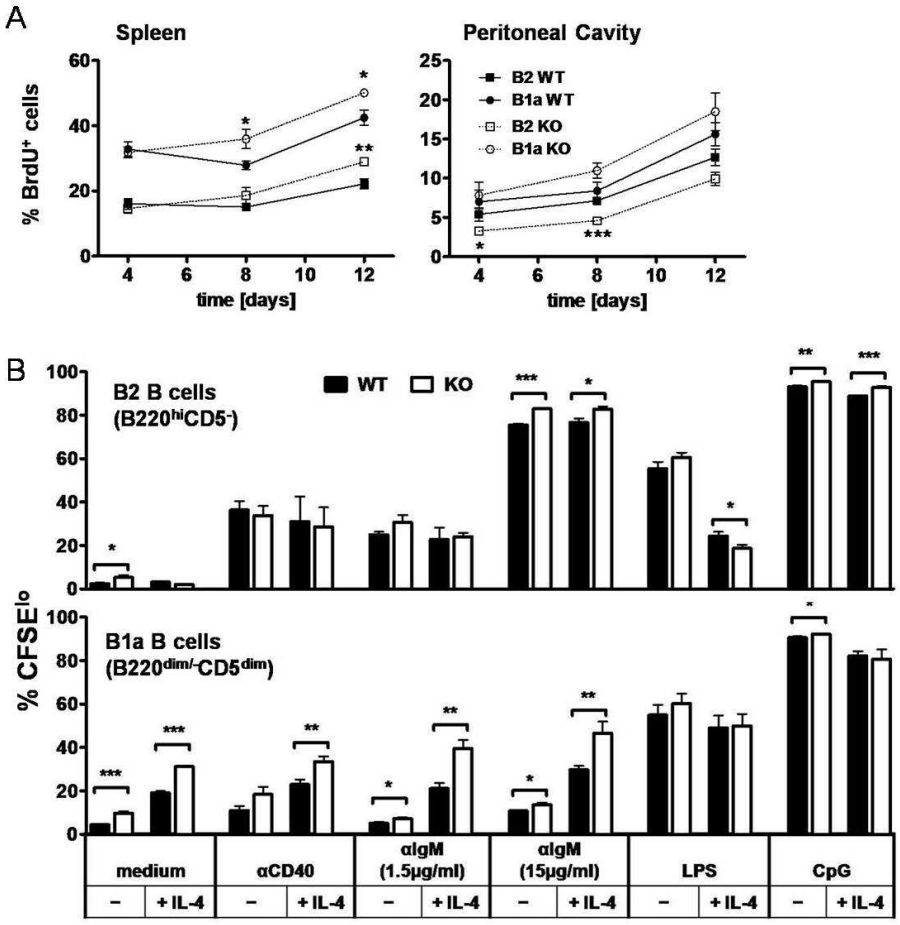

FIGURE 10. *Treml6*$^{-/-}$ B-1a B cells show enhanced homeostatic and IL-4 driven proliferation. ***A,*** Homeostatic proliferation of B-2 and B-1a B cells in spleens and peritoneal cavities of naïve WT and *treml6*$^{-/-}$ (KO) mice measured by BrdU incorporation. Mice received BrdU drinking water for 12 days. Results are means of two independent experiments with 4 mice per group and experiment. Error-bars represent the standard errors of the mean. ***B,*** *In vitro* proliferation of peritoneal B-2 and B-1a B cells from WT and *treml6*$^{-/-}$ (KO) mice. WT and *treml6*$^{-/-}$ (KO) B-2 (B220^{+}CD5^{-}) and B-1a B cells (B220^{dim}CD5^{dim}) from peritoneal cavities (pool of 7-10 mice per group) were sorted by FACS, stained with CFSE and incubated with different stimuli for 2.5 days. CFSE dilution was measured by flow cytometry; dead cells were excluded by 7-AAD staining. Results show mean values of two independent experiments each performed in triplicate. Error bars represent the standard error of mean. Significant differences between 2 groups are indicated by asterisks (Student's *t* test: *, $p < 0.05$, **, $p < 0.01$ and ***, $p < 0.001$).

4.1.5.2 BCR-dependent Calcium-signaling is not affected by the lack of *treml6*

Since F(ab')$_2$αIgM (15µg/ml) induced proliferation was marginally stronger in both peritoneal B-2 and B-1a B cells (w/o IL-4), we hypothesized that BCR-dependent calcium-signaling could be enhanced in *treml6*$^{-/-}$ mice. Therefore, we isolated leukocytes from spleens and peritoneal cavities, stained them with B-2 and B-1a B cell specific markers, and loaded them with indo-1. We measured Calcium-signaling as increases in free intracellular calcium in gated B cell populations as changes in ratio of Indo-violet (bound Ca^{2+}) to Indo-blue (unbound Ca^{2+}) signals

in real time. However, calcium responses to stimulation with high (10µg/ml) or low dose (1µg/ml) $F(ab')_2$αIgM by splenic B-2 B cells, peritoneal B-2 or B-1a B cells were identical for WT and *treml6*$^{-/-}$ B cells (Fig. 11A). Thus, *treml6* is dispensable for BCR-dependent Ca^{2+} signaling.

4.1.5.3 Impact of *treml6* deficiency on B cell maintenance and homing capacities

Reduced peritoneal B-1a B cells in *treml6*$^{-/-}$ mice might as well be a consequence of increased apoptosis or of impaired homing to peritoneal cavities.

Therefore, we measured frequencies of early apoptotic cells (AnnexinV^{+}7-AAD^{-}) within splenic and peritoneal B-2 and B-1a B cell populations and did not detect differences between WT and *treml6*$^{-/-}$ cell populations, indicating similar fitness of cells (Fig. 11B).

To investigate the homing capacities of B-2 and B-1a B cells in *treml6*$^{-/-}$ mice, we isolated RNA from BM, spleen, and peritoneal cavity and from FACS-sorted splenic and peritoneal T (B220^{-} CD5^{+}), B-2 B (B220^{hi}CD5^{-}) and B-1a B (B220$^{dim/-}$CD5^{dim}) cells, as well as from *in vitro* generated pre-B I cells. We then performed RT-PCRs specific for *cxcl13*, *cxcr5* and *ccr7* on transcribed cDNAs from these tissues and cells.The homeostatic chemokine, chemokine (C-X-C motif) ligand 13 (CXCL13) and its receptor CXCR5, as well as chemokine (C-C motif) receptor 7 (CCR7) are important for B-1 B cell homing to peritoneal cavities (159, 160). Moreover, CCR7 drives re-circulation of B-2 B cells after peritoneal passage (160). We detected no considerable differences in *cxcl13* mRNA expression between WT and *treml6*$^{-/-}$ tissues (Fig. 11C). *Cxcr5* mRNA expression did also not differ between WT and *treml6*$^{-/-}$ T, B-2 and B-1a B cells from spleen and peritoneal cavities, indicating that mature cells are able to home to the peritoneum. In contrast, *in vitro* generated *treml6*$^{-/-}$ pre-B I cells showed a 4-fold reduction in *cxcr5* mRNA compared to WT (Fig. 11D).

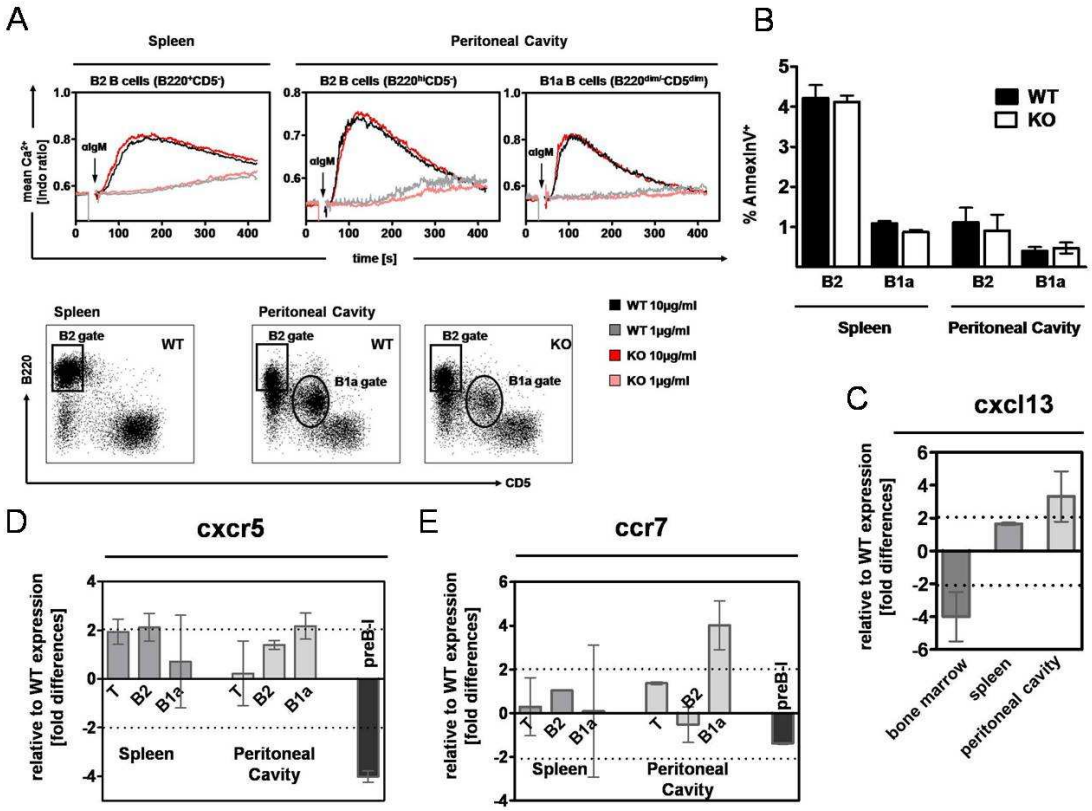

FIGURE 11. BCR-dependent Ca^{2+}-signaling in B-2 and B-1a B cells from WT and *treml6*$^{-/-}$ mice. ***A,*** Leukocytes from spleen and peritoneal cavities were isolated, surface stained for B220 and CD5 and, loaded with indo-1. Increases in free intracellular calcium in gated B cell populations were measured as changes in ratio of Indo-violet to Indo-blue signals in real time. Cells were stimulated with 10 µg/ml or 1 µg/ml $F(ab')_2$ αIgM. Results are representative for two independent experiments and show pooled graphs of 3 independent mice per group and experiment. ***B,*** Leukocytes from spleen and peritoneal cavities were isolated, surface stained for B220, CD19, CD43 and CD5, followed by AnnexinV and 7-AAD staining. Early apoptotic cells were defined as AnnexinV$^+$7-AAD$^-$. ***C,*** Fold differences of *cxcl13* mRNA expression in indicated tissues of *treml6*$^{-/-}$ (KO) mice relative to WT and ***D,*** Fold differences of *cxcr5* mRNA expression and ***E,*** Fold differences of *ccr7* mRNA expression in T and B cells from spleens and peritoneal cavities of *treml6*$^{-/-}$ mice relative to WT. ***D/E,*** WT and *treml6*$^{-/-}$ cells were sorted by FACS. ***C/D/E,*** Relative mRNA quantification was performed by real-time RT-PCR. Real-time PCR was performed using primers for *gapdh* and *β-actin* simultaneously as controls and intron spanning gene (*cxcl13*, *cxcr5*, and *ccr7*) specific primers for quantification. Dotted lines mark borders of 2-fold changes. Means of at least two experiments (each mean of triplicates) are shown. Error-bars represent standard error of means.

Ccr7 mRNA expression did not differ between WT and *treml6*$^{-/-}$ T cells and B-2 B cells. However, *treml6*$^{-/-}$ B-1a B cells showed a 4-fold up-regulation of *ccr7* mRNA compared to WT cells (Fig. 11E). In order to determine if the reduction of *ccr7* mRNA expression in *treml6*$^{-/-}$ B-1a B cells translates into higher protein expression of CCR7 receptor, we stained B-1a B cells with αCCR7 mAbs and analyzed them by means of flow cytometry. In contrast to mRNA expression, we observed no significant differences in surface CCR7 expression by WT and *treml6*$^{-/-}$ B-1a B cells. Conclusively, the upregulation of *ccr7* mRNA did not translate into measurable higher levels of receptor expression (data not shown).

4.1.6 Immune responses of WT and *treml6*$^{-/-}$ mice to TI-2 antigens

A hallmark of B cells is their ability to secrete antibodies; B-1 and MZ B cells are the mayor producers of natural antibodies, such as IgM and IgG3 (100). It is possible that changes in B-2:B-1a B cell ratios observed in *treml6*$^{-/-}$ mice, lead to differences in serum immunoglobulin levels. Therefore, we measured the amount of serum immunoglobulins in naïve WT and *treml6*$^{-/-}$ mice over age by multiplex analysis. At 9 to 10 weeks of age no differences in IgG1, IgG2b, IgG3, and IgM serum antibodies were detected between WT and *treml6*$^{-/-}$ mice. In between 12 to 20 weeks of age, *treml6*$^{-/-}$ mice showed a small, but significant reduction in IgM serum antibodies (Fig. 12A) compared to WT mice. IgG1, IgG2b, and IgG3 serum levels were identical between older (12-20 weeks) WT and *treml6*$^{-/-}$ mice (data not shown).

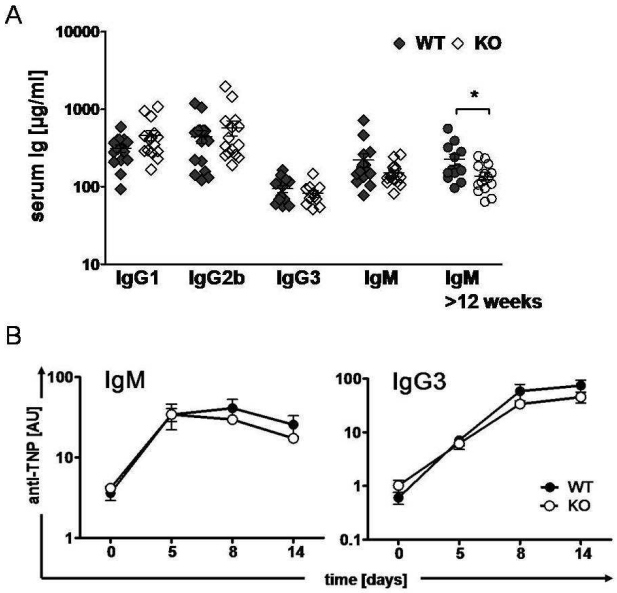

FIGURE 12. Lower IgM titers in aged *treml6*$^{-/-}$ mice and TI-2 immune responses.
A, Multiplex analysis of serum titers of immunoglobulins (Serum Ig) in 9-10 weeks old WT and *treml6*$^{-/-}$ (KO) mice and IgM titers in 12-20 weeks old WT and *treml6*$^{-/-}$ (KO) mice. Each symbol represents one mouse. Significant differences between 2 groups are indicated by asterisks (Mann-Whitney U test: *, $p < 0.05$). ***B,*** Immune responses of WT and *treml6*$^{-/-}$ (KO) mice after TI-2 immunization. Mice were immunized with 10µg TNP-Ficoll, and at days 0, 5, 8 and 14 post immunization serum samples were taken and TNP-specific IgM and IgG3 antibody responses were measured by ELISA. Results are representative for two independent experiments with 3-5 mice per group and experiment. AU, arbitrary units.

Since B-1 B cells are involved in TI-2 immune responses (100, 161), we measured the ability of *treml6*$^{-/-}$ mice to mount a normal antibody response. We immunized mice with trinitrophenol (TNP)-Ficoll as TI-2 antigen and followed TNP-specific IgM and IgG3 in sera. Both IgM and IgG3 responses were similar to WT responses (Fig. 12B). In sum, lack of *treml6* had no detectable

influence of TI-2 antibody responses against TNP-Ficoll, despite reduced levels of serum IgM in older *treml6*$^{-/-}$ mice.

4.1.7 Unimpaired reconstitution of Rag1$^{-/-}$ mice with *treml6*$^{-/-}$ BM

The observed contraction of the peritoneal B-1a B cell population in *treml6*$^{-/-}$ mice can be of either fetal or adult origin. Moreover, it can be either caused extrinsically by other cells expressing *treml6* and influencing the development and/or maintenance of the B-1a B cell population or it can be due to B cell intrinsic defects. Fetal pro-B cells as well as BM B-1 B cell progenitors have been described to give rise to B-1 B cells in the periphery (86, 118) and both were reduced in *treml6*$^{-/-}$ mice (Fig. 8). To investigate a putative connection with the peritoneal B-1a B cell paucity, we studied the ability of *treml6*$^{-/-}$ fetal liver-derived and *treml6*$^{-/-}$ BM cells to reconstitute the B-1 B cell compartment in spleens and peritoneal cavities in a WT environment, namely irradiated Rag1 deficient mice (Fig. 13).

In vitro generated pre-B I cells are known to preferentially fill the B-1 B cell compartment ((162) and (personal communication Szandor Simmons and Fritz Melchers)). Therefore, we generated pre-B I cells from WT and *treml6*$^{-/-}$ fetal livers (day 18 of gestation) *in vitro* and transplanted these cells into irradiated Rag1$^{-/-}$ hosts (Fig. 13A) to compare their capacity to generate B-1 B cells *in vivo*. Notably, this experiment has only been performed once and therefore conclusions should be drawn carefully. Yet, we observed reduced B-1a B cell numbers in peritoneal cavities (4 weeks, WT: 20% and KO: 11%; 12 weeks, WT: 42% and KO: 20%) and spleens after transfer of *treml6*$^{-/-}$ pre-B I cells compared to transfer of WT pre-B I cells 4 and 12 weeks post transfer, indicating that *treml6* is necessary for fetal liver-dependent B-1a B cell generation (Fig. 13B). Transfer of *treml6*$^{-/-}$ pre-B I cells resulted also in reduced B-2 B cell engraftment in spleens, but not in peritoneal cavities of recipient mice. To date we cannot explain why *treml6*$^{-/-}$ pre-B I cells were not as efficient as WT pre-B I cells in filling the B-2 B cell compartment in spleens. Notably, the differences were minor. Frequencies of B-2 B cells reached 5-4% (4 and 12 weeks) after transfer of WT cells and 2 and 3% (4 and 12 weeks) after transfer of *treml6*$^{-/-}$ pre-B I cells, and were thus far below normal B-2 B cell frequencies (60% of lymphocytes) found in spleen (Fig. 9B). Moreover, different numbers or fitness of transferred cells cannot have caused the

observed differences, since B-2 B cell populations in peritoneal cavity reached the same size after either transfer (Fig. 13B).

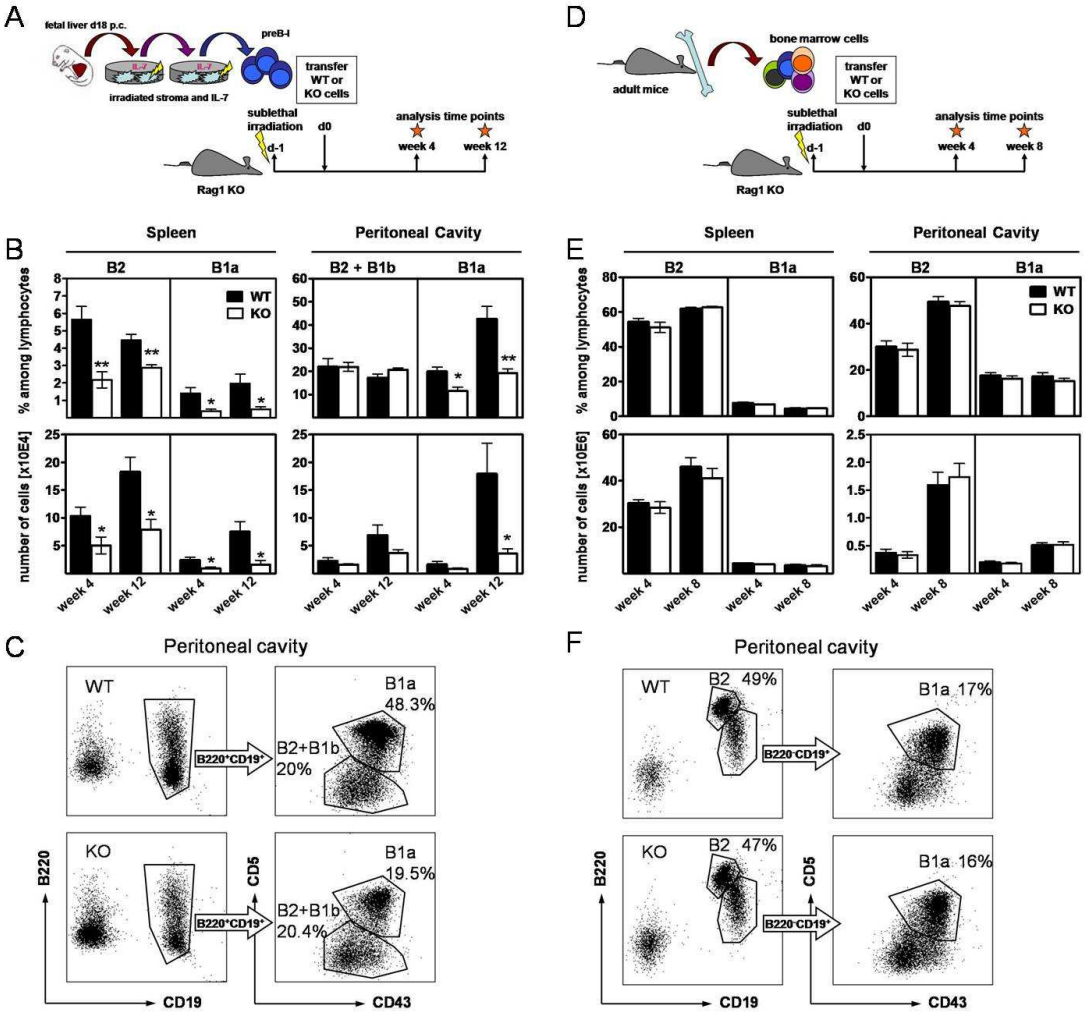

FIGURE 13. Transplantation of fetal liver derived pre-B I cells or adult BM into Rag1$^{-/-}$ mice. ***A,*** Scheme of pre-B I cell generation and cell transfer into Rag1$^{-/-}$ hosts. ***B,*** Frequencies and numbers of B-2 and B-1a B cells, at 4 and 12 weeks after reconstitution of Rag1$^{-/-}$ mice with *in vitro* generated WT or *treml6*$^{-/-}$ (KO) preB I B cells. Left dot blots show FSC/SSC gated lymphocytes. The respective B cell staining and gating strategy is depicted in dot blots of ***C.*** Results are from 1 experiment with 5 mice per time-point, group and, experiment. Error-bars represent the standard errors of the mean. ***D,*** Scheme of BM transfer, 1x 10^7 WT or *treml6*$^{-/-}$ (KO) BM cells were adoptively transferred upon Rag1$^{-/-}$ mice. ***E,*** Frequencies and numbers of B-2 and B-1a B cells after 4 and 8 weeks of re-constitution with BM cells in spleens and peritoneal cavities. Left dot blots show FSC/SSC gated lymphocytes. The respective B cell staining and gating strategy is depicted in dot blots of ***F.*** Results are means of 2 independent experiments with 5 mice per time-point, group and, experiment. Error-bars represent the standard errors of the mean. Significant differences between 2 groups are indicated by asterisks (Student's *t* test: *, $p < 0.05$, **, $p < 0.01$ and ***, $p < 0.001$).

We also transplanted WT and *treml6*$^{-/-}$ BM cells into Rag1$^{-/-}$ mice (Fig. 13D). We found that *treml6*-deficient B-1a B cells, like WT B-1a B cells, can be generated from progenitors found in adult BM. Notably, B-1a B cell frequencies among lymphocytes were around 15% at 4 and 8

weeks post WT or *treml6*$^{-/-}$ BM transfer (Fig. 13E) and therefore lower than normal B-1a B cell frequencies in WT animals (Fig. 9B). Eight weeks post transfer of either WT or *treml6*$^{-/-}$ BM frequencies of B-2 B cells in recipient spleens reached about 60% of lymphocytes, reflecting normal WT levels (Fig. 13E). Peritoneal cavities of reconstituted mice showed higher B-2 B cell frequencies than normally found in WT animals (Fig. 13E and 9B). Thus, BM from adult WT and *treml6*$^{-/-}$ mice possessed the same capacity to reconstitute all analyzed B cell subsets when transplanted in a WT environment (Rag1$^{-/-}$).

4.1.8 Concluding remarks on the role of *treml6* in immunity

In sum, we identified *treml6* as an ITIM-containing receptor with preferential mRNA expression in peritoneal cavities and lymphoid tissues. *Treml6*$^{-/-}$ mice revealed reduced B-1 B cell precursors in fetal liver (B-1Ps and pro-B cells) and bone marrow (B-1Ps), as well as reduced peritoneal B-1a B cells compared to WT mice. *Treml6* deficient peritoneal B-1a B cells showed a propensity for increased turnover and IL-4 driven proliferation. We detected no differences in BCR-triggered calcium responses or apoptosis rate between B-2 and B-1a B cell populations from *treml6*$^{-/-}$ or WT mice. However, we observed a) reduced expression of *cxcr5* mRNA – a chemokine receptor involved in homing to peritoneal cavities, and b) impaired B-1 B cell engraftment in Rag1$^{-/-}$ mice by *in vitro* generated *treml6*$^{-/-}$ pre-B I cells when compared to respective WT cells. In contrast, after transfer of *treml6*$^{-/-}$ BM or WT BM B cell engraftment of Rag1$^{-/-}$ mice was equal. TI-2 antibody responses to TNP-Ficoll were identical between *treml6*$^{-/-}$ and WT mice.

4.2 Impact of ICOS on T cell responses and protection against Mtb infection

In an attempt to compile the kinetics of multiple co-stimulatory molecules during Mtb infection, we observed that $CD4^+$ Th1 cells, notably IFN-γ-secretors, expressed ICOS during murine TB (Fig. 14B). Meanwhile, Quiroga *et al.* reported that the amount of IFN-γ secretion by T cells from patients with active TB disease correlates with their ICOS surface expression, and that ICOS signaling can increase IFN-γ secretion (155). Moreover, Urdahl and colleagues described that pulmonary Tregs express elevated level of ICOS during murine Mtb infection (66). These data point to ICOS as an important player during TB. Therefore, we investigated the role of ICOS co-stimulation in TB using $ICOS^{-/-}$ mice. Here we describe the expression pattern of ICOS during murine TB and its impact on T cell responses and disease outcome. We show that ICOS is strongly expressed on $CD4^+$ T cells during Mtb infection and that ICOS deficiency differentially affects $CD4^+$ and $CD8^+$ T cell responses, ultimately resulting in improved protection in the spleen during later stages of Mtb infection.

4.2.1 ICOS expression by $CD4^+$ and $CD8^+$ T cells during Mtb infection

Both $CD4^+$ and $CD8^+$ T cells are crucial for control of TB (124, 125, 127). In order to investigate the role of ICOS signaling in generation of Mtb-specific T cell responses, we first aimed at characterizing ICOS expression by T cells during Mtb infection (Fig. 14A). C57BL/6 wild type (WT) mice were infected via aerosol with a low dose of Mtb (approx. 200 CFU of strain H37Rv).

At different time points p.i., ICOS expression by T cells from spleen and lungs was determined by flow-cytometry. During the entire course of Mtb infection, numbers and frequencies of $CD8^+$ T cells expressing ICOS remained constant with less than 5% of all splenic and pulmonary $CD8^+$ T cells (< $3x\ 10^5$ $CD8^+$ T cells per organ) being $ICOS^+$ (Fig. 14A). In contrast to $CD8^+$ T cells, the fraction of $CD4^+$ T cells expressing ICOS constantly increased during the acute phase of infection. It reached its maximum at day 30 p.i. when up to 45% of all $CD4^+$ T cells expressed ICOS in lungs (~ $2x\ 10^6$ $ICOS^+CD4^+$ T cells), and up to 35% in spleen (~ $4x\ 10^6$ $ICOS^+CD4^+$ T cells). Between days 30 and 45 p.i., the $ICOS^+CD4^+$ T cell population contracted to approximately half the size, and re-expanded during the chronic phase of infection (days 45 to 120 p.i.) to reach levels similar to day 30 p.i.

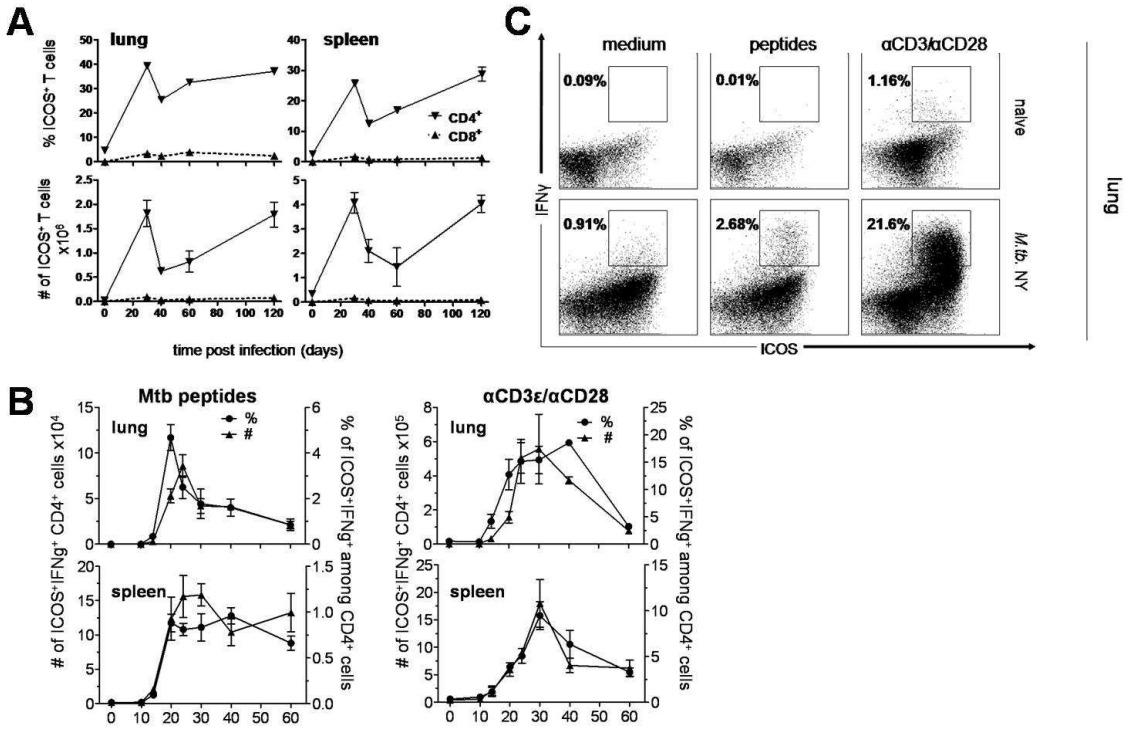

FIGURE 14. ICOS expression by CD4⁺ and CD8⁺ T cells during Mtb infection. ***A,*** Kinetics of frequencies and numbers of ICOS surface-expressing CD4⁺ and CD8⁺ lung and spleen T lymphocytes from Mtb infected C57BL/6 (WT) mice. At indicated time-points p.i. lung and spleen lymphocytes were isolated, surface-stained with αCD4 mAb, αCD8 mAb, and αICOS mAb, and analyzed by flow cytometry. Percentages refer to gated CD4⁺ or CD8⁺ lymphocytes. Results are representative for 3 independent experiments with 3 pools of 1-2 mice per group and experiment. Error-bars represent the standard errors of the mean. ***B,*** Kinetics of frequencies and numbers of ICOS⁺IFN-γ⁺CD4⁺ spleen and lung lymphocytes from Mtb infected WT mice. Isolated cells from 5-8 mice were pooled and re-stimulated *in vitro* with a mixture of Mtb MHC-II peptides or a mixture of αCD3ε/αCD28 mAbs. Subsequently, cells were surface-stained with αCD4 mAb and intracellularly with αICOS mAb and αIFN-γ mAb and analyzed by flow cytometry. Frequencies refer to gated CD4⁺ T lymphocytes. Cells cultured in medium served as background controls. Results represent means of 2 independent experiments with 2 pools of 5-8 mice per experiment. Error-bars represent standard errors of the mean. ***C,*** Representative dot blots of IFN-γ and ICOS expressing CD4⁺ lung lymphocytes from naïve and Mtb infected (day 24 p.i.) WT mice. Black squares indicate gating of ICOS⁺IFN-γ⁺ CD4⁺ T cells.

To further define the nature and cytokine secretion patterns of these $ICOS^+CD4^+$ T cells, we performed intracellular cytokine staining after short term *in vitro* re-stimulation with either Mtb-derived peptides or αCD3ε/αCD28 monoclonal antibodies (polyclonal stimulation) (Fig. 14B). In either setting, almost all IFN-γ secreting cells also co-expressed ICOS (Fig. 14C) suggesting a mayor role of ICOS co-stimulation in the development of Th1 cells during Mtb infection.

4.2.2 Impact of ICOS deficiency on Mtb burden and pathology

Since ICOS was expressed by almost all IFN-γ secreting $CD4^+$ T cells during Mtb infection, we next studied consequences of ICOS deficiency on TB disease progression. We infected ICOS-gene deficient mice and WT animals with Mtb and followed bacterial burdens and pathology in lungs and spleens during the course of infection (Fig. 15 and 16). We observed no differences in Mtb numbers in lungs between both groups at all time-points analyzed (days 15 to 120 p.i.). In contrast, spleens of ICOS-deficient mice revealed a significantly reduced bacterial burden on days 60 and 120 p.i. (Fig. 15).

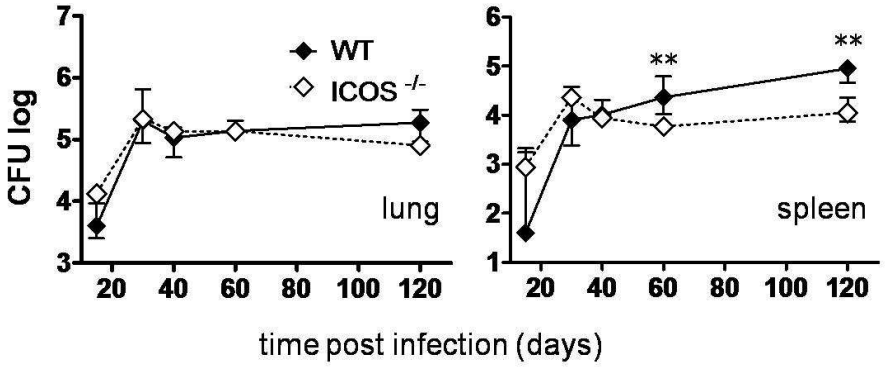

FIGURE 15. Mtb burden in lungs and spleen during Mtb infection. $ICOS^{-/-}$ and WT mice were infected with Mtb by aerosol. At indicated time-points p.i., mice were killed and bacterial burdens in lungs and spleens were determined. Medians with range of log CFU are plotted versus time. Open or filled diamonds represent $ICOS^{-/-}$ or WT mice, respectively. Data are representative of 3 independent experiments with 5 mice per group per time-point. Significant differences between 2 groups are indicated by asterisks (Mann-Whitney U test: *, $p < 0.05$ and **, $p < 0.01$).

During the course of Mtb infection we observed no apparent differences in pathology of lungs between WT and $ICOS^{-/-}$ mice (Fig. 15B). At day 30 p.i. lung parenchyma presented infiltrates with granulomatous appearance, but no great differences were revealed between the groups in terms of frequency or cellular composition of the inflammatory foci. Alveolitis, perivascular and peribronchiolar accumulations of macrophages and lymphocytes were as well comparable between WT and $ICOS^{-/-}$ mice. During chronic Mtb infection (120 p.i.) lung lesions extended to almost the entire respiratory tissue. They became consolidated with defined clusters of mononuclear cells, mostly lymphocytes. Within the inflammatory infiltrates and particularly in proximity to the remnant alveolar spaces large foamy macrophages were present in both animal strains. Compensatory emphysema and relatively few intact alveoli were present at this stage of Mtb infection.

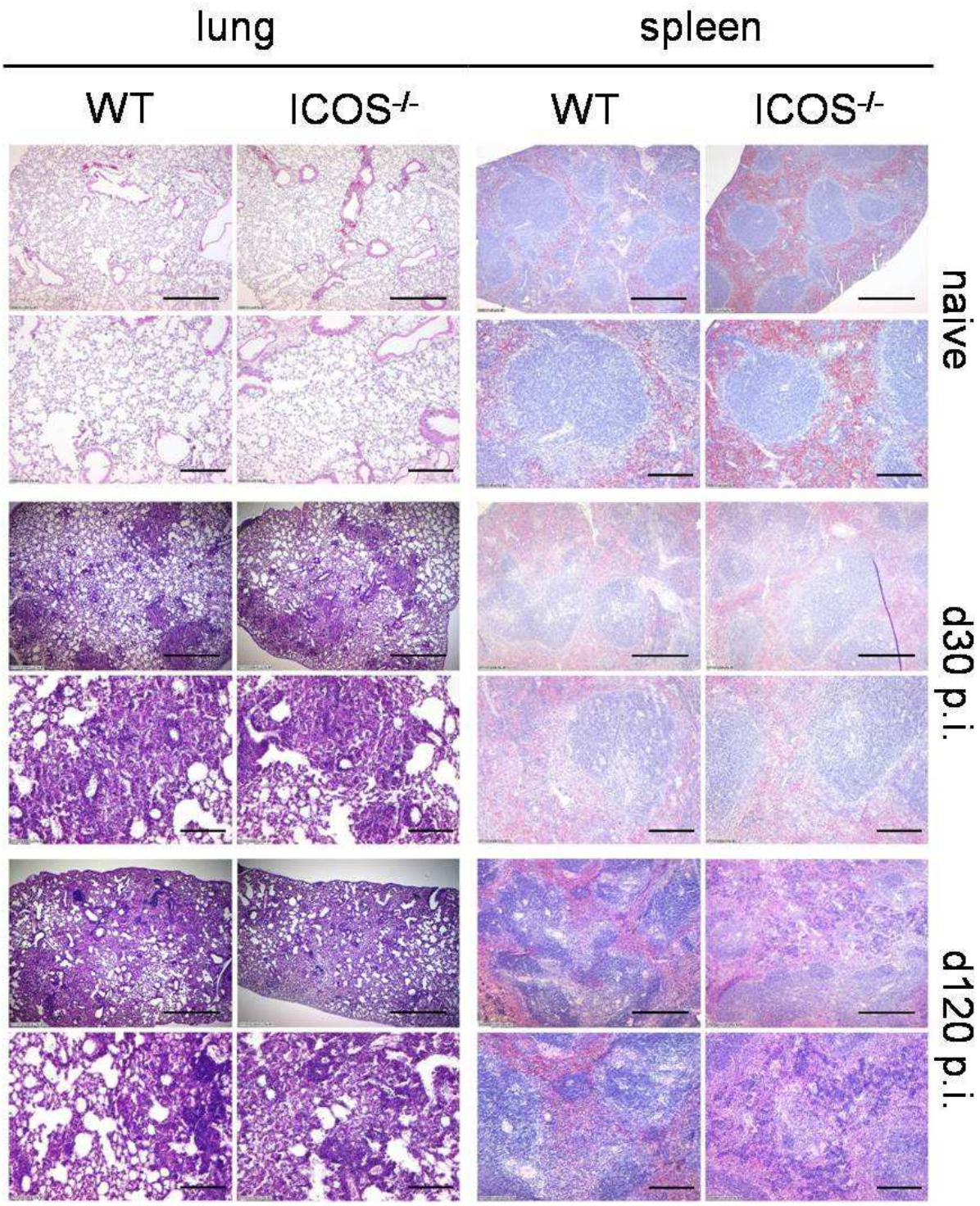

FIGURE 16. Pathology of lungs and spleen during Mtb infection. ICOS$^{-/-}$ and WT mice were infected with Mtb by aerosol. Hematoxylin and eosin staining of lung and spleen sections from naïve and Mtb-infected C57BL/6 and ICOS$^{-/-}$ mice; Upper panels of each time point, scale bar 500μm; lower panels of each time point, scale bar 200μm.

The pathology of the spleens differed only slightly during the chronic phase of Mtb infection (Fig. 16). During the acute phase of Mtb infection (day 30 p.i.) spleen architecture was not

dramatically changed. In both, WT and ICOS$^{-/-}$ mice spleen follicles were intact and sparse mononuclear cell infiltrates were observed within the red pulp. At day 120 p.i. partial disruption of the spleen follicles was recorded for both WT and ICOS$^{-/-}$ mice and slightly more infiltration of the perifollicular space was noticed in ICOS$^{-/-}$ mice compared to WT mice.

4.2.3 Impact of ICOS deficiency on generation of CD4^{+} Th1 responses during Mtb infection

The CD4^{+} Th1 response and its major effector cytokine IFN-γ are crucial for defense against Mtb (125, 127). To gain detailed information about the kinetics and activation of the Th1 response in absence of ICOS signaling, we infected WT and ICOS$^{-/-}$ mice with Mtb. At various time points after infection, we isolated spleen and lung lymphocytes and restimulated them *in vitro* either polyclonally (αCD3ε/αCD28) or with a cocktail of Mtb peptides (PepA, Ag85A$_{241-260}$, Ag85B$_{240-260}$ and ESAT6$_{1-20}$). We subsequently stained and analyzed these cells for co-expression of CD4 (and CD8; Fig. 19A), IFN-γ and TNF-α (Fig. 17).

Kinetics of initial and late phase Mtb (ESAT6, Ag85A and Ag85B)-specific Th1 responses were similar between WT and ICOS$^{-/-}$ mice, only the contraction of the response on day 40 p.i. was less pronounced in ICOS$^{-/-}$ mice than in WT mice. Accordingly more than twice as many Mtb-peptide-specific CD4^{+} T cells were identified in lungs and spleens of ICOS$^{-/-}$ mice (~3.2x 10^5 in ICOS$^{-/-}$ vs. ~1.5x 10^5 in WT lungs, and ~5x 10^5 in ICOS$^{-/-}$ and ~2x 10^5 in WT spleens). The total IFN-γ secreting CD4^{+} T cell response (after αCD3ε/αCD28 mAbs restimulation) differed significantly between the two groups of mice in the chronic stage of infection. In ICOS$^{-/-}$ mice the Th1 response did not contract as profoundly as in WT mice, and remained elevated throughout the later stage of infection, evidenced by significantly increased frequencies and numbers of IFN-γ^{+}CD4^{+} T cells in lungs and spleen of ICOS-deficient mice.

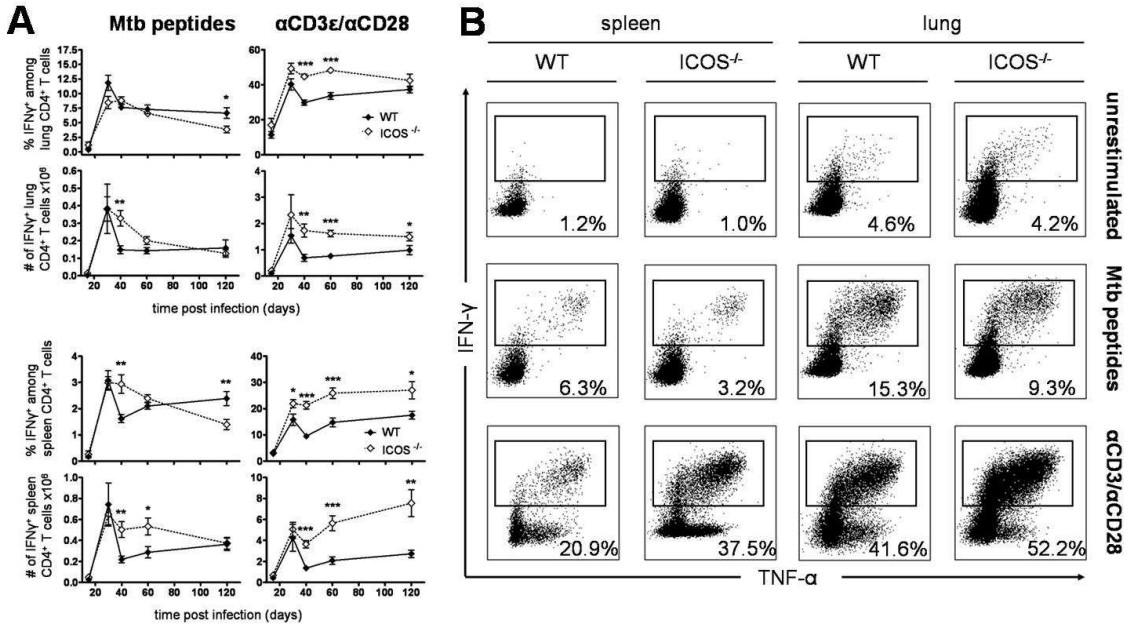

FIGURE 17. Increased frequencies of total IFN-γ⁺CD4⁺ T cells in ICOS$^{-/-}$ mice during late stage of Mtb infection. ***A,*** Kinetics of frequencies and numbers of IFN-γ⁺CD4⁺ spleen and lung lymphocytes from Mtb infected WT and ICOS$^{-/-}$ mice. WT and ICOS$^{-/-}$ mice were infected with Mtb and cells were isolated, re-stimulated, stained, and analyzed, as in Fig. 14B. Percentages refer to gated CD4⁺ T lymphocytes. Results are mean values of 2 to 3 independent experiments with 3 pools of 1-2 mice per group and experiment. Error-bars represent the standard errors of the mean. Significant differences between 2 groups are indicated by asterisks (Student's *t* test: *, $p < 0.05$, **, $p < 0.01$ and ***, $p < 0.001$). ***B,*** Representative dot blots of IFN-γ and TNF-α expression by CD4⁺ lung and spleen lymphocytes from Mtb infected (day 120 p.i.) WT and ICOS$^{-/-}$ mice. Black squares indicate gating of IFN-γ⁺ CD4⁺ T cells.

From day 30 to 40 p.i., numbers of total IFN-γ producing CD4$^+$ T cells contracted approximately by half in lungs of WT mice and only by a quarter in lungs of ICOS-deficient mice. After the contraction phase, the amount of total IFN-γ producing CD4$^+$ T cells remained at about the same level in both groups of mice until day 120 p.i. (~0.8x 10^6 in WT and 1.6x 10^6 in ICOS$^{-/-}$ lungs). In spleens differences in contraction strength between the two groups of mice were even more pronounced. From day 30 to 40 p.i. numbers of total IFN-γ producing CD4$^+$ T cells contracted approximately by two-third in spleens of WT mice and only by a quarter in spleens of ICOS-deficient mice. After the contraction of the CD4$^+$ Th1 response, numbers of total IFN-γ producing CD4$^+$ T cells doubled in both groups from day 40 p.i. to 120 p.i. (~1.3x 10^6 to ~2.7x 10^6 in WT mice and ~3.6x 10^6 to ~7.5x 10^6 in ICOS$^{-/-}$ mice). While, ICOS-deficient mice had the highest levels of total IFN-γ producing CD4$^+$ T cells on day 120 p.i. (~7.5x 10^6), WT mice showed highest numbers on day 30 p.i. at the peak of the acute immune response (~4.2x 10^6) (Fig. 17A). Thus, we assume that the contraction of the acute CD4$^+$ T cell response is likely governed by

ICOS signaling and that at later stages of infection, $CD4^+$ Th1 responses are restricted in an ICOS-dependent manner.

4.2.4 Impaired maintenance of Mtb-specific effector $CD8^+$ T cells in $ICOS^{-/-}$ mice

In addition to $CD4^+$ Th1 cells, $CD8^+$ T cells contribute to protection against Mtb (124, 163, 164). They secrete the mayor Th1 effector cytokine IFN-γ, and also lyse infected cells directly (140).

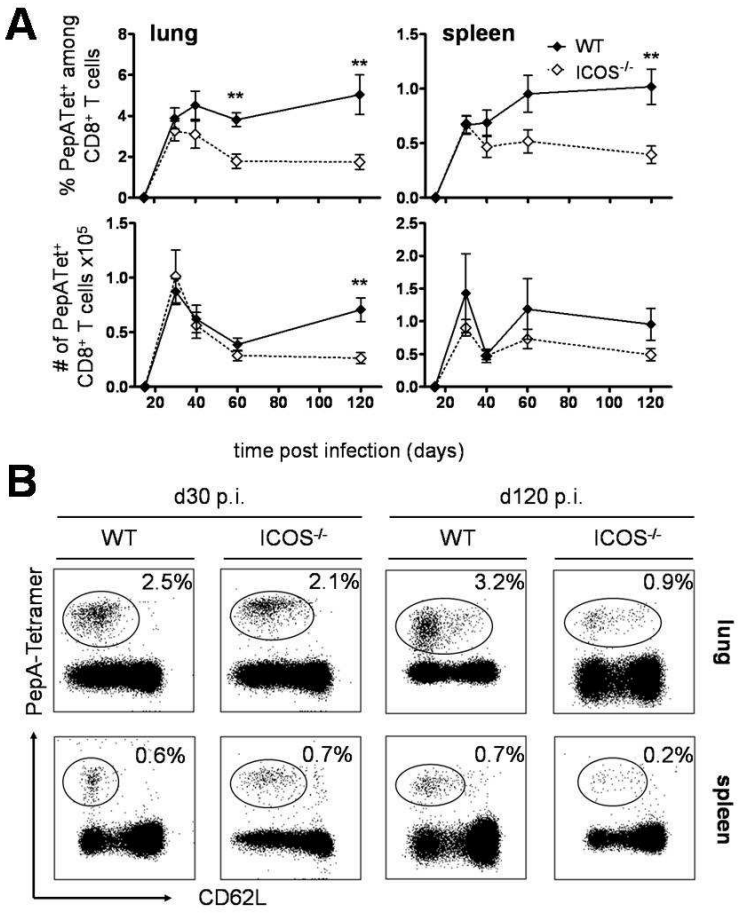

FIGURE 18. Reduced numbers of PepA-specific $CD8^+$ T cells in chronically Mtb infected $ICOS^{-/-}$ mice. ***A,*** Kinetics of frequencies and numbers of PepA-$Tetramer^+CD8^+$ spleen and lung lymphocytes from Mtb infected $ICOS^{-/-}$ and WT mice. WT and $ICOS^{-/-}$ mice were infected with Mtb and cells were isolated as in Fig. 17. Isolated cells were surface-stained with αCD8 mAb, PepA-Tetramer and αCD62L mAb and analyzed by flow cytometry. Percentages refer to gated $CD8^+$ T lymphocytes. Results are mean values of 2 to 3 independent experiments with 3 pools of 1-2 mice per group and experiment. Error-bars represent standard errors of the mean. Significant differences between 2 groups are indicated by asterisks (Student's *t* test: *, $p < 0.05$, **, $p < 0.01$ and ***, $p < 0.001$). ***B,*** Representative dot blots of PepA-Tetramer binding and CD62L expression by $CD8^+$ lung and spleen lymphocytes from Mtb infected (days 30 and 120 p.i.) $ICOS^{-/-}$ and WT mice. Black circles indicate gating of PepA-$Tetramer^+CD62L^{low}$ $CD8^+$ T cells.

We stained PepA-specific $CD8^+$ T cells using fluorochrome-labeled MHCI-peptide-tetramers (Fig. 18). The initial acute $CD8^+$ T cell response did not differ between WT and ICOS-deficient mice, whilst the late phase response did. At day 60 p.i., 4% and at day 120 p.i., about 5% of all $CD8^+$ T cells were specific for PepA in lungs of Mtb-infected WT mice. In contrast, at the same time points only about 2% of all $CD8^+$ T cells were PepA-specific in lungs of Mtb-infected $ICOS^{-/-}$ mice resulting in significantly reduced numbers of these cells at day 120 p.i. ($0.25x\ 10^5$ in $ICOS^{-/-}$ and $0.7x\ 10^5$ in WT mice). We also observed reduced PepA-specific $CD8^+$ T cell responses in spleens of $ICOS^{-/-}$ mice. At day 120 p.i., 0.4% of all $ICOS^{-/-}$ $CD8^+$ T cells and about 1% of all $CD8^+$ T cells in WT mice were PepA-specific. Not only frequencies, but also numbers of PepA-specific $CD8^+$ T cells were reduced in spleens of $ICOS^{-/-}$ mice; however they did not differ significantly from numbers in WT animals (Fig. 18A).

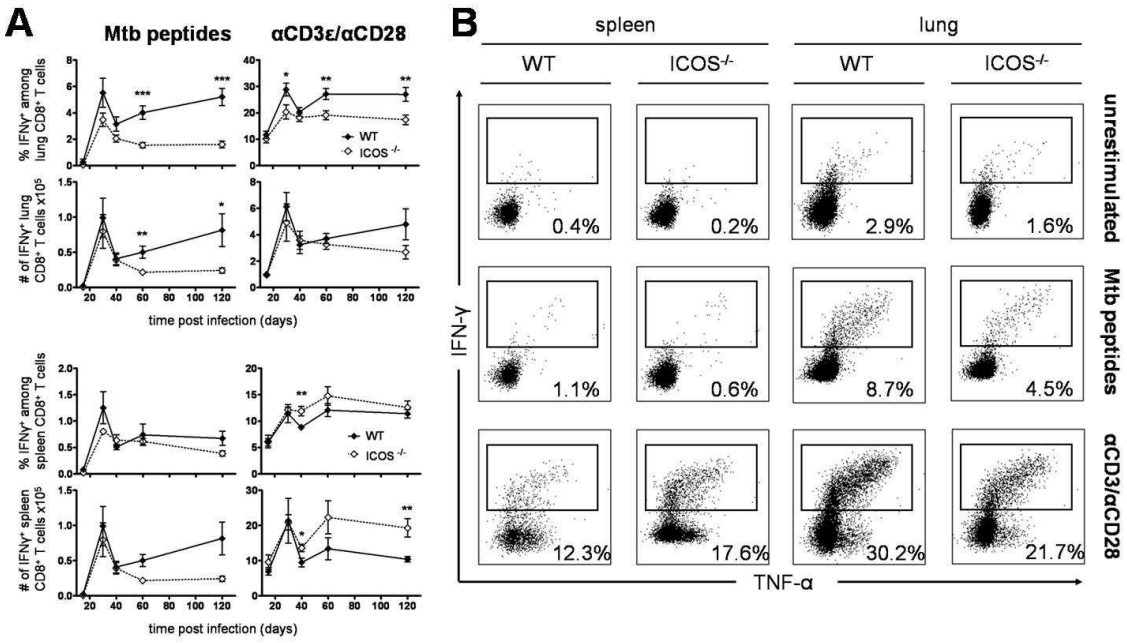

FIGURE 19. Reduced numbers of IFN-γ secreting PepA-specific $CD8^+$ T cells in chronically Mtb infected $ICOS^{-/-}$ mice. ***A,*** Kinetics of frequencies and numbers of IFN-γ^+CD8^+ spleen and lung lymphocytes from Mtb infected $ICOS^{-/-}$ and WT mice. WT and $ICOS^{-/-}$ mice were infected with Mtb and cells were isolated as in Fig. 17. Isolated cells were *in vitro* restimulated with an Mtb MHC-I peptide or a mixture of αCD3ε/αCD28 mAbs. Subsequently, cells were surface-stained with αCD8 mAb and intracellularly with αTNF-α and αIFN-γ mAbs, and analyzed by flow cytometry. Percentages refer to gated $CD8^+$ T lymphocytes. Cells cultured in medium served as a background controls. Results are mean values of 2 to 3 independent experiments with 3 pools of 1-2 mice per group and experiment. Error-bars represent the standard errors of the mean. Significant differences between 2 groups are indicated by asterisks (Student's *t* test: *, $p < 0.05$, **, $p < 0.01$ and ***, $p < 0.001$). ***B,*** Representative dot blots of IFN-γ and TNF-α expression by $CD8^+$ lung and spleen cells from Mtb infected (day 120 p.i.) $ICOS^{-/-}$ and WT mice. Black squares indicate gating of IFN-γ^+ $CD4^+$ T cells.

In order to assess effector functions of the $CD8^+$ T cell response, we first analyzed their ability to produce IFN-γ and TNF-α after short term *in vitro* restimulation with PepA peptide (Fig. 19). $CD8^+$ T cells from $ICOS^{-/-}$ mice were not affected in their ability to produce effector cytokines. Frequencies and numbers of $CD8^+$ T cells secreting IFN-γ upon restimulation with Mtb-peptide PepA were comparable to those of PepA-TCR expressing $CD8^+$ T cells as assessed by MHC-I-tetramer staining. At day 120 p.i. we measured 2% PepA-TCR-specific $CD8^+$ T cells (Fig. 18A), as well as 2% IFN-γ secreting PepA-specific $CD8^+$ T cells in $ICOS^{-/-}$ mice (Fig 19A). Although during the late stage of infection lack of ICOS co-stimulation led to reduced PepA-specific CTL response in magnitude, it did not affect their capacity to secrete IFN-γ (Fig. 18A and 19A).

Compared to WT mice, $ICOS^{-/-}$ mice had less PepA-TCR-specific $CD8^+$ T cells as well as PepA-specific IFN-γ secreting $CD8^+$ T cells. However, pulmonary total IFN-γ-secreting $CD8^+$ T cells – assessed through *in vitro* restimulation with αCD3ε/αCD28 mAbs – were only reduced in frequencies, but not numbers, in $ICOS^{-/-}$ mice. Of note, in spleens of $ICOS^{-/-}$ mice the total IFN-γ secreting $CD8^+$ T cell response was even elevated in the late stage of Mtb infection (Fig. 19A).

4.2.4.1 Reduced killing by PepA-specific $CD8^+$ T cell in $ICOS^{-/-}$ mice

A hallmark of $CD8^+$ T cell function is their ability to lyse target cells (165). To further address the effector functions of the weakened PepA-specific $CD8^+$ T cell response in $ICOS^{-/-}$ mice, we examined whether PepA-specific $CD8^+$ T cells in Mtb infected mice were capable of lysing target cells presenting this epitope *in vivo* (Fig. 20).

We used an *in vivo* cytotoxicity assay, in which equal numbers of differentially CFSE-labeled splenocytes from naïve mice, pulsed either with control peptide LLO_{91-99} or pulsed with Mtb-derived peptide PepA, were adoptively transferred upon Mtb infected mice. Peptide-specific lysis of transferred cells was assessed by flow cytometric analysis of spleens of recipient mice and quantification of residual CFSE high (PepA pulsed) and CFSE low (LLO_{91-99} pulsed) donor cells. WT and $ICOS^{-/-}$ mice showed killing upon transfer of target cells. The CTL activity of PepA-specific $CD8^+$ T cell was significantly stronger in WT mice (~40%-specific killing of PepA loaded cells) as compared to $ICOS^{-/-}$ mice (~25%-specific killing) (Fig. 20A). The observed reduction in killing of donor cells can be due to either reduced killing capacity of PepA-specific $CD8^+$ T cells or be a consequence of reduced numbers and frequencies of PepA-specific $CD8^+$ T cells in ICOS-deficient mice.

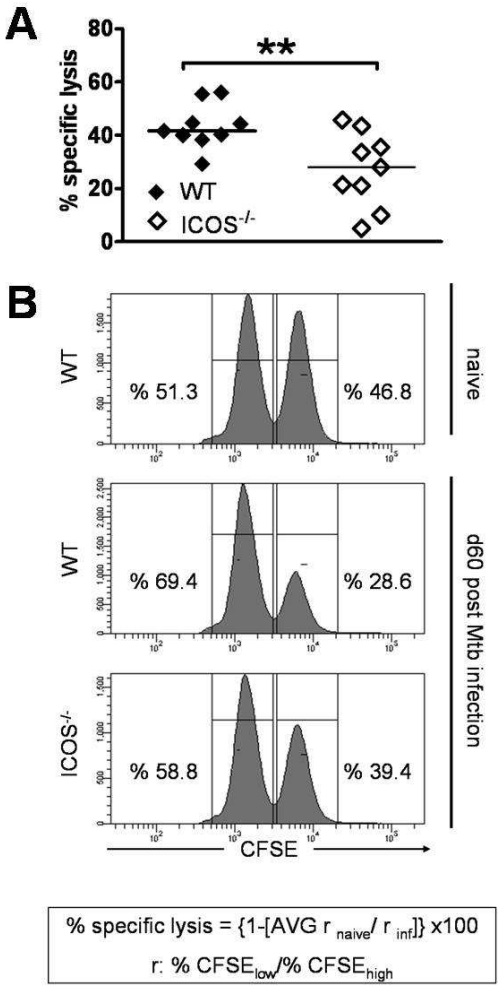

FIGURE 20. Reduced PepA-specific *in vivo* lysis in chronically Mtb infected ICOS$^{-/-}$ mice. ***A,*** CTL activity of PepA-specific CD8^{+} T cells *in vivo*. Listeriolysin O (control peptide) loaded splenocytes ($CFSE_{low}$) and PepA-loaded splenocytes ($CFSE_{high}$) from naive mice were transferred upon Mtb infected mice (day 60 p.i.). Reduction in $CFSE_{high}$ populations reflects the amount of splenocytes killed *in vivo* by PepA-specific CD8^{+} T cells. Significant differences between 2 groups are indicated by asterisks (Student's *t* test: *, $p < 0.05$, **, $p < 0.01$ and ***, $p < 0.001$). ***B,*** Representative histograms show frequencies of $CFSE_{high}$ and $CFSE_{low}$ populations. Specific lysis was calculated as indicated. Calculation: % specific lysis = 1-[AVG r_{naive}/ r_{inf}] x100. AVG r_{naive}: average of $CFSE_{low}/CFSE_{high}$ ratios from individual naïve mice; AVG r_{naive} has been calculated for each experiment independently. r_{inf}: $CFSE_{low}/CFSE_{high}$ ratios of individual infected mice. Scatter plots show data from 3 independent experiments with 3 mice per group and experiment. Results were pooled with each diamond representing one mouse.

4.2.5 Impaired CD8^{+} effector memory maintenance during chronic Mtb infection in ICOS$^{-/-}$ mice

ICOS signaling has been suggested to serve as survival factor for effector and effector memory T cells (85). We were interested in contribution of ICOS signaling on the generation or stimulation of memory T cells in the context of a chronic TB disease (Fig. 21). Memory phenotype of PepA-specific CD8^{+} T cells was assessed by staining for CD127, a surface marker expressed only on naïve and on memory T cells, and for CD62L, to differentiate between central and effector memory cells (166).

No differences in numbers of effector and central memory CD8^{+} T cells were detected in spleens at days 60 and 120 p.i. between WT and ICOS$^{-/-}$ mice. Moreover, central memory T cells were not affected by the lack of ICOS signals in lungs of Mtb infected mice as numbers did not differ from those in WT mice. However, we observed differences in numbers of effector memory T

cells. PepA-specific effector memory $CD8^+$ T cells in WT mice increased from 1.8x 10^4 cells at day 60 p.i. to about 3x 10^4 cells at day 120 p.i., whilst effector memory $CD8^+$ T cells in $ICOS^{-/-}$ mice remained at a stable level of 1.8x 10^4 cells (Fig. 21A). In sum, lack of ICOS had no impact on the development of central memory T cells, but impaired formation and/or maintenance of PepA-specific effector memory $CD8^+$ T cells in lungs of Mtb infected mice.

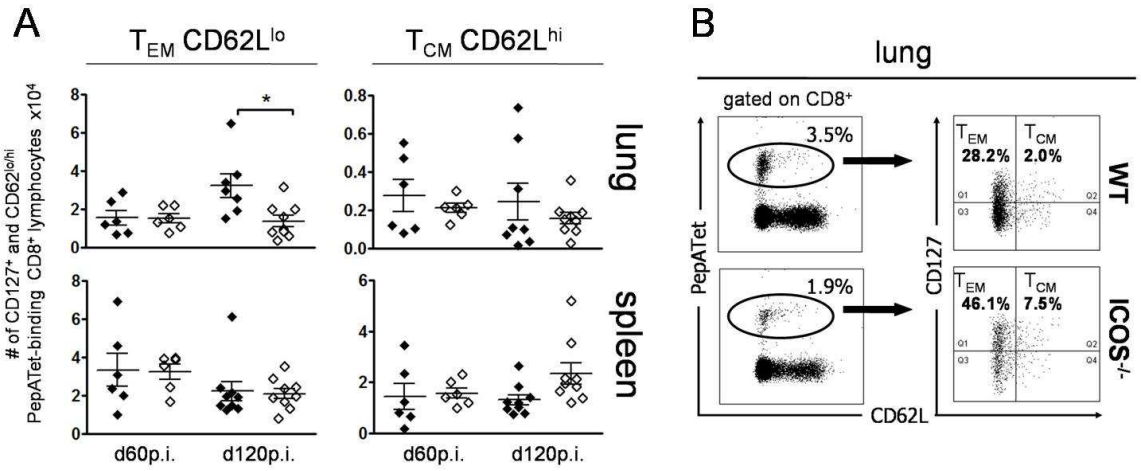

FIGURE 21. Reduced PepA-specific $CD8^+$ effector memory T cells at day 120 p.i. in $ICOS^{-/-}$ mice. ***A,*** Numbers of $CD127^+$ and $CD62L^{lo}$/$CD62L^{hi}$ PepA-Tetramer$^+CD8^+$ spleen and lung lymphocytes from Mtb infected $ICOS^{-/-}$ and WT mice on days 60 and 120 p.i. WT and $ICOS^{-/-}$ mice were infected with Mtb and cells were isolated as in Fig. 17. Isolated cells were surface-stained with αCD8 mAb, PepA-Tetramer, αCD127 mAb and αCD62L mAb and analyzed by flow cytometry. Results are mean values of 2 to 3 independent experiments with 3 pools of 1-2 mice per group and experiment. Error-bars represent standard errors of the mean. Significant differences between 2 groups are indicated by asterisks (Student's *t* test: *, $p < 0.05$, **, $p < 0.01$ and ***, $p < 0.001$). ***B,*** Representative dot blots demonstrating PepA-Tetramer-binding and CD62L expression by $CD8^+$ gated lung lymphocytes from Mtb infected (day 120 p.i.) WT and $ICOS^{-/-}$ mice. Black circles indicate gating of PepA-tetramer-binding $CD8^+$ T cells. Arrows point to dot blots which demonstrate further analysis of CD127 and CD62L expression of the PepA-tetramer binding $CD8^+$ T cells.

4.2.6 Reduced frequencies and numbers of Treg in $ICOS^{-/-}$ mice during Mtb infection

Treg control the immune response against Mtb (64-66), and Treg upregulate ICOS surface expression during Mtb infection (66), suggesting ICOS as a key regulator for these cells in TB. We found that throughout the course of Mtb infection Treg frequencies were significantly reduced in ICOS-deficient mice as compared to WT mice (Fig. 22). This also held true for Treg numbers in the later stage of Mtb infection.

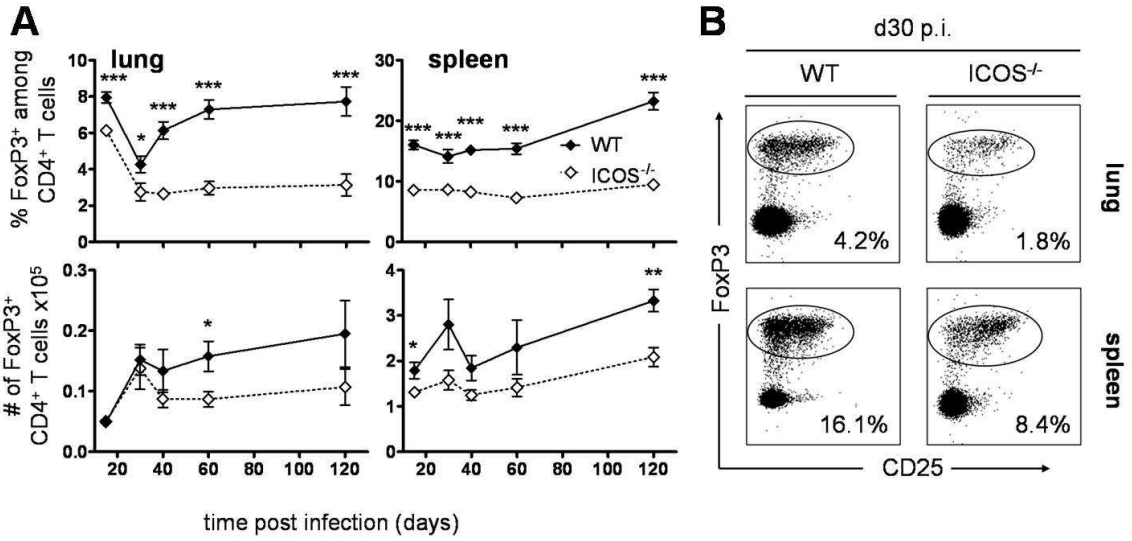

FIGURE 22. Reduced frequencies and numbers of Treg in ICOS$^{-/-}$ mice throughout Mtb infection. ***A,*** Kinetics of frequencies and numbers of FoxP3^{+}CD4^{+} spleen and lung lymphocytes from Mtb infected WT and ICOS$^{-/-}$ mice. WT and ICOS$^{-/-}$ mice were infected with Mtb and cells were isolated as in Fig. 17. Cells were surface-stained with αCD4 mAb and αCD25 mAb and intranuclearly with αFoxP3 mAb, and analyzed by flow cytometry. Percentages refer to gated CD4^{+} T lymphocytes. Results are mean values of 2 to 3 independent experiments with 3 pools of 1-2 mice per group and experiment. Error-bars represent standard errors of the mean. Significant differences between 2 groups at analyzed time-points are indicated by asterisks (Student's *t* test: *, $p < 0.05$, **, $p < 0.01$ and ***, $p < 0.001$). ***B,*** Representative dot blots of FoxP3 and CD25 expression by CD4^{+} lung and spleen cells from Mtb infected (day 30 p.i.) ICOS$^{-/-}$ and WT mice. Black circles indicate gating of CD4^{+}FoxP3^{+} cells.

Frequencies of Treg in spleen and lung of Mtb infected WT and ICOS-deficient mice were altered reciprocally to the Th1 response. The Th1 response peaked around day 30 p.i. whereas the Treg response contracted at this time point. WT Treg decreased from 8% at day 15 p.i. to about 4% of CD4^{+} T cells at day 30 p.i. Similarly, ICOS-deficient Treg decreased from 6% at day 15 p.i. to about 2-3% of all CD4^{+} T cells at day 30 p.i., indicating similar kinetics despite lower frequencies during the acute response to Mtb in ICOS$^{-/-}$ mice. However, while the Treg response in WT mice recovered and increased after day 30 p.i. (up to 7-8% of all CD4^{+} T cells at days 60 and 120 p.i.), Treg frequencies in lungs of ICOS$^{-/-}$ mice remained at a constant low level of 2-3% of all CD4^{+} T cells (Fig. 22A).

4.2.7 Concluding remarks on the role of ICOS during murine Mtb infection

In sum, all major T cell populations were altered in the absence of ICOS signaling during murine Mtb infection. ICOS deficiency resulted in an increased polyclonal CD4^{+} Th1 response against Mtb, most likely caused by robustly reduced numbers and frequencies of Tregs in these mice. In

contrast to the $CD4^+$ Th1 response, the Mtb-specific $CD8^+$ T cell response during the later stage of infection was reduced. In addition, not only Mtb-specific effector $CD8^+$ T cells, but also effector memory $CD8^+$ T cells were reduced in Mtb infected $ICOS^{-/-}$ mice. As a result, Mtb infected $ICOS^{-/-}$ mice were less susceptible during the late chronic stage of infection as compared to wild type (WT) controls evidenced by decreased bacterial burden in the spleen.

5 DISCUSSION

5.1 *Treml6* is a positive regulator of B-1a B cell development

This thesis is the first report describing *treml6*$^{-/-}$ mice and investigating the function of murine *treml6*, an ITIM-containing receptor of the TREM protein family (12, 13). TREM receptors are of particular interest in infection immunology since many members regulate inflammatory responses by either amplifying or dampening TLR signals (12). In this context, we got interested in the TREM family and in particular in *treml6* as a putative inhibitor of inflammation. The basis for understanding the role of a molecule in infection is a careful immunological characterization of its function in the steady state.

As a result of this analysis, we provide data that expand the function of TREM receptors from regulators of inflammation to regulators of lymphocyte development. In fact, we identified *treml6* as a positive regulator of B-1a B cell development. Its role in regulation of B-1a B cell development was manifested in reduced B-1P in fetal liver and adult BM, and finally resulted in a strong reduction of peritoneal B-1a B cells in young and adult *treml6*$^{-/-}$ mice. Moreover, *treml6* deficient peritoneal B-1a B cells showed a propensity for increased turnover and IL-4 driven proliferation that possibly led to re-normalized B-1a B cell levels in aged *treml6*$^{-/-}$ mice (older than 17 weeks). We found no indications linking *treml6*-dependent regulation to BCR signaling or increased apoptosis.

Treml6$^{-/-}$ mice were fertile and showed normal growth. Moreover, the initial immunological analysis of *treml6*$^{-/-}$ mice revealed regular immune cell composition. In addition, t*reml6* gene expression showed preferential expression in peritoneal cavities and lymphoid tissues, such as bone marrow and spleen. Though, it was not focused to a specific cell population. In latter regard, *treml6* is not an exception in the TREM family, since other TREM members are also widely expressed on various innate immune cells of the myeloid lineage, and on T and B lymphocytes (12). Our assessment of *treml6* expression was limited to mRNA expression analysis by the unavailability of commercial αTLT-6 antibodies. Future plans comprise the generation of a TLT-6-specific antibody to define the protein expression profile.

Although we observed high *treml6* mRNA expression in bone marrow leukocyte populations, we initially detected no differences in size of these populations in *treml6*$^{-/-}$ mice. Moreover, B-2 B cell development was normal in BM of *treml6*$^{-/-}$ mice, evidenced in normal-sized pro-B, pre-B1,

pre-B2, and immature as well mature B cell subsets (87, 167). However, numbers of the newly described B-1Ps were reduced in the BM of adult *treml6*$^{-/-}$ mice. This was particularly interesting, since B-1 B cell ontogeny is still poorly understood and controversial, with two general models proposed. The 'lineage model' claims that B-1 and B-2 B cells are derived from two developmentally distinct cell lineages, and the alternative 'induced-differentiation' model proposes that B-1a B cells derive from B-2 B cells exposed to strong BCR signals (86, 97, 100, 101). However, both models acknowledge the importance of the fetal microenvironment in B-1 B cell generation (95, 100). In line with these reports, we showed that *treml6* was not only necessary for B-1Ps generation in BM, but also in fetal livers (day 18 of gestation). In addition, pro-B cells were reduced in fetal livers of *treml6*$^{-/-}$ mice, but fetal pre-B1 and pre-B2 populations were unaffected. The reduction in fetal liver pro-B, but not bone marrow pro-B cells was consistent with a specific role of *treml6* in B-1 B cell development. Early cell transfer studies by Hardy and Hayakawa with committed D-J rearranged B cell precursor, isolated from fetal liver or bone marrow and transferred into adult scid mice, showed that most fetal-derived cells become B-1 B cells, whereas most bone marrow-derived cells become B-2 B cells (86).

We could further underline the importance of *treml6* in B-1 B cell development, by showing that the defects in B-1 precursor (B-1Ps and fetal liver pro-B cells) translated into reduced peripheral B-1 B cell numbers as early as at the age of 4-5 weeks. Notably, only frequencies and numbers of B-1a B cells, but not B-2 and B-1b B cells were reduced in peritoneal cavities of adult *treml6*$^{-/-}$ mice. We observed the *treml6*-dependent paucity in peritoneal B-1a B cells until the age of 11 weeks. Interestingly, in aged *treml6*$^{-/-}$ mice (17-23 weeks) earlier differences in B-1a and B-2 B cell populations had normalized to WT levels. This reconstitution of WT levels was most likely due to the proliferative and self-renewing capacity of B-1a B cells (168). Peritoneal B-1a B cells showed a higher, while peritoneal B-2 B cells showed a lower turnover rate in adult *treml6*$^{-/-}$ mice compared to WT mice. Moreover, basal and IL-4 driven *in vitro* proliferation was increased in *treml6*$^{-/-}$ B-1a B cells, indicating a higher activation state of these cells (169). Similar observations were made in IL-5$^{-/-}$ mice that lack the B-1 B cell growth factor IL-5, reduction in B-1a B cells at the age of 2 weeks normalized by the age of 6-8 weeks (168). Notably, peripheral B-1a and B-2 B cell populations in peritoneal cavities and spleens of *treml6*$^{-/-}$ mice did not comprise more apoptotic cells than WT B cell populations. Thus, different degrees in fitness cannot explain the paucity in peritoneal B-1a B cells that we observed in *treml6*$^{-/-}$ mice.

In spleens of *treml6*$^{-/-}$ mice, no differences in any mature B cell subset (MZ, FC, B-2, B-1a B cells) were detected. Referring to our previous observation of normal B-2 B cell development in adult BM, we expected the B-2 B cell compartment to be unaffected. However, it was puzzling to us why the reduction in B-1 B cell precursors in fetal liver and adult bone marrow of *treml6*$^{-/-}$ mice resulted in reduced peritoneal B-1a B cells, but not in reduced peritoneal B-1b and splenic B-1a B cells, in respective mice.

Coinciding with independent roles of B cell subsets – and in support of our data that *treml6* exclusively regulates peritoneal B-1a B cells - are recent studies that strengthen the hypothesis that B-1a, B-1b and B-2 cells derive from distinct lineages (118, 170-172). Supporters of the 'lineage model' and 'unified model' (Fig. 3) of B-1 B cell development claim that B-1a B cells are generated from fetal precursors, while precursor cells for B-1b B cells are present during fetal and adult B cell development. Moreover, they showed that transferred adult bone marrow-derived B-1Ps preferentially give rise to B-1b B cells, while fetal B-1Ps (BM and liver) preferentially generate B-1a B cells (118, 170). In the context of these models, the reduced numbers of B-1a B cells and WT-like numbers of B-1b B cells further underline that solely fetal B-1 B cell development depends on *treml6*. Notably, the observed reduction of B-1Ps in adult bone marrow in *treml6*$^{-/-}$ mice did not translate into reduced peripheral B-1b B cells. Conclusively, either *treml6*$^{-/-}$ B-1b B cells must possess the propensity to compensate reduced precursor numbers through a yet unknown mechanism, or other B-1b B cell precursor apart from B-1P exist in the BM, or - despite its high expression in BM, and more probable, - *treml6* only operates in the fetal environment and reduced numbers of B-1Ps in BM could be a relic of defective B-1Ps generation in fetal livers of *treml6*$^{-/-}$ mice.

B-1a and B-1b B cells differ not only in phenotype, but also in immunological function. While B-1a B cells participate in innate immune responses, B-1b B cells mediate a type of T cell independent adaptive immune response, including an IgM memory response as has been reported by two studies with *Streptococcus pneumoniae* and *Borrelia hermsii* (96, 173). Notably, despite reduced numbers of B-1a B cells in *treml6*$^{-/-}$ mice, we detected no differences in TI-2 IgM and IgG3 antibody responses against TNP-Ficoll between WT and *treml6*$^{-/-}$ mice. One explanation could be that although B-1a B cells are involved in TI-2 responses (100), they do not respond strongly to TNP-Ficoll (161). Instead, MZ B cells and B-1b B cell appear to be the main population responding to this antigen (174, 175). Conclusively, WT-like anti-TNP antibody

responses mounted by *treml6*$^{-/-}$ mice reflect normal MZ and B-1b B cell populations, in respective mice. A similar explanation could be envisioned for unaffected serum titers of IgM, IgG1, IgG2b and IgG3 in naïve *treml6*$^{-/-}$ mice. Although B-1 B cells - together with MZ B cells - are the major source of serum IgM (94), the reduction in B-1a B cells is most likely not sufficiently pronounced to translate into detectable reduction of serum IgM levels in *treml6*$^{-/-}$ mice. Currently, we cannot explain why IgM levels in older *treml6*$^{-/-}$ mice (17-23 weeks) were reduced, despite normalized B-1a B cell numbers in these mice.

In contrast to the observed reduction in peritoneal B-1a B cells, the splenic B-1a B cell population was normal in *treml6*$^{-/-}$ mice. Notably, it has been demonstrated that splenic B-1a B cells rather resemble splenic B-2 B cells than peritoneal B-1a B cells in terms of transcription factor and gene expression, and in signaling for cell cycle progression (176). Conclusively, our data support the hypothesis that peritoneal B-1a B cells and splenic B-1a B cells might be distinct lineages with distinct developmental pathways (176). Given all these observations underlining the phenotypical, transcriptional, functional, and developmental differences between peritoneal B-1a, splenic B-1a and peritoneal B-1b cells, we were no longer surprised that *treml6* exclusively influences peritoneal B-1a cells.

Treml6 mRNA expression was not restricted to B cells; all analyzed leukocyte populations showed *treml6* mRNA expression. Thus, the reduction of peritoneal B-1a B cells could originate from two possible mechanisms. First, it could be caused by an extrinsic mechanism – such as other *treml6* expressing cells or tissues influencing the B cells. Second, it could also be a B-1a B cell autonomous defect caused by B cell intrinsic *treml6* deficiency. We designed cell transfer experiments that would help elucidate, or at least provide evidence to, whether B cell autonomous or extrinsic mechanisms are operative. Moreover, these experiments were designed to discriminate whether the observed peripheral defect in B-1a B cells is rooted in fetal or adult B cell development.

Our transfer of fetal liver-derived *in vitro* generated pre-B I cells confirmed previous studies, showing that these cells indeed preferentially fill the B-1 compartment ((87) and (personal communication Szandor Simmons and Fritz Melchers)). Notably, compared to WT pre-B I cells, transfer of *treml6*-deficient pre-B I cells resulted in reduced engraftment of B-1a B cells, while numbers of peritoneal B-2 B cells were equal in recipient mice. This observation demonstrated that fetal-derived *treml6*$^{-/-}$ cells were defective in B-1a B cell engraftment of a WT environment.

It is tempting to speculate that the observed impairment in B-1a B cell generation by *treml-6*$^{-/-}$ pre-B I cells is a B cell autonomous defect. But given the fact that pre-B I cells were generated with fetal liver cells from day 18 of gestation, we cannot fully exclude that by that time other *treml6* expressing cells could have imprinted the B-1 pathway on the precursor cells. Moreover, the fetal liver pre-B I cell transfer experiment has only been performed once and we acknowledge the weakness of drawn conclusions. Nevertheless, resulting findings match our previous observations strikingly and support the existence of a *treml6*-dependent regulatory mechanism that origins in fetal B-1a B cell development.

Transfer of BM from adult WT or *treml6*$^{-/-}$ mice resulted in similar reconstitution patterns of all B cell compartments in recipient mice. In either transfer B-2 B cell populations dominated over other B cell populations, supporting previous reports that BM transfer favors B-2 B cell development (97, 100). Thus, as WT BM, BM from adult *treml6*-deficient mice can give rise to B-1a and B-1b B cells, confirming our previous observation that reduced B-1Ps in adult *treml6*$^{-/-}$ BM did not translate into reduced peripheral B-1b B cells. These results allow the following conclusion: peripheral reduction of B-1a B cells did not result from a B cell autonomous defect in adult BM precursor cells. However, the possibility of 'trans' effects on BM precursors or peripheral B cells by other *treml6* expressing cells still exists, e.g. through cytokine or chemokine secretion – thereby altering the development or homing of B-1a B cells.

Hence, we measured the expression of CXCL13, a homeostatic chemokine crucial for B-1 B cell homing to peritoneal cavities (159, 160). We did not detect significant differences in *cxcl13* mRNA expression between peritoneal cavities of WT or *treml6*-deficient mice, providing strong evidence that regarding the homing capacity no extrinsic mechanism operates in the periphery. Nevertheless, ultimately only a transfer of WT BM into a *treml6*-deficient environment would help us clarify this issue.

On the B cell side, CXCR5 - the receptor for CXCL13 - as well as CCR7 are important for B-1 B cell homing to peritoneal cavities (159, 160). Moreover, CCR7 drives re-circulation of B-2 B cells after peritoneal passage (160). We found that *treml6*$^{-/-}$ T cells, B-1a cells, and B2 cells from peritoneal cavity and spleen were fully functional in terms of *cxcr5* mRNA expression. Moreover, no alteration in CCR7 surface expressions were detected on any cell type, despite increased mRNA levels of *ccr7* in peritoneal *treml6*$^{-/-}$ B-1a B cells. Notably, *in vitro* generated *treml6*$^{-/-}$ pre-B I cells had decreased levels of *cxcr5* mRNA expression compared to WT cells, indicating that

impaired homing capacities might have led to reduced B-1a B cell engraftment after transfer of *treml6*$^{-/-}$ pre-B I cells.

An important factor, involved in controlling the development and/or persistence, of both B-1a and B-2 B cells, is BCR signaling strength as indicated by multiple studies of genetically manipulated mice. Mutations that impair BCR signal strength (e.g., CD19 deletion, vav-1 deletion, or phospholipase PLCγ deletion) result in reduced B-1a cell numbers (100, 107-109), whereas mutations that enhance BCR signaling (e.g., SH2 domain containing phosphatase-1 (SHP-1) deletion, CD22 deletion, CD72 deletion, Siglec-G deletion, or protein tyrosine kinase Lyn deletion), lead to the expansion of the B-1a B cell population (100, 110-112, 114). Since *treml6* affected B-1a B cell development, we speculated whether *treml6* signaling influences BCR signals. We found that *treml6* only marginally affected BCR-triggered *in vitro* proliferation of peritoneal B-2 and B-1a B cells. Moreover, BCR-induced calcium responses in *treml6*$^{-/-}$ splenic B-2 B cells, and *treml6*$^{-/-}$ peritoneal B-2 and B-1a B cells were similar to those of respective WT cells. Notably, as shown by a previous report B-1P as well as pro-B cells do not have rearranged immunoglobulin heavy chain V gene, meaning they do not express BCR or pre-BCR (95, 170). Conclusively, the observed *treml6* dependent effects on B-1P and pro-B cell populations could not have been caused by alterations of BCR signaling. We cannot exclude that BCR-signaling in fetal precursors that express the pre-BCR is affected by *treml6*, but absence of regulation of BCR-signaling on mature B cells strongly suggest that mechanism other than strength of BCR signal lead to depletion of precursor and peritoneal B-1a B cells in *treml6*$^{-/-}$ mice.

Treml6 contains two intracellular ITIM motifs that can be bound by src homology 2 (SH2) domain bearing proteins, such as SHP-1, SHP-2 and SHIP. Opposing to our results, mice that carry a general mutation in Shp-1 (motheathen mice) or a specific Shp-1 deficiency in B cells have increased numbers of B-1a B cells (114, 177). The signal-attenuating effects of SHP-1 are believed to be mediated primarily via its binding to inhibitory receptors (178). B cells express several of such ITIM-containing receptors, including CD72, CD22, Siglec-G, and paired Ig-like receptor (PIR)-B (179). The phenotypes of mice lacking these inhibitory receptors show deficiencies in B-1a B cell development (110, 111, 180-185). As discussed above, these receptors as well as SHP-1 act by inhibiting BCR signals and we excluded this as the mode of action of *treml6*. Conclusively, the current data contradict the possibility of SHP-1 binding to *treml6*.

A possible intracellular binding partner for *treml6* is Bruton's tyrosine kinase (btk), which contains both SH2 and SH3 domains. Moreover, btk deficient mice, like *treml6* deficient mice, have reduced levels of B-1Ps in fetal livers (170). Thus, btk is involved in B cell development prior to pre-BCR expression (170). On the other hand, opposing to *treml6*$^{-/-}$ mice, btk$^{-/-}$ mice have increased numbers of B-1P in adult BM (171). In fact, the role of btk in BCR signaling is well established and btk$^{-/-}$ mice show, like other mediators of BCR signaling, a defect in mature B-1 B cells (186-188). Thus, *treml6* activity through btk would have to be restricted to the fetal microenvironment. However, unless binding experiments demonstrate interaction of Btk and *treml6*, this interaction remains speculative.

In sum, this study ascribes a new function to the TREM receptor family, namely regulation of lymphocyte development. We could show that TREM family member, *treml6* is a positive regulator of B-1a B cell development. The reduction in B-1 B cell specific progenitors in the fetal liver, as well as the impairment in B-1a B cell engraftment of Rag1$^{-/-}$ mice by *treml6*$^{-/-}$ pre-B I cells and normal engraftment after transfer of adult *treml6*$^{-/-}$ BM, point to developmental defects during fetal hematopoiesis. The paucity of B-1a B cells in peritoneal cavities is possibly caused due to impaired homing capacities of fetal-derived precursors, evidenced in reduced expression of *cxcr5* mRNA by *in vitro* generated *treml6*$^{-/-}$ pre-B I cells. Moreover, maintenance of peripheral B-1a B cells is most likely not affected by the lack of *treml6.*

Due to increased B-1a- and decreased B-2-homeostatic turnover, peripheral *treml6* deficient B-1a and B-2 B cells were able to restore B-1:B-2 WT ratios in peritoneal cavities of *treml6*$^{-/-}$ mice at the age of 17-23 weeks. The specific paucity in peritoneal B-1a B cells, but not other B-1 B cell subsets, underlines the high specificity of *treml6* in regulating solely the fetal development of B-1a B cells and thereby supports the 'lineage model' and 'unified model' of B-1 B cell development.

Nevertheless, it remains an open question whether B-1 precursors or the fetal microenvironment or both depend on *treml6*. In addition, the modes of *treml6* signal transductions as well as extracellular ligands remain elusive. We excluded interference with BCR signaling, but possible roles of *btk* and, in the context of TREM family function, TLR signaling (discussed separately below), will have to be subjects of future studies. Since *treml6* has no known ortholog in humans, further studies on *treml6* could provide new insights into differences of murine and human B-1 B cell development.

Possible involvement of *treml6* in TLR signaling

Most TREM family receptors were described to act as regulators of inflammation by either amplifying or dampening TLR signaling. Even though we are missing direct evidence, it is likely that this family characteristic, namely regulation of TLR signaling, also applies to *treml6*.

In line with this thinking, it is a very interesting fact that the role of TLR signaling in hematopoiesis begins to be established. It has recently been described that HSC and multipotent progenitors from humans (189-191), or mice (192) express TLRs and respond to some of their ligands by secreting cytokines and producing preferentially a myeloid progeny, namely DCs, macrophages, and granulocytes. This feedback to the site of hematopoiesis was interpreted to be beneficial in fighting bacterial or viral infections as it ensures the rapid production and thus replacement of the mainly short-lived myeloid cells (192, 193). Interestingly, this does not only apply to HSC and common myeloid progenitors, but also to CLPs. Mouse CLPs cultured in conditions that generate B lymphocytes, supplemented with TLR2, TLR4 or TLR9 ligands, PAM3, LPS, and CpG, respectively, showed a greatly reduced B cell production and yielded preferentially DC-like cells (192, 193). More relevant to our study is the so far unpublished observation by Lalanne AI and Vieira P, that TLR9 ligand CpG controls the pool size of pre-B 1 cells, through the induction of apoptosis of respective cells, in both fetal liver and bone marrow (Lalanne AI and Vieira P, personal communication).

A link to potential regulation of TLR9 signaling by *treml6* stems from *in vitro* proliferation experiments (Fig. 10B), *treml6*$^{-/-}$ B-1a B cells proliferated marginally, but significantly stronger in response to CpG. Moreover, another TREM family member PDC-TREM amplifies TLR9 signals (CpG) through association with DAP12 and Plexin-A1 in pDCs (18) and *in silico* analysis showed that *treml6* shares striking homology (86.9% identity and 90% similarity) to the first 130aa of the extracellular domain of PDC-TREM. In contrast to *treml6*, PDC-TREM signals by binding the ITAM-containing adaptor protein DAP12. In most cases, ITAM and ITIM receptors control each other by binding the same or similar ligands; in this regard *treml6* was predicted to be the counter-receptor of PDC-TREM (13). Conclusively, subjects of future studies would be to investigate a) whether *treml6* and PDC-TREM are in fact counter-receptors and b) whether *treml6* is linked to TLR9 signaling and involved in the CpG induced apoptosis of pre-B 1 cells described by Lalanne AI and Vieira P and thereby regulates B-1a B cell development.

Independent of a putative connection of *treml6* with TLR signaling future studies would also have to comprise a) generation of a *treml6* specific antibody to compare mRNA expression profile with the protein expression profile, b) identification of the putative ligand of *treml6*, and c) analysis of signaling pathways operating downstream of *treml6*.

5.2 ICOS co-stimulation shapes T cell responses against Mtb

Acquired T-cell immunity is crucial for efficient control of Mtb infection, and its failure results in TB disease outbreak (124, 125, 127). We studied the contribution of ICOS co-stimulation on generation of protective T-cell immunity against Mtb in mice. Analysis of Mtb burden and tissue pathology in WT and $ICOS^{-/-}$ mice revealed no apparent differences at the primary site of infection, the lungs. In contrast, Mtb burden in spleens was significantly reduced in $ICOS^{-/-}$ mice in the late phase of infection, suggesting that ICOS signaling influenced control of Mtb during chronic stages. This notion is consistent with exclusive ICOS expression on activated T cells which formerly led to the conclusion that ICOS sustains functions of effector and/or memory T cells rather than participating in priming of naïve T cells (68, 81, 194).

The initial acute $CD4^+$ Th1 response was comparable in WT and $ICOS^{-/-}$ mice. In contrast, in the late stage of Mtb infection we observed significantly higher frequencies of total IFN-γ secreting $CD4^+$ effector T cells in lungs and spleens of $ICOS^{-/-}$ mice. This was particularly interesting since in the steady state in naïve $ICOS^{-/-}$ mice, $CD4^+$ effector and effector memory T cells are reduced (85). Furthermore, the majority of studies addressing a role of ICOS in infection with intracellular pathogens revealed that in the absence or blockage of ICOS signaling, $CD4^+$ T cell responses remained either unaffected (e.g lymphocytic choriomeningitis virus (LCMV) (77)), or were reduced (e.g. *Leishmania mexicana*, *Nippostrongylus brasiliensis, Toxoplasma gondii* and vesicular stomatitis virus (77, 79, 81)). In murine listeriosis, inhibiting ICOS signaling impaired *Listeria monocytogenes*-specific $CD4^+$, as well as $CD8^+$ T cell responses, and resulted in higher susceptibility of mice (76). In contrast to the studies described above, but similar to our observations in murine TB, genital tract infection with *Chlamydia trachomatis* increased $CD4^+$ Th1 responses in $ICOS^{-/-}$ mice compared to WT controls (78). On the whole, depending on the type of infection analyzed, absence of ICOS signaling can lead to reduced, equal, or as for *C. trachomatis* and Mtb even increased $CD4^+$ T cell responses.

It has been proposed that all effector T-cell populations express ICOS (85). We found that during murine Mtb infection $CD4^+$, but not $CD8^+$ effector T cells surface expressed ICOS. Moreover, comparison of naive $CD8^+$ T cells with PepA(Mtb)-specific effector $CD8^+$ T cells, did not reveal increased ICOS density (data not shown). Yet, the $CD8^+$ T cell response was affected by the lack of ICOS, manifested in a weaker Mtb-specific $CD8^+$ T cell response during the late stage of Mtb infection. Our data only allow speculations on whether this effect is caused by either $CD8^+$ T-cell intrinsic or extrinsic mechanisms. Several studies have analyzed influence of ICOS on $CD8^+$ T cell responses (76, 80, 195-197). In most infection models, (e.g. *Nippostrongylus brasiliensis*, LCMV and vesicular stomatitis virus infection) the $CD8^+$ T cell response remained normal in the absence of ICOS signaling (77). However, if $CD8^+$ T cell responses depended on ICOS signaling (76, 80), it was difficult to discriminate between direct effects of ICOS signaling on $CD8^+$ T cells, and indirect effects e.g. ICOS dependent $CD4^+$ T cell help (198, 199). To answer this question Vidric *et al.* performed *in vitro* stimulation assays showing that αICOS mAb can provide co-stimulation to naïve $CD8^+$ T cells directly in the absence of $CD4^+$ T cell help (80). Yet, this experiment does not fully reflect the *in vivo* situation during an infection, where $CD4^+$ T cells strongly up-regulate ICOS, while $CD8^+$ T cells do not. Indeed, in the presence of inflammatory stimuli $CD8^+$ T cell responses can be generated without $CD4^+$ T cell help. Yet, memory $CD8^+$ T cell responses will be defective without $CD4^+$ T cell help during primary responses (166, 198, 199). Further, $CD4^+$ T cells are important for $CD8^+$ memory T cell survival, as evidenced by the decline of memory $CD8^+$ T cells in mice lacking $CD4^+$ T cells (200, 201). Moreover, during viral infections with persisting antigen, chronically stimulated $CD8^+$ T cells require $CD4^+$ T cells for survival (202-204). It is tempting to speculate that ICOS signaling is involved in this dependence. In chronic infections, when $CD8^+$ T cell survival depends on $CD4^+$ T cells (202-204), activated $CD4^+$ T cells strongly express ICOS which promotes their interactions with APCs or epithelial cells expressing ICOS-L. Such interactions in turn can stimulate CD40L surface expression on $CD4^+$ T cells (74, 205). CD40L can then interact directly with $CD8^+$ T cells expressing CD40 or indirectly with CD40 expressed on APCs, licensing them to stimulate $CD8^+$ T cell responses (41-43, 198, 199, 206, 207). Consequently, lack of ICOS would lead to reduced $CD8^+$ T cell responses during secondary challenge or in the chronic phase of infection as observed by us in murine TB.

Generation of $CD8^+$ effector memory, rather than central memory T cells depends on CD40 stimulation (166). It is possible that the described feedback loop is already operative during the priming phase, promoting the generation of effector memory $CD8^+$ T cells. Indeed, in the

absence of ICOS signaling we observed a reduction of effector memory, but not central memory $CD8^+$ T cells on day 120 of Mtb infection in lungs. $CD4^+$ T cells can help $CD8^+$ T cells via IL-2 (41). Diminished IL-2 secretion by $CD4^+$ T cells could therefore also impair $CD8^+$ T cell responses. We consider this scenario of $CD4^+$ T cell help less likely in our study, since we observed as many IL-2 secreting $CD4^+$ T cells in $ICOS^{-/-}$ mice as in WT mice (data not shown). Studies analyzing the biological role of $CD8^+$ T cells in TB revealed increased bacterial load from day 90 in CD8α-deficient mice (163, 164). Analysis of these and other $CD8^+$ T cell defective mouse strains stressed the importance of $CD8^+$ T cells in control of chronic pulmonary TB (163, 164). Although, we observed impaired $CD8^+$ T cell responses during the chronic phase of Mtb infection, $ICOS^{-/-}$ mice showed improved control of Mtb at this stage. We conclude that the subtle reduction in $CD8^+$ T cell responses in $ICOS^{-/-}$ mice did not suffice to increase susceptibility to Mtb, and was perhaps compensated for by elevated $CD4^+$ Th1 responses.

The role of Treg during Mtb infection has already been addressed by several studies which generally indicate that Treg suppress protective Th1 responses against Mtb (64-66). Since Treg express high levels of ICOS during murine Mtb infection, we were interested in how the absence of ICOS signaling would influence their response (66). Our studies revealed constant Treg numbers during chronic murine TB in $ICOS^{-/-}$ mice, compared to WT mice, in which numbers of Treg continuously increased throughout Mtb infection. This is consistent with a role of ICOS as survival factor for Treg in the steady state in naïve mice and humans (85, 208). Moreover, Umetsu and colleagues showed that antigen-specific Treg which protect from allergen-induced airway hyperreactivity in the lung mucosa develop via the ICOS-ICOS-L pathway (209). Since Treg have been shown to suppress Th1 responses against Mtb, we assume that their reduction allowed a stronger Th1 response as evidenced by increased IFN-γ secretion by bulk $CD4^+$ T cells in $ICOS^{-/-}$ mice. In genital tract infection with *C. trachomatis* ICOS drives Th2 immunity and anti-inflammation through IL-10 production and promotion of Treg populations (78). In line with these results is the finding that blockage of ICOS co-stimulation during priming in Experimental Autoimmune Encephalomyelitis (EAE) leads to increased IFN-γ secretion and Th1 polarization causing exacerbated immunopathology (84). It is tempting to speculate that during Mtb infection ICOS deficiency not only reduced Treg but also Th2 responses leading to enhanced IFN-γ secretion by $CD4^+$ T cells (210, 211).

Impact of ICOS deficiency on T cell responses differed in strength between the organs. Overall, Mtb-peptide specific $CD4^+$ Th1 responses developed normal in the absence of ICOS co-stimulation, whereas bulk IFN-γ^+ -secreting $CD4^+$ T cell responses were increased in the late phase of Mtb infection. In addition, ICOS signaling was necessary for the maintenance of Mtb-specific $CD8^+$ T cell - and Treg responses. In combination however, these effects at the level of single T cell subpopulations influenced each other. Thus mutual interdependency could explain minor effects on control of Mtb infection. Notably, ICOS deficiency did not affect Mtb load in lungs. We assume that beneficial effects of increased $CD4^+$ Th1 cell responses were countered by the detrimental reduction of pulmonary $CD8^+$ T cell responses. Reduced Mtb numbers in spleens of $ICOS^{-/-}$ mice resulted most likely from increased protective IFN-γ secreting $CD4^+$ T cells, in combination with marginally reduced Mtb-specific $CD8^+$ T cell responses. Thus different outcomes in distinct organs were the result of differential balances between T cell populations notably $CD4^+$ Th1, Treg, and $CD8^+$ T cells.

6 SUMMARY

6.1 *Treml6* regulates B-1a B cell development

TREM receptors are of particular interest in infection immunology since they are able to regulate inflammatory responses by either amplifying or dampening TLR signals (12). Here we investigated the immunological function of TLT-6 (gene: *treml6*), a so far undescribed ITIM-containing receptor of the TREM protein family (12, 13) using *treml6*-WT and in-house generated *treml6*$^{-/-}$ mice.

Treml6 mRNA was broadly expressed among leukocytes of the peritoneal cavity and lymphoid tissues. *Treml6*$^{-/-}$ mice were fertile and showed normal growth. Analysis of their immune cell composition revealed reduced numbers of B-1 B cell specific precursors in fetal liver and adult BM of *treml6*$^{-/-}$ mice. Likely as a consequence of this reduction, young and adult *treml6*$^{-/-}$ mice bared reduced numbers of peritoneal B-1a B cells. Notably, solely peritoneal B-1a B cells, but no other B-1 or B-2 B cell subsets were affected by the lack of *treml6*. No abnormalities in maintenance of B-1a B cells or in their functionality, such as increased apoptosis rates of B cells or altered antibody responses, respectively, were evident in *treml6*$^{-/-}$ mice. Moreover, in contrast to most B-1 B cell defects described in the literature, the defect observed in *treml6*$^{-/-}$ mice was independent of BCR signaling. By means of transplantation experiments it became apparent that the origin of the peritoneal B-1a B cell defect in *treml6*$^{-/-}$ mice was rooted in a defect during the fetal B cell development. Transplantation of *treml6*$^{-/-}$ adult BM cells resulted in normal - WT-like - B cell engraftment of Rag1$^{-/-}$ mice. In contrast, transplantation of *treml6*$^{-/-}$ fetal liver-derived pre-B I cells resulted in poorer B-1a B cell engraftment of recipient Rag1$^{-/-}$ mice when compared to WT pre-B I cells.

In sum, we propose that *treml6* is a positive regulator of fetal B-1a B cell development. Hence, our data provide new insights into B-1a B cell development; an area of research that is still controversial. Moreover, our study expands the knowledge of the TREM receptor family by ascribing it an additional function, namely regulation of lymphocyte development.

6.2 ICOS co-stimulation shapes T cell responses against Mtb

Mtb is still a global health threat. T cells, notably $CD4^+$ Th1 cells and their major effector cytokine IFN-γ are crucial for protective immunity against Mtb. However, the immune responses including the T cell response are not sufficient to eliminate the bacilli and to provide sterile immunity. In an initial attempt to identify factors that shape the Th1 response, we observed that $CD4^+$ Th1 cells, notably IFN-γ-secretors, co-expressed ICOS during murine TB. These data pointed to ICOS as an important player in the formation of Th1 responses against Mtb.

To gain detailed information about the kinetics and nature of the T cell response in absence of ICOS signaling, we infected WT and $ICOS^{-/-}$ mice with Mtb. ICOS deficiency resulted in an increased polyclonal $CD4^+$ Th1 response against Mtb, most likely caused by robustly reduced numbers and frequencies of Treg in these mice. In contrast to the $CD4^+$ Th1 response, the Mtb-specific $CD8^+$ T cell response was reduced in the absence of ICOS, but only during the later stage of infection. In addition, not only Mtb-specific effector $CD8^+$ T cells, but also effector memory $CD8^+$ T cells were reduced in Mtb infected $ICOS^{-/-}$ mice. The reduction in $CD8^+$ T cells was most likely not $CD8^+$ T cell intrinsic – since $CD8^+$ T cells revealed only marginal ICOS surface expression, but caused by impaired $CD4^+$ T cell help.

In sum, we confirmed our initial assumption; ICOS indeed influenced the Th1 cell response against Mtb, and moreover presence of ICOS was mandatory for normal Treg responses. The extent to which ICOS influenced single T cell populations, notably $CD4^+$ Th1, Treg, and $CD8^+$ T cells, and conclusively the interaction among themselves, differed between spleen and lung. As a result, $ICOS^{-/-}$ mice showed improved control of Mtb in the spleens, but not in the lungs during the late chronic phase of infection.

7 ZUSAMMENFASSUNG

7. 1 *Treml6* reguliert die Entwicklung von B-1a B Zellen

TREM Rezeptoren sind aus infektionsimmunologischer Sicht von großem Interesse, da sie TLR Signale inhibieren bzw. verstärken können und somit in der Lage sind, inflammatorische Immunantworten zu regulieren (12). Diese Doktorarbeit untersucht die immunologische Funktion von murinem TLT-6 (Gen: *treml6*), einem bislang unerforschten ITIM-tragenden Rezeptor der TREM Rezeptor Familie (12, 13), mittels Analyse von *treml6*-WT und eigens generierten *treml6*$^{-/-}$ Mäusen.

Treml6 mRNA wurde vornehmlich von Leukozyten der Peritonealhöhle und lymphoiden Organen exprimiert. *Treml6*$^{-/-}$ Mäuse waren fortpflanzungsfähig und zeigten normales Wachstum. Die Analyse ihrer Immunzellzusammensetzung zeigte, dass *treml6*$^{-/-}$ Mäuse eine verringerte Anzahl an B-1 B Vorläuferzellen in der fetalen Leber und im adulten Knochenmark aufwiesen. Möglicherweise bedingt durch diese Reduktion an Vorläuferzellen, hatten sowohl junge als auch erwachsene *treml6*$^{-/-}$ Mäusen weniger peritoneale B-1a B Zellen als WT Mäuse. Andere B-1 oder B-2 Zellpopulationen in *treml6*$^{-/-}$ Mäusen waren hingegen nicht beeinträchtigt. Ferner wiesen *treml6*$^{-/-}$ Mäusen keine Defekte in der Aufrechterhaltung von B-1a B Zellen in der Peripherie, wie zum Beispiel eine erhöhte Apoptosisrate der B Zellen, noch Unterschiede in der Funktionalität der B Zellen, wie z.B. abnormale Antikörpersekretion, auf. Der B-1a B Zelldefekt in *treml6*$^{-/-}$ Mäusen kann, im Gegensatz zum Großteil der in der Literatur bekannten B-1 B Zelldefekte, ebenfalls nicht auf eine veränderte Signaltransduktion des BCR zurückgeführt werden. Die Ursache für die Reduktion der peritonealen B-1a B Zellen vermuten wir vielmehr in einem Defekt im fetalen Stadium der B-1a B Zellentwicklung in *treml6*$^{-/-}$ Mäusen. Hinweise hierfür lieferten Zelltransferexperimente. Entsprechend resultierte die Transplantation von adultem *treml6*$^{-/-}$ KM in Rag1$^{-/-}$ Mäuse in einer normalen Rekonstitution aller B Zellpopulationen des Rezipienten. Transplantierten wir jedoch aus *treml6*$^{-/-}$ fetalen Leberzellen generierte pre-B I Zellen, so zeigte sich, dass sie im Vergleich zu WT pre-B I B Zellen, eine beschränkte Fähigkeit aufwiesen, das B-1a B Zellkompartiment im Rag1$^{-/-}$ Rezipienten zu füllen.

Zusammenfassend schlussfolgern wir, dass *treml6* ein positiver Regulator der fetalen B-1a B Zellentwicklung ist. Unsere Daten liefern somit neue Einblicke in die Regulation der B-1a B Zellentwicklung, einem nach wie vor stark diskutierten Forschungsfeld. Ferner haben unsere

Untersuchungen die Erkenntnisse über die TREM Rezeptor Familie um eine weitere Funktion, nämlich ihre Beteiligung an der Regulation der Lymphozytenentwicklung, erweitert.

7.2 Kostimulation durch ICOS prägt die T Zellantwort gegen Mtb

Mtb ist weiterhin als globale gesundheitliche Bedrohung anzusehen. T Zellen, insbesondere $CD4^+$ Th1 Zellen und ihr wichtigstes Effektorzytokin IFN-γ, sind für eine schützende Immunantwort gegen Mtb entscheidend. Dessen ungeachtet gelingt es der Immunantwort inklusive der T Zellantwort nicht, die Bakterien vollständig zu eliminieren und Sterilität zu erreichen. Im Zuge vorrausgehender Bemühungen, Faktoren zu identifizieren, die die Th1 Antwort gegen Mtb beeinflussen, stellten wir fest, dass in der murinen Mtb Infektion ein Großteil der IFN-γ sekretierenden $CD4^+$ Th1 Zellen ICOS exprimierten. Dementsprechend lag die Vermutung nahe, dass ICOS eine wichtige Rolle in der Ausbildung der Th1 Antwort gegen Mtb spielt.

Wir infizierten WT und $ICOS^{-/-}$ Mäuse mit Mtb, um ein detailiertes Bild der Kinetik und der Art der T Zellantwort in Abwesenheit von ICOS-Kostimulation zu erhalten. ICOS-Defizienz führte zu einer verstärkten polyklonalen $CD4^+$ Th1 Antwort gegen Mtb. Die Ursache hierfür lässt sich in der stark reduzierten Anzahl und Frequenzen der Treg in $ICOS^{-/-}$ Mäusen vermuten. Im Gegensatz zur $CD4^+$ Th1 war die Mtb-spezifische $CD8^+$ T Zellantwort in $ICOS^{-/-}$ Mäusen in der chronischen Phase der Infektion abgeschwächt. Die Reduktion betraf nicht nur Effektor $CD8^+$ T Zellen, sondern auch Effektor-Gedächtnis $CD8^+$ T Zellen in Mtb infizierten $ICOS^{-/-}$ Mäusen. Da nur eine marginale ICOS Expression auf $CD8^+$ T Zellen während der Mtb Infektion festzustellen war, lässt sich die Reduktion der Mtb-spezifischen $CD8^+$ T Zellen nicht auf intrinsische Defekte zurückführen, sondern wurde wahrscheinlich durch beeinträchtigte $CD4^+$ T Zell-Hilfe in $ICOS^{-/-}$ Mäusen verursacht.

Insgesamt bestätigten wir unsere Anfangsvermutung, dass ICOS die Th1 T Zellantwort gegen Mtb maßgeblich beeinflusst und konnten zusätzlich zeigen, dass die Stärke der Treg Antwort ICOS-abhängig war. Das Ausmaß, in dem ICOS die einzelnen T Zellpopulationen wie $CD4^+$ Th1, Treg und $CD8^+$ T Zellen und somit auch ihre Interaktion untereinander beeinflusste, unterschied sich zwischen Milz und Lunge. So zeigten $ICOS^{-/-}$ Mäuse in der späten chronischen Phase der Mtb Infektion eine bessere Kontrolle der Erreger in der Milz, nicht aber in der Lunge.

8 REFERENCES

1. Medzhitov, R., and C. Janeway, Jr. 2000. Innate immune recognition: mechanisms and pathways. *Immunol.Rev.* 173:89-97.
2. Delves, P. J., and I. M. Roitt. 2000. The immune system. Second of two parts. *N.Engl.J.Med.* 343:108-117.
3. Delves, P. J., and I. M. Roitt. 2000. The immune system. First of two parts. *N.Engl.J.Med.* 343:37-49.
4. Zipfel, P. F. 2009. Complement and immune defense: from innate immunity to human diseases. *Immunol Lett* 126:1-7.
5. Creagh, E. M., and L. A. O'Neill. 2006. TLRs, NLRs and RLRs: a trinity of pathogen sensors that co-operate in innate immunity. *Trends Immunol* 27:352-357.
6. Willment, J. A., and G. D. Brown. 2008. C-type lectin receptors in antifungal immunity. *Trends Microbiol* 16:27-32.
7. O'Neill, L. A., and A. G. Bowie. 2007. The family of five: TIR-domain-containing adaptors in Toll-like receptor signalling. *Nat Rev Immunol* 7:353-364.
8. Medzhitov, R., and C. A. Janeway, Jr. 2000. How does the immune system distinguish self from nonself? *Semin.Immunol.* 12:185-188.
9. O'Neill, L. A. 2006. How Toll-like receptors signal: what we know and what we don't know. *Curr.Opin.Immunol.* 18:3-9.
10. Colonna, M. 2003. TREMs in the immune system and beyond. *Nat Rev Immunol* 3:445-453.
11. Klesney-Tait, J., I. R. Turnbull, and M. Colonna. 2006. The TREM receptor family and signal integration. *Nat Immunol* 7:1266-1273.
12. Ford, J. W., and D. W. McVicar. 2009. TREM and TREM-like receptors in inflammation and disease. *Curr Opin Immunol* 21:38-46.
13. Daeron, M., S. Jaeger, L. Du Pasquier, and E. Vivier. 2008. Immunoreceptor tyrosine-based inhibition motifs: a quest in the past and future. *Immunol Rev* 224:11-43.
14. Bouchon, A., J. Dietrich, and M. Colonna. 2000. Cutting edge: inflammatory responses can be triggered by TREM-1, a novel receptor expressed on neutrophils and monocytes. *J Immunol* 164:4991-4995.
15. Bouchon, A., F. Facchetti, M. A. Weigand, and M. Colonna. 2001. TREM-1 amplifies inflammation and is a crucial mediator of septic shock. *Nature* 410:1103-1107.
16. Turnbull, I. R., S. Gilfillan, M. Cella, T. Aoshi, M. Miller, L. Piccio, M. Hernandez, and M. Colonna. 2006. Cutting edge: TREM-2 attenuates macrophage activation. *J Immunol* 177:3520-3524.
17. Hamerman, J. A., J. R. Jarjoura, M. B. Humphrey, M. C. Nakamura, W. E. Seaman, and L. L. Lanier. 2006. Cutting edge: inhibition of TLR and FcR responses in macrophages by triggering receptor expressed on myeloid cells (TREM)-2 and DAP12. *J Immunol* 177:2051-2055.
18. Watarai, H., E. Sekine, S. Inoue, R. Nakagawa, T. Kaisho, and M. Taniguchi. 2008. PDC-TREM, a plasmacytoid dendritic cell-specific receptor, is responsible for augmented production of type I interferon. *Proc Natl Acad Sci U S A* 105:2993-2998.
19. Barrow, A. D., E. Astoul, A. Floto, G. Brooke, I. A. Relou, N. S. Jennings, K. G. Smith, W. Ouwehand, R. W. Farndale, D. R. Alexander, and J. Trowsdale. 2004. Cutting edge: TREM-like transcript-1, a platelet immunoreceptor tyrosine-based inhibition motif encoding costimulatory immunoreceptor that enhances, rather than inhibits, calcium signaling via SHP-2. *J Immunol* 172:5838-5842.
20. Washington, A. V., R. L. Schubert, L. Quigley, T. Disipio, R. Feltz, E. H. Cho, and D. W. McVicar. 2004. A TREM family member, TLT-1, is found exclusively in the alpha-granules of megakaryocytes and platelets. *Blood* 104:1042-1047.
21. Hashiguchi, M., H. Kobori, P. Ritprajak, Y. Kamimura, H. Kozono, and M. Azuma. 2008. Triggering receptor expressed on myeloid cell-like transcript 2 (TLT-2) is a counter-receptor for B7-H3 and enhances T cell responses. *Proc Natl Acad Sci U S A* 105:10495-10500.
22. Hume, D. A. 2008. Macrophages as APC and the dendritic cell myth. *J Immunol* 181:5829-5835.

23. Sokol, C. L., N. Q. Chu, S. Yu, S. A. Nish, T. M. Laufer, and R. Medzhitov. 2009. Basophils function as antigen-presenting cells for an allergen-induced T helper type 2 response. *Nat Immunol* 10:713-720.
24. Yoshimoto, T., K. Yasuda, H. Tanaka, M. Nakahira, Y. Imai, Y. Fujimori, and K. Nakanishi. 2009. Basophils contribute to T(H)2-IgE responses in vivo via IL-4 production and presentation of peptide-MHC class II complexes to CD4+ T cells. *Nat Immunol* 10:706-712.
25. Perrigoue, J. G., S. A. Saenz, M. C. Siracusa, E. J. Allenspach, B. C. Taylor, P. R. Giacomin, M. G. Nair, Y. Du, C. Zaph, N. van Rooijen, M. R. Comeau, E. J. Pearce, T. M. Laufer, and D. Artis. 2009. MHC class II-dependent basophil-CD4+ T cell interactions promote T(H)2 cytokine-dependent immunity. *Nat Immunol* 10:697-705.
26. Cresswell, P. 2005. Antigen processing and presentation. *Immunol.Rev.* 207:5-7.
27. Porcelli, S. A., and G. Hammerling. 2006. Antigen processing and recognition. *Curr.Opin.Immunol.* 18:61-63.
28. Krogsgaard, M., and M. M. Davis. 2005. How T cells 'see' antigen. *Nat.Immunol.* 6:239-245.
29. Mosmann, T. R., and R. L. Coffman. 1989. TH1 and TH2 cells: different patterns of lymphokine secretion lead to different functional properties. *Annu.Rev.Immunol.* 7:145-173.
30. Lenschow, D. J., T. L. Walunas, and J. A. Bluestone. 1996. CD28/B7 system of T cell costimulation. *Annu.Rev.Immunol.* 14:233-258.
31. Sharpe, A. H., and G. J. Freeman. 2002. The B7-CD28 superfamily. *Nat Rev Immunol* 2:116-126.
32. Schwartz, R. H. 1992. Costimulation of T lymphocytes: the role of CD28, CTLA-4, and B7/BB1 in interleukin-2 production and immunotherapy. *Cell* 71:1065-1068.
33. Hutloff, A., A. M. Dittrich, K. C. Beier, B. Eljaschewitsch, R. Kraft, I. Anagnostopoulos, and R. A. Kroczek. 1999. ICOS is an inducible T-cell co-stimulator structurally and functionally related to CD28. *Nature* 397:263-266.
34. Wilson, E. H., C. Zaph, M. Mohrs, A. Welcher, J. Siu, D. Artis, and C. A. Hunter. 2006. B7RP-1-ICOS interactions are required for optimal infection-induced expansion of CD4+ Th1 and Th2 responses. *J Immunol* 177:2365-2372.
35. Sallusto, F., D. Lenig, R. Forster, M. Lipp, and A. Lanzavecchia. 1999. Two subsets of memory T lymphocytes with distinct homing potentials and effector functions. *Nature* 401:708-712.
36. Seder, R. A., and R. Ahmed. 2003. Similarities and differences in CD4+ and CD8+ effector and memory T cell generation. *Nat.Immunol.* 4:835-842.
37. Hsieh, C. S., S. E. Macatonia, C. S. Tripp, S. F. Wolf, A. O'Garra, and K. M. Murphy. 1993. Development of TH1 CD4+ T cells through IL-12 produced by Listeria-induced macrophages. *Science* 260:547-549.
38. Amsen, D., C. G. Spilianakis, and R. A. Flavell. 2009. How are T(H)1 and T(H)2 effector cells made? *Curr Opin Immunol* 21:153-160.
39. Gordon, S. 2003. Alternative activation of macrophages. *Nat Rev Immunol* 3:23-35.
40. Martinez, F. O., L. Helming, and S. Gordon. 2009. Alternative activation of macrophages: an immunologic functional perspective. *Annu Rev Immunol* 27:451-483.
41. Wilson, E. B., and A. M. Livingstone. 2008. Cutting edge: CD4+ T cell-derived IL-2 is essential for help-dependent primary CD8+ T cell responses. *J Immunol* 181:7445-7448.
42. Ridge, J. P., F. Di Rosa, and P. Matzinger. 1998. A conditioned dendritic cell can be a temporal bridge between a CD4+ T-helper and a T-killer cell. *Nature* 393:474-478.
43. Schoenberger, S. P., R. E. Toes, E. I. van der Voort, R. Offringa, and C. J. Melief. 1998. T-cell help for cytotoxic T lymphocytes is mediated by CD40-CD40L interactions. *Nature* 393:480-483.
44. Shinkai, K., M. Mohrs, and R. M. Locksley. 2002. Helper T cells regulate type-2 innate immunity in vivo. *Nature* 420:825-829.
45. Parker, D. C. 1993. T cell-dependent B cell activation. *Annu Rev Immunol* 11:331-360.
46. Ivanov, II, B. S. McKenzie, L. Zhou, C. E. Tadokoro, A. Lepelley, J. J. Lafaille, D. J. Cua, and D. R. Littman. 2006. The orphan nuclear receptor RORgammat directs the differentiation program of proinflammatory IL-17+ T helper cells. *Cell* 126:1121-1133.

47. Harrington, L. E., R. D. Hatton, P. R. Mangan, H. Turner, T. L. Murphy, K. M. Murphy, and C. T. Weaver. 2005. Interleukin 17-producing CD4+ effector T cells develop via a lineage distinct from the T helper type 1 and 2 lineages. *Nat.Immunol.* 6:1123-1132.
48. Park, H., Z. Li, X. O. Yang, S. H. Chang, R. Nurieva, Y. H. Wang, Y. Wang, L. Hood, Z. Zhu, Q. Tian, and C. Dong. 2005. A distinct lineage of CD4 T cells regulates tissue inflammation by producing interleukin 17. *Nat.Immunol.* 6:1133-1141.
49. Bettelli, E., Y. Carrier, W. Gao, T. Korn, T. B. Strom, M. Oukka, H. L. Weiner, and V. K. Kuchroo. 2006. Reciprocal developmental pathways for the generation of pathogenic effector TH17 and regulatory T cells. *Nature* 441:235-238.
50. Mangan, P. R., L. E. Harrington, D. B. O'Quinn, W. S. Helms, D. C. Bullard, C. O. Elson, R. D. Hatton, S. M. Wahl, T. R. Schoeb, and C. T. Weaver. 2006. Transforming growth factor-beta induces development of the T(H)17 lineage. *Nature* 441:231-234.
51. Langrish, C. L., Y. Chen, W. M. Blumenschein, J. Mattson, B. Basham, J. D. Sedgwick, T. McClanahan, R. A. Kastelein, and D. J. Cua. 2005. IL-23 drives a pathogenic T cell population that induces autoimmune inflammation. *J.Exp.Med.* 201:233-240.
52. Gaffen, S. L. 2004. Biology of recently discovered cytokines: interleukin-17--a unique inflammatory cytokine with roles in bone biology and arthritis. *Arthritis Res.Ther.* 6:240-247.
53. Ye, P., F. H. Rodriguez, S. Kanaly, K. L. Stocking, J. Schurr, P. Schwarzenberger, P. Oliver, W. Huang, P. Zhang, J. Zhang, J. E. Shellito, G. J. Bagby, S. Nelson, K. Charrier, J. J. Peschon, and J. K. Kolls. 2001. Requirement of interleukin 17 receptor signaling for lung CXC chemokine and granulocyte colony-stimulating factor expression, neutrophil recruitment, and host defense. *J.Exp.Med.* 194:519-527.
54. Lee, Y. K., R. Mukasa, R. D. Hatton, and C. T. Weaver. 2009. Developmental plasticity of Th17 and Treg cells. *Curr Opin Immunol* 21:274-280.
55. Lohr, J., B. Knoechel, and A. K. Abbas. 2006. Regulatory T cells in the periphery. *Immunol.Rev.* 212:149-162.
56. Sakaguchi, S. 2004. Naturally arising CD4+ regulatory t cells for immunologic self-tolerance and negative control of immune responses. *Annu.Rev.Immunol.* 22:531-562.
57. Sakaguchi, S., N. Sakaguchi, M. Asano, M. Itoh, and M. Toda. 1995. Immunologic self-tolerance maintained by activated T cells expressing IL-2 receptor alpha-chains (CD25). Breakdown of a single mechanism of self-tolerance causes various autoimmune diseases. *J.Immunol.* 155:1151-1164.
58. Belkaid, Y., and K. Tarbell. 2009. Regulatory T cells in the control of host-microorganism interactions (*). *Annu Rev Immunol* 27:551-589.
59. Mittrucker, H. W., and S. H. Kaufmann. 2004. Mini-review: regulatory T cells and infection: suppression revisited. *Eur.J.Immunol.* 34:306-312.
60. Suvas, S., and B. T. Rouse. 2006. Treg control of antimicrobial T cell responses. *Curr.Opin.Immunol.* 18:344-348.
61. Belkaid, Y., C. A. Piccirillo, S. Mendez, E. M. Shevach, and D. L. Sacks. 2002. CD4+CD25+ regulatory T cells control Leishmania major persistence and immunity. *Nature* 420:502-507.
62. Kursar, M., K. Bonhagen, J. Fensterle, A. Kohler, R. Hurwitz, T. Kamradt, S. H. Kaufmann, and H. W. Mittrucker. 2002. Regulatory CD4+CD25+ T cells restrict memory CD8+ T cell responses. *J.Exp.Med.* 196:1585-1592.
63. Hisaeda, H., Y. Maekawa, D. Iwakawa, H. Okada, K. Himeno, K. Kishihara, S. Tsukumo, and K. Yasutomo. 2004. Escape of malaria parasites from host immunity requires CD4+ CD25+ regulatory T cells. *Nat.Med.* 10:29-30.
64. Kursar, M., M. Koch, H. W. Mittrucker, G. Nouailles, K. Bonhagen, T. Kamradt, and S. H. Kaufmann. 2007. Cutting Edge: Regulatory T cells prevent efficient clearance of Mycobacterium tuberculosis. *J Immunol* 178:2661-2665.
65. Quinn, K. M., R. S. McHugh, F. J. Rich, L. M. Goldsack, G. W. de Lisle, B. M. Buddle, B. Delahunt, and J. R. Kirman. 2006. Inactivation of CD4(+)CD25(+) regulatory T cells during early

mycobacterial infection increases cytokine production but does not affect pathogen load. *Immunol.Cell Biol.* 84:467-474.

66. Scott-Browne, J. P., S. Shafiani, G. Tucker-Heard, K. Ishida-Tsubota, J. D. Fontenot, A. Y. Rudensky, M. J. Bevan, and K. B. Urdahl. 2007. Expansion and function of Foxp3-expressing T regulatory cells during tuberculosis. *J Exp Med* 204:2159-2169.
67. Zhou, L., M. M. Chong, and D. R. Littman. 2009. Plasticity of CD4+ T cell lineage differentiation. *Immunity* 30:646-655.
68. Yoshinaga, S. K., J. S. Whoriskey, S. D. Khare, U. Sarmiento, J. Guo, T. Horan, G. Shih, M. Zhang, M. A. Coccia, T. Kohno, A. Tafuri-Bladt, D. Brankow, P. Campbell, D. Chang, L. Chiu, T. Dai, G. Duncan, G. S. Elliott, A. Hui, S. M. McCabe, S. Scully, A. Shahinian, C. L. Shaklee, G. Van, T. W. Mak, and G. Senaldi. 1999. T-cell co-stimulation through B7RP-1 and ICOS. *Nature* 402:827-832.
69. Coyle, A. J., S. Lehar, C. Lloyd, J. Tian, T. Delaney, S. Manning, T. Nguyen, T. Burwell, H. Schneider, J. A. Gonzalo, M. Gosselin, L. R. Owen, C. E. Rudd, and J. C. Gutierrez-Ramos. 2000. The CD28-related molecule ICOS is required for effective T cell-dependent immune responses. *Immunity* 13:95-105.
70. McAdam, A. J., T. T. Chang, A. E. Lumelsky, E. A. Greenfield, V. A. Boussiotis, J. S. Duke-Cohan, T. Chernova, N. Malenkovich, C. Jabs, V. K. Kuchroo, V. Ling, M. Collins, A. H. Sharpe, and G. J. Freeman. 2000. Mouse inducible costimulatory molecule (ICOS) expression is enhanced by CD28 costimulation and regulates differentiation of CD4+ T cells. *J Immunol* 165:5035-5040.
71. Greenwald, R. J., G. J. Freeman, and A. H. Sharpe. 2005. The B7 family revisited. *Annu Rev Immunol* 23:515-548.
72. Kroczek, R. A., H. W. Mages, and A. Hutloff. 2004. Emerging paradigms of T-cell co-stimulation. *Curr Opin Immunol* 16:321-327.
73. Tafuri, A., A. Shahinian, F. Bladt, S. K. Yoshinaga, M. Jordana, A. Wakeham, L. M. Boucher, D. Bouchard, V. S. Chan, G. Duncan, B. Odermatt, A. Ho, A. Itie, T. Horan, J. S. Whoriskey, T. Pawson, J. M. Penninger, P. S. Ohashi, and T. W. Mak. 2001. ICOS is essential for effective T-helper-cell responses. *Nature* 409:105-109.
74. McAdam, A. J., R. J. Greenwald, M. A. Levin, T. Chernova, N. Malenkovich, V. Ling, G. J. Freeman, and A. H. Sharpe. 2001. ICOS is critical for CD40-mediated antibody class switching. *Nature* 409:102-105.
75. Dong, C., A. E. Juedes, U. A. Temann, S. Shresta, J. P. Allison, N. H. Ruddle, and R. A. Flavell. 2001. ICOS co-stimulatory receptor is essential for T-cell activation and function. *Nature* 409:97-101.
76. Mittrucker, H. W., M. Kursar, A. Kohler, D. Yanagihara, S. K. Yoshinaga, and S. H. Kaufmann. 2002. Inducible costimulator protein controls the protective T cell response against Listeria monocytogenes. *J.Immunol.* 169:5813-5817.
77. Kopf, M., A. J. Coyle, N. Schmitz, M. Barner, A. Oxenius, A. Gallimore, J. C. Gutierrez-Ramos, and M. F. Bachmann. 2000. Inducible costimulator protein (ICOS) controls T helper cell subset polarization after virus and parasite infection. *J Exp Med* 192:53-61.
78. Marks, E., M. Verolin, A. Stensson, and N. Lycke. 2007. Differential CD28 and inducible costimulatory molecule signaling requirements for protective CD4+ T-cell-mediated immunity against genital tract Chlamydia trachomatis infection. *Infect Immun* 75:4638-4647.
79. Wilson, E. H., C. Zaph, M. Mohrs, A. Welcher, J. Siu, D. Artis, and C. A. Hunter. 2006. B7RP-1-ICOS interactions are required for optimal infection-induced expansion of CD4+ Th1 and Th2 responses. *J.Immunol.* 177:2365-2372.
80. Vidric, M., A. T. Bladt, U. Dianzani, and T. H. Watts. 2006. Role for inducible costimulator in control of Salmonella enterica serovar Typhimurium infection in mice. *Infect Immun* 74:1050-1061.
81. Greenwald, R. J., A. J. McAdam, D. Van der Woude, A. R. Satoskar, and A. H. Sharpe. 2002. Cutting edge: inducible costimulator protein regulates both Th1 and Th2 responses to cutaneous leishmaniasis. *J Immunol* 168:991-995.

82. Humphreys, I. R., L. Edwards, R. J. Snelgrove, A. J. Rae, A. J. Coyle, and T. Hussell. 2006. A critical role for ICOS co-stimulation in immune containment of pulmonary influenza virus infection. *Eur J Immunol* 36:2928-2938.
83. Ozkaynak, E., W. Gao, N. Shemmeri, C. Wang, J. C. Gutierrez-Ramos, J. Amaral, S. Qin, J. B. Rottman, A. J. Coyle, and W. W. Hancock. 2001. Importance of ICOS-B7RP-1 costimulation in acute and chronic allograft rejection. *Nat Immunol* 2:591-596.
84. Rottman, J. B., T. Smith, J. R. Tonra, K. Ganley, T. Bloom, R. Silva, B. Pierce, J. C. Gutierrez-Ramos, E. Ozkaynak, and A. J. Coyle. 2001. The costimulatory molecule ICOS plays an important role in the immunopathogenesis of EAE. *Nat Immunol* 2:605-611.
85. Burmeister, Y., T. Lischke, A. C. Dahler, H. W. Mages, K. P. Lam, A. J. Coyle, R. A. Kroczek, and A. Hutloff. 2008. ICOS controls the pool size of effector-memory and regulatory T cells. *J Immunol* 180:774-782.
86. Hardy, R. R., and K. Hayakawa. 1991. A developmental switch in B lymphopoiesis. *Proc Natl Acad Sci U S A* 88:11550-11554.
87. Rolink, A., U. Grawunder, T. H. Winkler, H. Karasuyama, and F. Melchers. 1994. IL-2 receptor alpha chain (CD25, TAC) expression defines a crucial stage in pre-B cell development. *Int Immunol* 6:1257-1264.
88. Cobaleda, C., A. Schebesta, A. Delogu, and M. Busslinger. 2007. Pax5: the guardian of B cell identity and function. *Nat Immunol* 8:463-470.
89. Allman, D. M., S. E. Ferguson, V. M. Lentz, and M. P. Cancro. 1993. Peripheral B cell maturation. II. Heat-stable antigen(hi) splenic B cells are an immature developmental intermediate in the production of long-lived marrow-derived B cells. *J Immunol* 151:4431-4444.
90. Rajewsky, K. 1996. Clonal selection and learning in the antibody system. *Nature* 381:751-758.
91. Genestier, L., M. Taillardet, P. Mondiere, H. Gheit, C. Bella, and T. Defrance. 2007. TLR agonists selectively promote terminal plasma cell differentiation of B cell subsets specialized in thymus-independent responses. *J Immunol* 178:7779-7786.
92. Martin, F., A. M. Oliver, and J. F. Kearney. 2001. Marginal zone and B1 B cells unite in the early response against T-independent blood-borne particulate antigens. *Immunity* 14:617-629.
93. Snapper, C. M., H. Yamada, D. Smoot, R. Sneed, A. Lees, and J. J. Mond. 1993. Comparative in vitro analysis of proliferation, Ig secretion, and Ig class switching by murine marginal zone and follicular B cells. *J Immunol* 150:2737-2745.
94. Allman, D., and S. Pillai. 2008. Peripheral B cell subsets. *Curr Opin Immunol* 20:149-157.
95. Hardy, R. R. 2006. B-1 B cell development. *J Immunol* 177:2749-2754.
96. Haas, K. M., J. C. Poe, D. A. Steeber, and T. F. Tedder. 2005. B-1a and B-1b cells exhibit distinct developmental requirements and have unique functional roles in innate and adaptive immunity to S. pneumoniae. *Immunity* 23:7-18.
97. Kantor, A. B., and L. A. Herzenberg. 1993. Origin of murine B cell lineages. *Annu Rev Immunol* 11:501-538.
98. Hardy, R. R., and K. Hayakawa. 1994. CD5 B cells, a fetal B cell lineage. *Adv Immunol* 55:297-339.
99. Kantor, A. B., A. M. Stall, S. Adams, and L. A. Herzenberg. 1992. Differential development of progenitor activity for three B-cell lineages. *Proc Natl Acad Sci U S A* 89:3320-3324.
100. Berland, R., and H. H. Wortis. 2002. Origins and functions of B-1 cells with notes on the role of CD5. *Annu Rev Immunol* 20:253-300.
101. Haughton, G., L. W. Arnold, A. C. Whitmore, and S. H. Clarke. 1993. B-1 cells are made, not born. *Immunol Today* 14:84-87; discussion 87-91.
102. Cong, Y. Z., E. Rabin, and H. H. Wortis. 1991. Treatment of murine CD5- B cells with anti-Ig, but not LPS, induces surface CD5: two B-cell activation pathways. *Int Immunol* 3:467-476.
103. Murakami, M., T. Tsubata, M. Okamoto, A. Shimizu, S. Kumagai, H. Imura, and T. Honjo. 1992. Antigen-induced apoptotic death of Ly-1 B cells responsible for autoimmune disease in transgenic mice. *Nature* 357:77-80.

104. Arnold, L. W., C. A. Pennell, S. K. McCray, and S. H. Clarke. 1994. Development of B-1 cells: segregation of phosphatidyl choline-specific B cells to the B-1 population occurs after immunoglobulin gene expression. *J Exp Med* 179:1585-1595.
105. Tatu, C., J. Ye, L. W. Arnold, and S. H. Clarke. 1999. Selection at multiple checkpoints focuses V(H)12 B cell differentiation toward a single B-1 cell specificity. *J Exp Med* 190:903-914.
106. Clarke, S. H., and L. W. Arnold. 1998. B-1 cell development: evidence for an uncommitted immunoglobulin (Ig)M+ B cell precursor in B-1 cell differentiation. *J Exp Med* 187:1325-1334.
107. Tarakhovsky, A., M. Turner, S. Schaal, P. J. Mee, L. P. Duddy, K. Rajewsky, and V. L. Tybulewicz. 1995. Defective antigen receptor-mediated proliferation of B and T cells in the absence of Vav. *Nature* 374:467-470.
108. Wang, D., J. Feng, R. Wen, J. C. Marine, M. Y. Sangster, E. Parganas, A. Hoffmeyer, C. W. Jackson, J. L. Cleveland, P. J. Murray, and J. N. Ihle. 2000. Phospholipase Cgamma2 is essential in the functions of B cell and several Fc receptors. *Immunity* 13:25-35.
109. Rickert, R. C., K. Rajewsky, and J. Roes. 1995. Impairment of T-cell-dependent B-cell responses and B-1 cell development in CD19-deficient mice. *Nature* 376:352-355.
110. Pan, C., N. Baumgarth, and J. R. Parnes. 1999. CD72-deficient mice reveal nonredundant roles of CD72 in B cell development and activation. *Immunity* 11:495-506.
111. Nitschke, L., R. Carsetti, B. Ocker, G. Kohler, and M. C. Lamers. 1997. CD22 is a negative regulator of B-cell receptor signalling. *Curr Biol* 7:133-143.
112. Hoffmann, A., S. Kerr, J. Jellusova, J. Zhang, F. Weisel, U. Wellmann, T. H. Winkler, B. Kneitz, P. R. Crocker, and L. Nitschke. 2007. Siglec-G is a B1 cell-inhibitory receptor that controls expansion and calcium signaling of the B1 cell population. *Nat Immunol* 8:695-704.
113. Chan, V. W., F. Meng, P. Soriano, A. L. DeFranco, and C. A. Lowell. 1997. Characterization of the B lymphocyte populations in Lyn-deficient mice and the role of Lyn in signal initiation and down-regulation. *Immunity* 7:69-81.
114. Pao, L. I., K. P. Lam, J. M. Henderson, J. L. Kutok, M. Alimzhanov, L. Nitschke, M. L. Thomas, B. G. Neel, and K. Rajewsky. 2007. B cell-specific deletion of protein-tyrosine phosphatase Shp1 promotes B-1a cell development and causes systemic autoimmunity. *Immunity* 27:35-48.
115. Sato, S., N. Ono, D. A. Steeber, D. S. Pisetsky, and T. F. Tedder. 1996. CD19 regulates B lymphocyte signaling thresholds critical for the development of B-1 lineage cells and autoimmunity. *J Immunol* 157:4371-4378.
116. Hardy, R. R. 2006. B-1 B cells: development, selection, natural autoantibody and leukemia. *Curr Opin Immunol* 18:547-555.
117. Casola, S. 2007. Control of peripheral B-cell development. *Curr Opin Immunol* 19:143-149.
118. Montecino-Rodriguez, E., H. Leathers, and K. Dorshkind. 2006. Identification of a B-1 B cell-specified progenitor. *Nat Immunol* 7:293-301.
119. Vosshenrich, C. A., A. Cumano, W. Muller, J. P. Di Santo, and P. Vieira. 2003. Thymic stromal-derived lymphopoietin distinguishes fetal from adult B cell development. *Nat Immunol* 4:773-779.
120. Kaufmann, S. H. 2005. Robert Koch, the Nobel Prize, and the ongoing threat of tuberculosis. *N.Engl.J.Med.* 353:2423-2426.
121. North, R. J., and Y. J. Jung. 2004. Immunity to tuberculosis. *Annu.Rev.Immunol.* 22:599-623.
122. Camus, J. C., M. J. Pryor, C. Medigue, and S. T. Cole. 2002. Re-annotation of the genome sequence of Mycobacterium tuberculosis H37Rv. *Microbiology* 148:2967-2973.
123. Cole, S. T., R. Brosch, J. Parkhill, T. Garnier, C. Churcher, D. Harris, S. V. Gordon, K. Eiglmeier, S. Gas, C. E. Barry, III, F. Tekaia, K. Badcock, D. Basham, D. Brown, T. Chillingworth, R. Connor, R. Davies, K. Devlin, T. Feltwell, S. Gentles, N. Hamlin, S. Holroyd, T. Hornsby, K. Jagels, A. Krogh, J. McLean, S. Moule, L. Murphy, K. Oliver, J. Osborne, M. A. Quail, M. A. Rajandream, J. Rogers, S. Rutter, K. Seeger, J. Skelton, R. Squares, S. Squares, J. E. Sulston, K. Taylor, S. Whitehead, and B. G. Barrell. 1998. Deciphering the biology of Mycobacterium tuberculosis from the complete genome sequence. *Nature* 393:537-544.
124. Kaufmann, S. H. 2006. Tuberculosis: back on the immunologists' agenda. *Immunity.* 24:351-357.

125. Flynn, J. L., and J. Chan. 2001. Immunology of tuberculosis. *Annu Rev Immunol* 19:93-129.
126. World Health Organization. 2009. *Global tuberculosis control : epidemiology, planning, financing : WHO report 2009*. World Health Organization, Geneva.
127. Cooper, A. M. 2009. Cell-mediated immune responses in tuberculosis. *Annu Rev Immunol* 27:393-422.
128. Kaufmann, S. H., S. T. Cole, V. Mizrahi, E. Rubin, and C. Nathan. 2005. Mycobacterium tuberculosis and the host response. *J.Exp.Med.* 201:1693-1697.
129. Kaufmann, S. H., and A. J. McMichael. 2005. Annulling a dangerous liaison: vaccination strategies against AIDS and tuberculosis. *Nat.Med.* 11:S33-S44.
130. Kaufmann, S. H., and B. D. Walker. 2006. Host-pathogen interactions. *Curr.Opin.Immunol.* 18:371-373.
131. Cohen, J. 2006. Infectious disease. Extensively drug-resistant TB gets foothold in South Africa. *Science* 313:1554.
132. Armstrong, J. A., and P. D. Hart. 1971. Response of cultured macrophages to Mycobacterium tuberculosis, with observations on fusion of lysosomes with phagosomes. *J Exp Med* 134:713-740.
133. Algood, H. M., J. Chan, and J. L. Flynn. 2003. Chemokines and tuberculosis. *Cytokine & growth factor reviews* 14:467-477.
134. Reiley, W. W., M. D. Calayag, S. T. Wittmer, J. L. Huntington, J. E. Pearl, J. J. Fountain, C. A. Martino, A. D. Roberts, A. M. Cooper, G. M. Winslow, and D. L. Woodland. 2008. ESAT-6-specific CD4 T cell responses to aerosol Mycobacterium tuberculosis infection are initiated in the mediastinal lymph nodes. *Proc Natl Acad Sci U S A* 105:10961-10966.
135. Chackerian, A. A., J. M. Alt, T. V. Perera, C. C. Dascher, and S. M. Behar. 2002. Dissemination of Mycobacterium tuberculosis is influenced by host factors and precedes the initiation of T-cell immunity. *Infect Immun* 70:4501-4509.
136. Wolf, A. J., L. Desvignes, B. Linas, N. Banaiee, T. Tamura, K. Takatsu, and J. D. Ernst. 2008. Initiation of the adaptive immune response to Mycobacterium tuberculosis depends on antigen production in the local lymph node, not the lungs. *J Exp Med* 205:105-115.
137. Ulrichs, T., and S. H. Kaufmann. 2006. New insights into the function of granulomas in human tuberculosis. *J.Pathol.* 208:261-269.
138. Flynn, J. L. 2004. Immunology of tuberculosis and implications in vaccine development. *Tuberculosis.(Edinb.)* 84:93-101.
139. Winau, F., S. H. Kaufmann, and U. E. Schaible. 2004. Apoptosis paves the detour path for CD8 T cell activation against intracellular bacteria. *Cell Microbiol.* 6:599-607.
140. Saunders, B. M., and W. J. Britton. 2007. Life and death in the granuloma: immunopathology of tuberculosis. *Immunol Cell Biol* 85:103-111.
141. Schaible, U. E., and S. H. Kaufmann. 2000. CD1 and CD1-restricted T cells in infections with intracellular bacteria. *Trends Microbiol* 8:419-425.
142. Behar, S. M., and S. A. Porcelli. 2007. CD1-restricted T cells in host defense to infectious diseases. *Curr Top Microbiol Immunol* 314:215-250.
143. Houben, E. N., L. Nguyen, and J. Pieters. 2006. Interaction of pathogenic mycobacteria with the host immune system. *Curr.Opin.Microbiol.* 9:76-85.
144. Washington, A. V., L. Quigley, and D. W. McVicar. 2002. Initial characterization of TREM-like transcript (TLT)-1: a putative inhibitory receptor within the TREM cluster. *Blood* 100:3822-3824.
145. Hayakawa, K., R. R. Hardy, D. R. Parks, and L. A. Herzenberg. 1983. The "Ly-1 B" cell subpopulation in normal immunodefective, and autoimmune mice. *J Exp Med* 157:202-218.
146. Hayakawa, K., R. R. Hardy, M. Honda, L. A. Herzenberg, and A. D. Steinberg. 1984. Ly-1 B cells: functionally distinct lymphocytes that secrete IgM autoantibodies. *Proc Natl Acad Sci U S A* 81:2494-2498.
147. Manohar, V., E. Brown, W. M. Leiserson, and T. M. Chused. 1982. Expression of Lyt-1 by a subset of B lymphocytes. *J Immunol* 129:532-538.

148. Hayakawa, K., R. R. Hardy, and L. A. Herzenberg. 1985. Progenitors for Ly-1 B cells are distinct from progenitors for other B cells. *J Exp Med* 161:1554-1568.
149. Lam, K. P., and K. Rajewsky. 1999. B cell antigen receptor specificity and surface density together determine B-1 versus B-2 cell development. *J Exp Med* 190:471-477.
150. Dorshkind, K., and E. Montecino-Rodriguez. 2007. Fetal B-cell lymphopoiesis and the emergence of B-1-cell potential. *Nat Rev Immunol* 7:213-219.
151. Perlman, D. C., W. M. el-Sadr, E. T. Nelson, J. P. Matts, E. E. Telzak, N. Salomon, K. Chirgwin, and R. Hafner. 1997. Variation of chest radiographic patterns in pulmonary tuberculosis by degree of human immunodeficiency virus-related immunosuppression. The Terry Beirn Community Programs for Clinical Research on AIDS (CPCRA). The AIDS Clinical Trials Group (ACTG). *Clin Infect Dis* 25:242-246.
152. Mogues, T., M. E. Goodrich, L. Ryan, R. LaCourse, and R. J. North. 2001. The relative importance of T cell subsets in immunity and immunopathology of airborne Mycobacterium tuberculosis infection in mice. *J Exp Med* 193:271-280.
153. Caruso, A. M., N. Serbina, E. Klein, K. Triebold, B. R. Bloom, and J. L. Flynn. 1999. Mice deficient in CD4 T cells have only transiently diminished levels of IFN-gamma, yet succumb to tuberculosis. *J Immunol* 162:5407-5416.
154. Flynn, J. L., J. Chan, K. J. Triebold, D. K. Dalton, T. A. Stewart, and B. R. Bloom. 1993. An essential role for interferon gamma in resistance to Mycobacterium tuberculosis infection. *J Exp Med* 178:2249-2254.
155. Quiroga, M. F., V. Pasquinelli, G. J. Martinez, J. O. Jurado, L. C. Zorrilla, R. M. Musella, E. Abbate, P. A. Sieling, and V. E. Garcia. 2006. Inducible costimulator: a modulator of IFN-gamma production in human tuberculosis. *J.Immunol.* 176:5965-5974.
156. Kissenpfennig, A., S. Henri, B. Dubois, C. Laplace-Builhe, P. Perrin, N. Romani, C. H. Tripp, P. Douillard, L. Leserman, D. Kaiserlian, S. Saeland, J. Davoust, and B. Malissen. 2005. Dynamics and function of Langerhans cells in vivo: dermal dendritic cells colonize lymph node areas distinct from slower migrating Langerhans cells. *Immunity* 22:643-654.
157. Staub, E., A. Rosenthal, and B. Hinzmann. 2004. Systematic identification of immunoreceptor tyrosine-based inhibitory motifs in the human proteome. *Cell Signal* 16:435-456.
158. LeBien, T. W., and T. F. Tedder. 2008. B lymphocytes: how they develop and function. *Blood* 112:1570-1580.
159. Ansel, K. M., R. B. Harris, and J. G. Cyster. 2002. CXCL13 is required for B1 cell homing, natural antibody production, and body cavity immunity. *Immunity* 16:67-76.
160. Hopken, U. E., A. H. Achtman, K. Kruger, and M. Lipp. 2004. Distinct and overlapping roles of CXCR5 and CCR7 in B-1 cell homing and early immunity against bacterial pathogens. *J Leukoc Biol* 76:709-718.
161. Forster, I., and K. Rajewsky. 1987. Expansion and functional activity of Ly-1+ B cells upon transfer of peritoneal cells into allotype-congenic, newborn mice. *Eur J Immunol* 17:521-528.
162. Rolink, A. G., C. Schaniel, M. Busslinger, S. L. Nutt, and F. Melchers. 2000. Fidelity and infidelity in commitment to B-lymphocyte lineage development. *Immunol Rev* 175:104-111.
163. Rolph, M. S., B. Raupach, H. H. Kobernick, H. L. Collins, B. Perarnau, F. A. Lemonnier, and S. H. Kaufmann. 2001. MHC class Ia-restricted T cells partially account for beta2-microglobulin-dependent resistance to Mycobacterium tuberculosis. *Eur J Immunol* 31:1944-1949.
164. Turner, J., C. D. D'Souza, J. E. Pearl, P. Marietta, M. Noel, A. A. Frank, R. Appelberg, I. M. Orme, and A. M. Cooper. 2001. CD8- and CD95/95L-dependent mechanisms of resistance in mice with chronic pulmonary tuberculosis. *Am J Respir Cell Mol Biol* 24:203-209.
165. Masopust, D., V. Vezys, E. J. Wherry, and R. Ahmed. 2007. A brief history of CD8 T cells. *Eur J Immunol* 37 Suppl 1:S103-110.
166. Huster, K. M., V. Busch, M. Schiemann, K. Linkemann, K. M. Kerksiek, H. Wagner, and D. H. Busch. 2004. Selective expression of IL-7 receptor on memory T cells identifies early CD40L-dependent generation of distinct CD8+ memory T cell subsets. *Proc.Natl.Acad.Sci.U.S.A* 101:5610-5615.

167. Hardy, R. R., and K. Hayakawa. 2001. B cell development pathways. *Annu Rev Immunol* 19:595-621.
168. Kopf, M., F. Brombacher, P. D. Hodgkin, A. J. Ramsay, E. A. Milbourne, W. J. Dai, K. S. Ovington, C. A. Behm, G. Kohler, I. G. Young, and K. I. Matthaei. 1996. IL-5-deficient mice have a developmental defect in CD5+ B-1 cells and lack eosinophilia but have normal antibody and cytotoxic T cell responses. *Immunity* 4:15-24.
169. Nelms, K., A. D. Keegan, J. Zamorano, J. J. Ryan, and W. E. Paul. 1999. The IL-4 receptor: signaling mechanisms and biologic functions. *Annu Rev Immunol* 17:701-738.
170. Kouro, T., M. Ikutani, A. Kariyone, and K. Takatsu. 2009. Expression of IL-5Ralpha on B-1 cell progenitors in mouse fetal liver and involvement of Bruton's tyrosine kinase in their development. *Immunol Lett* 123:169-178.
171. Esplin, B. L., R. S. Welner, Q. Zhang, L. A. Borghesi, and P. W. Kincade. 2009. A differentiation pathway for B1 cells in adult bone marrow. *Proc Natl Acad Sci U S A* 106:5773-5778.
172. Tung, J. W., M. D. Mrazek, Y. Yang, and L. A. Herzenberg. 2006. Phenotypically distinct B cell development pathways map to the three B cell lineages in the mouse. *Proc Natl Acad Sci U S A* 103:6293-6298.
173. Alugupalli, K. R., J. M. Leong, R. T. Woodland, M. Muramatsu, T. Honjo, and R. M. Gerstein. 2004. B1b lymphocytes confer T cell-independent long-lasting immunity. *Immunity* 21:379-390.
174. Guinamard, R., M. Okigaki, J. Schlessinger, and J. V. Ravetch. 2000. Absence of marginal zone B cells in Pyk-2-deficient mice defines their role in the humoral response. *Nat Immunol* 1:31-36.
175. Hsu, M. C., K. M. Toellner, C. G. Vinuesa, and I. C. Maclennan. 2006. B cell clones that sustain long-term plasmablast growth in T-independent extrafollicular antibody responses. *Proc Natl Acad Sci U S A* 103:5905-5910.
176. Fischer, G. M., L. A. Solt, W. D. Hastings, K. Yang, R. M. Gerstein, B. S. Nikolajczyk, S. H. Clarke, and T. L. Rothstein. 2001. Splenic and peritoneal B-1 cells differ in terms of transcriptional and proliferative features that separate peritoneal B-1 from splenic B-2 cells. *Cell Immunol* 213:62-71.
177. Sidman, C. L., L. D. Shultz, R. R. Hardy, K. Hayakawa, and L. A. Herzenberg. 1986. Production of immunoglobulin isotypes by Ly-1+ B cells in viable motheaten and normal mice. *Science* 232:1423-1425.
178. Neel, B. G., H. Gu, and L. Pao. 2003. The 'Shp'ing news: SH2 domain-containing tyrosine phosphatases in cell signaling. *Trends Biochem Sci* 28:284-293.
179. Pritchard, N. R., and K. G. Smith. 2003. B cell inhibitory receptors and autoimmunity. *Immunology* 108:263-273.
180. Ujike, A., K. Takeda, A. Nakamura, S. Ebihara, K. Akiyama, and T. Takai. 2002. Impaired dendritic cell maturation and increased T(H)2 responses in PIR-B(-/-) mice. *Nat Immunol* 3:542-548.
181. Sato, S., A. S. Miller, M. Inaoki, C. B. Bock, P. J. Jansen, M. L. Tang, and T. F. Tedder. 1996. CD22 is both a positive and negative regulator of B lymphocyte antigen receptor signal transduction: altered signaling in CD22-deficient mice. *Immunity* 5:551-562.
182. Otipoby, K. L., K. B. Andersson, K. E. Draves, S. J. Klaus, A. G. Farr, J. D. Kerner, R. M. Perlmutter, C. L. Law, and E. A. Clark. 1996. CD22 regulates thymus-independent responses and the lifespan of B cells. *Nature* 384:634-637.
183. O'Keefe, T. L., G. T. Williams, S. L. Davies, and M. S. Neuberger. 1996. Hyperresponsive B cells in CD22-deficient mice. *Science* 274:798-801.
184. Lajaunias, F., L. Nitschke, T. Moll, E. Martinez-Soria, I. Semac, Y. Chicheportiche, R. M. Parkhouse, and S. Izui. 2002. Differentially regulated expression and function of CD22 in activated B-1 and B-2 lymphocytes. *J Immunol* 168:6078-6083.
185. Bikah, G., J. Carey, J. R. Ciallella, A. Tarakhovsky, and S. Bondada. 1996. CD5-mediated negative regulation of antigen receptor-induced growth signals in B-1 B cells. *Science* 274:1906-1909.
186. Hayakawa, K., R. R. Hardy, and L. A. Herzenberg. 1986. Peritoneal Ly-1 B cells: genetic control, autoantibody production, increased lambda light chain expression. *Eur J Immunol* 16:450-456.

187. Khan, W. N., F. W. Alt, R. M. Gerstein, B. A. Malynn, I. Larsson, G. Rathbun, L. Davidson, S. Muller, A. B. Kantor, L. A. Herzenberg, and et al. 1995. Defective B cell development and function in Btk-deficient mice. *Immunity* 3:283-299.
188. Hendriks, R. W., M. F. de Bruijn, A. Maas, G. M. Dingjan, A. Karis, and F. Grosveld. 1996. Inactivation of Btk by insertion of lacZ reveals defects in B cell development only past the pre-B cell stage. *EMBO J* 15:4862-4872.
189. De Luca, K., V. Frances-Duvert, M. J. Asensio, R. Ihsani, E. Debien, M. Taillardet, E. Verhoeyen, C. Bella, S. Lantheaume, L. Genestier, and T. Defrance. 2009. The TLR1/2 agonist PAM(3)CSK(4) instructs commitment of human hematopoietic stem cells to a myeloid cell fate. *Leukemia* 23:2063-2074.
190. Kim, J. M., N. I. Kim, Y. K. Oh, Y. J. Kim, J. Youn, and M. J. Ahn. 2005. CpG oligodeoxynucleotides induce IL-8 expression in CD34+ cells via mitogen-activated protein kinase-dependent and NF-kappaB-independent pathways. *Int Immunol* 17:1525-1531.
191. Sioud, M., Y. Floisand, L. Forfang, and F. Lund-Johansen. 2006. Signaling through toll-like receptor 7/8 induces the differentiation of human bone marrow CD34+ progenitor cells along the myeloid lineage. *J Mol Biol* 364:945-954.
192. Nagai, Y., K. P. Garrett, S. Ohta, U. Bahrun, T. Kouro, S. Akira, K. Takatsu, and P. W. Kincade. 2006. Toll-like receptors on hematopoietic progenitor cells stimulate innate immune system replenishment. *Immunity* 24:801-812.
193. Welner, R. S., R. Pelayo, Y. Nagai, K. P. Garrett, T. R. Wuest, D. J. Carr, L. A. Borghesi, M. A. Farrar, and P. W. Kincade. 2008. Lymphoid precursors are directed to produce dendritic cells as a result of TLR9 ligation during herpes infection. *Blood* 112:3753-3761.
194. Gonzalo, J. A., J. Tian, T. Delaney, J. Corcoran, J. B. Rottman, J. Lora, A. Al-garawi, R. Kroczek, J. C. Gutierrez-Ramos, and A. J. Coyle. 2001. ICOS is critical for T helper cell-mediated lung mucosal inflammatory responses. *Nat Immunol* 2:597-604.
195. Wallin, J. J., L. Liang, A. Bakardjiev, and W. C. Sha. 2001. Enhancement of CD8+ T cell responses by ICOS/B7h costimulation. *J Immunol* 167:132-139.
196. Liu, X., X. F. Bai, J. Wen, J. X. Gao, J. Liu, P. Lu, Y. Wang, P. Zheng, and Y. Liu. 2001. B7H costimulates clonal expansion of, and cognate destruction of tumor cells by, CD8(+) T lymphocytes in vivo. *J Exp Med* 194:1339-1348.
197. Bertram, E. M., A. Tafuri, A. Shahinian, V. S. Chan, L. Hunziker, M. Recher, P. S. Ohashi, T. W. Mak, and T. H. Watts. 2002. Role of ICOS versus CD28 in antiviral immunity. *Eur J Immunol* 32:3376-3385.
198. Shedlock, D. J., and H. Shen. 2003. Requirement for CD4 T cell help in generating functional CD8 T cell memory. *Science* 300:337-339.
199. Sun, J. C., and M. J. Bevan. 2003. Defective CD8 T cell memory following acute infection without CD4 T cell help. *Science* 300:339-342.
200. Sun, J. C., M. A. Williams, and M. J. Bevan. 2004. CD4+ T cells are required for the maintenance, not programming, of memory CD8+ T cells after acute infection. *Nat Immunol* 5:927-933.
201. Bevan, M. J. 2006. Cross-priming. *Nat Immunol* 7:363-365.
202. Kalams, S. A., and B. D. Walker. 1998. The critical need for CD4 help in maintaining effective cytotoxic T lymphocyte responses. *J Exp Med* 188:2199-2204.
203. Matloubian, M., R. J. Concepcion, and R. Ahmed. 1994. CD4+ T cells are required to sustain CD8+ cytotoxic T-cell responses during chronic viral infection. *J Virol* 68:8056-8063.
204. Zajac, A. J., K. Murali-Krishna, J. N. Blattman, and R. Ahmed. 1998. Therapeutic vaccination against chronic viral infection: the importance of cooperation between CD4+ and CD8+ T cells. *Curr Opin Immunol* 10:444-449.
205. Akiba, H., K. Takeda, Y. Kojima, Y. Usui, N. Harada, T. Yamazaki, J. Ma, K. Tezuka, H. Yagita, and K. Okumura. 2005. The role of ICOS in the CXCR5+ follicular B helper T cell maintenance in vivo. *J Immunol* 175:2340-2348.
206. Bennett, S. R., F. R. Carbone, F. Karamalis, R. A. Flavell, J. F. Miller, and W. R. Heath. 1998. Help for cytotoxic-T-cell responses is mediated by CD40 signalling. *Nature* 393:478-480.

207. Bourgeois, C., B. Rocha, and C. Tanchot. 2002. A role for CD40 expression on CD8+ T cells in the generation of CD8+ T cell memory. *Science* 297:2060-2063.
208. Takahashi, N., K. Matsumoto, H. Saito, T. Nanki, N. Miyasaka, T. Kobata, M. Azuma, S. K. Lee, S. Mizutani, and T. Morio. 2009. Impaired CD4 and CD8 effector function and decreased memory T cell populations in ICOS-deficient patients. *J Immunol* 182:5515-5527.
209. Akbari, O., G. J. Freeman, E. H. Meyer, E. A. Greenfield, T. T. Chang, A. H. Sharpe, G. Berry, R. H. DeKruyff, and D. T. Umetsu. 2002. Antigen-specific regulatory T cells develop via the ICOS-ICOS-ligand pathway and inhibit allergen-induced airway hyperreactivity. *Nat Med* 8:1024-1032.
210. Lohning, M., A. Hutloff, T. Kallinich, H. W. Mages, K. Bonhagen, A. Radbruch, E. Hamelmann, and R. A. Kroczek. 2003. Expression of ICOS in vivo defines CD4+ effector T cells with high inflammatory potential and a strong bias for secretion of interleukin 10. J Exp Med 197:181-193.
211. Hubbard, V. M., J. M. Eng, T. Ramirez-Montagut, K. H. Tjoe, S. J. Muriglan, A. A. Kochman, T. H. Terwey, L. M. Willis, R. Schiro, G. Heller, G. F. Murphy, C. Liu, O. Alpdogan, and M. R. van den Brink. 2005. Absence of inducible costimulator on alloreactive T cells reduces graft versus host disease and induces Th2 deviation. Blood 106:3285-3292.

9 ACKNOWLEDGEMENTS

Mein besonderer Dank gilt Prof. Stefan H. E. Kaufmann, dafür dass er mir ermöglichte diese Doktorarbeit in seiner Abteilung durchzuführen. Ich möchte Ihm auch für die anregenden Diskussion, seine Betreuung und vor allem seine Unterstützung danken, als das „treml“ Projekt uns unerwarteterweise in infektionsfreie B-Zellgefilde führte.

Mein ausdrücklicher Dank gilt auch Herrn Prof. Roland Lauster für seine Tätigkeit als Betreuer und Ratgeber. Ich danke auch Prof. Dr. Jens Kurreck für seine Bereitschaft Gutachter dieser Doktorarbeit zu sein.

Dr. Mischo Kursar und Dr. Markus Koch möchte ich ebenfalls von ganzem Herzen danken, für die Betreuung dieser Doktorarbeit, für die zahlreichen und lehrreichen Diskussion, für ihre Unterstützung und für ihr Vertrauen. Diese Arbeit wäre nicht möglich gewesen ohne ihren unermüdlichen Einsatz. Ich möchte auch Dr. Mischo Kursar dafür danken, dass er mich weiter betreut hat und bei Sorgen und Problemen für mich da war, nachdem er das MPIIB bereits verlassen hatte und dafür, dass er diese Arbeit korrekturgelesen hat.

Ich möchte für die Mitarbeit am ICOS Projekt Dr. Tracey Walker, Pia Gamradt, Steffi Kuhlmann und Delia Loewe danken. Tausend Dank geht auch an Dr. Anca Dorhoi und Lydia Pradl für ihre Unterstützung bei der histologischen Untersuchung. Mein Dank gilt auch Andraes Hutloff für die ICOS Mäuse und Diskussionen der Daten. Im Rahmen des *treml6* Projektes möchte ich insbesondere Szandor Simmons danken, für die experimentelle Unterstützung und für Nachhilfestunden in B Zellimmunologie. Mein Dank gilt ebenfalls Prof. Melchers und Marco Knoll für ihre Unterstützung und Diskussionen. Vielen Dank auch an Steffi Kuhlmann für ihren unermüdlichen Einsatz.

Nicht unerwähnt bleiben sollten auch January Weiner, vielen Dank für die Nachhilfestunde in *in silico* Analyse, Christian Köberle für das FACS Analyser Programm, Julia Jellusova für die TI-2 Immunisierungsprotokolle und Robert Hurwitz für die PepA-Tetramere.

Danken möchte ich auch allen Kollegen und Doktoranden für eine herzliche, inspirierende und motivierende Atmosphäre in und außerhalb des Instituts. Insbesondere danke ich Dr. Christian Ganoza, der so freundlich war diese Arbeit ebenfalls Korrektur zu lesen. Auch meiner Freundin Lisa Marit Otte möchte ich dafür danken, dass sie diese Arbeit korrekturgelesen hat.

Meine Liebsten zum Schluss, ein riesen Dank für ihre Unterstützung geht an meine Freunde, Mischo, Tracey, Lisa, Katrin und Anke und an meine Familie. Julien, mein Bruderherz, Du bist mein Fels in der Brandung. Papa, Dein naturwissenschaftliches Wissen, von Pflanzen und Tieren bis zur Physik war mir viele Jahre ein unerschöpflich scheinendes lebendiges Lehrbuch. Merci. An meine Mama unendlichen Dank natürlich dafür, dass Du immer für mich da warst und bist, aber auch dafür, dass Du mich immer darin bestärkt hast neugierig zu sein, die Welt zu hinterfragen und mir meine eigene Meinung zu bilden. Tausend Dank.

10 ABBREVIATIONS

α	anti
aa	amino acid
Ag85A	Antigen 85A
Ag85B	Antigen 85B
AP	alkaline phosphatase
APC	antigen presenting cell
β-actin	beta-actin
B-1P	B-1 B cell progenitor
BCG	Bacille Calmette-Guérin
BCR	b cell receptor
BM	bone marrow
BrdU	bromodeoxyuridine
BSA	bovine serum albumin
btk	Bruton's tyrosine kinase
Ca^{2+}	calcium
CCR	chemokine (C-C motif) receptor
CD	cluster of differentiation
$CD4^+$ Th1 cells	$CD4^+$ T cells of Th1 type
cDNA	complementary DNA
CFP10	culture filtrate protein 10
CFSE	carboxy-fluorescein diacetate succinimidyl ester
CFU	colony forming units
CLPs	common lymphoid progenitors
CLRs	C-type lectin receptors
CO_2	carbon dioxide
CpG ODN	oligodinucleotides containing CpG motifs
Cre	causes recombination
cRPMI	complete RPMI
c_t	threshold cycle
CTL	cytotoxic T lymphocytes
CXCL	chemokine (C-X-C motif) ligand
CXCR	chemokine (C-X-C motif) receptor
DAP-12	DNAX activating protein of 12kDa
DC	dendritic cell
ddH_2O	double distilled H_2O
DMSO	dimethyl sulfoxide
DNA	deoxyribonucleic acid
EDTA	ethylenediaminetetraacetic acid
EEJ	exon-exon junctions
ELISA	enzyme-linked immuno sorbent assay
ES cells	embryonic stem cells

ESAT6	six kilodalton early secretory antigenic target
$F(ab')_2$αIgM	$F(ab')_2$ fragment goat anti-mouse IgM
FACS	fluorescence activated cell sorting
FCS	fetal calf serum
FMO	fluorescence minus one
FO	follicular
FoxP3	forkhead box transcription factor P3
γδ T cells	gamma delta T cells
gapdh	glyceraldehyde-3-phosphate dehydrogenase
H&E	hematoxylin and eosin Y
HA	homology arm
HIV	human immunodeficiency virus
HSC	hematopoietic stem cells
i.p.	intraperitoneal
i.v.	intravenous
ICOS	inducible co-stimulatory molecule
ICOS-L	ICOS-ligand
ICS	intracellular cytokine staining
IFNγ	interferon-gamma
Ig	immunoglobulin
IL	interleukin
IMDM	Iscove‘s modified Dulbecco‘s medium
ITAM	immunoreceptor tyrosine-based activating
ITIM	immunoreceptor tyrosine-based inhibitory
ITIM-Rs	ITIM-containing receptors
iTreg	induced Treg
KO	knock-out
lacZ	beta-galactosidase
LCMV	lymphocytic choriomeningitis virus
LLO	listeriolysin
loxP	locus of X-ing over
LPS	lipopolysaccharide
mAb	monoclonal antibody
MEM	minimum essential medium
MHC	major histocompatibility complex
MHCI	MHC class I
MHCII	MHC class II
MLN	mesenteric lymph nodes
Mtb	Mycobacterium tuberculosis
MZ	marginal zone
NLRs	nucleotide-binding domain and leucine-rich repeat containing molecules
NOD	nucleotide oligomerization domain

nTreg	naturally occurring Treg
OP9-PH	puromycine-hygromycine-resistant OP9 cells
p.i.	post infection
PBS	phosphate buffered saline
PBST	PBS/Tween solution
PCR	poly chain reaction
pDC	plasmacytoid dendritic cell
PepA	Mtb32A-derived peptide
PFA	paraformaldehyde
PIR	paired Ig-like receptor
PMN	polymorphonuclear leukocytes
PMT	photo multiplier tubes
PRR	pattern recognition receptors
Rag	recombination-activating gene
rIL-7	recombinant IL-7
RLRs	RIG-I-like receptors
RNA	ribonucleic acid
RORγt	retinoic acid-related orphan receptor γ expressed in T cells
RPMI	Roswell Park Memorial Institute
RT	room temperature
RT-PCR	real-time polymerase chain reaction
SH2	src homology 2
SH3	src homology 3
SHP-1	SH2 domain containing phosphatase-1
STAT	signal transducer and activator of transcription
tACE	testes-specific promoter from the angiotensin-converting enzyme gene
TB	tuberculosis
T_{CM}	central memory T cells
TCR	T cell receptor
T_{EM}	effector memory T cells
TGF-ß	transforming growth factor beta
Th1 cells	helper T cells type 1
Th2 cells	helper T cells type 2
Th17 cells	helper T cells type 17
TI	T-independent
TI-2	thymus independent-type-2
TK	thymidine-kinase
TLT	TREM-like transcript (alternative name for TREML, used for protein)
TNF-α	tumor necrosis factor alpha
TNP-Ficoll	trinitrophenol
Treg	regulatory T cells
TREM	triggering receptors expressed on myeloid cells

TREML	TREM-like (alternative name for TLT, used for genes)
T-bet	T box transcription factor
V_H	heavy chain variable region
WHO	World Health Organization
WT	wild-type
XDR	extensively drug-resistant
7-AAD	7-amino-actinomycin D

APPENDIX 1: MATERIAL

APPENDIX 1.1: Buffers and solutions

Standard laboratory chemicals used to prepare buffers were purchased from Sigma, Merck or Roth. Solutions were prepared with a Millipore purified H_2O and sterilized by autoclaving for 25 min at 121°C or filter-sterilized through a 0.2 µm membrane.

1x phosphate buffered saline (1x PBS)	8 g NaCl 0.2 g KCl 1.44 g Na_2PO_4*$2H_2O$ 0.24 g KH_2PO_4 add to 1000 ml with H_2O
PBS, 0.2% bovine serum albumin (PBS/BSA) solution	2 g BSA add to 1000 ml with 1x PBS
PBS, 0.1% bovine serum albumin	1 g BSA add to 1000 ml with 1x PBS
4% Paraformaldehyde (4% PFA) solution	40 g PFA add to 1000 ml with 1x PBS stir O/N at 50°C, keep dark
Saponin buffer	5 g saponin 500 ml PBS/BSA add to 1000 ml with H_2O
Red Blood Cell Lysis buffer	8.29 g NH_4Cl 1 g $KHCO_3$ 0.037 g EDTA add to 1000 ml with H_2O
Trypan blue solution	10 ml 10x trypan blue add to 100 ml with 1x PBS
PBST (PBS/Tween solution)	5 ml Tween20 add to 1000 ml with 1x PBS
40% Percoll/RPMI	40 ml Percoll add to 100 ml with RPMI solution
70% Percoll/RPMI	70 ml Percoll add to 100 ml with RPMI solution
TAE 1x	40 mM TRIS (pH 8.0) 1 mM EDTA
Krebs-Ringer solution [+CaCl2]	140 mM NaCl 4 mM KCl 1 mM $MgCl_2$

	10 mM D-Glucose 10 mM HEPES (pH 7.4) with or without 1 mM $CaCl_2$ add to 1000 ml with ddH_2O sterile filtration, store at 4°C
Proteinase K buffer	50 mM TRIS (pH 8.0), 100 mM NaCl, 100 mM EDTA, 1% SDS in dH2O
TE	10 mM TRIS (pH 8.0), 1 mM EDTA in dH2O
6x Gel loading dye	30% Glycerol 0.25% Bomophenol blue in dH20
ELISA blocking solution	1 % BSA 0.05% sodium azide in 1x PBS
ELISA dilution buffer	0.1 % BSA 0.05 % sodium azide
FACS Clean	*BD Pharmingen*
FACS Rinse	*BD Pharmingen*

APPENDIX 1.2: Media and cell culture reagents

IMDM	*Gibco*
MEM alpha medium	*Gibco*
RPMI (L-Glutamine)	*Gibco*
D-MEM	*Gibco*
Opti-MEM	*Gibco*
PBS Dulbeccos (low endotoxin)	*Biochrom AG*
FCS	*Sigma-Aldrich*
L-Glutamine	*Gibco*
2-Mercapto-ethanol	*Fluka*
Trypsin/EDTA 5%	*Gibco*
Insulin	*Sigma-Aldrich*
Penicillin/Streptomycin (100x)	*PAA*
MEM non-essential amino acids	*Gibco*
Primatone RL	*Quest*
RPMI-10 complete medium	RPMI media plus:

	0.2 mM L-Glutamine 10 U/ml Penicillin/Streptomycin 10 mM HEPES buffer 0.05 mM β-mercaptoethanol 10% heat inactivated (1 h 65°C) FCS
Collagenase medium	RPMI-10 complete medium plus: 0.3 mg/ml Collagenase D 0.7 mg/ml Collagenase VIII
Freezing medium	45 ml FCS 5 ml DMSO
5% RPMI	RPMI media plus: 5% heat inactivated FCS
IMDM based serum-free medium	5 l dddH2O 1 can IMDM powder, dissolve 30.24 g NaHCO3 100 ml Kanamycin Sulphate (100x) 100 ml MEM non-essential amino acids solution (100x) 10 ml insulin (5 mg/ml), sterile 10 ml 2-Mercapto-ethanol (50 mM) 30 ml Primatone RL 10% solution, sterile Fill up with triple-distilled H2O to 10 l total volume Set pH to 7 with NaOH 10 M Filtrate with 1 l sterile filter-units (0.22 µm) into 1 l sterile flasks
αMEM based serum-free medium	5 l dddH2O 1 can αMEM powder, dissolve 20.02 g NaHCO3 100 ml Kanamycin Sulphate (100x) 100 ml MEM non-essential amino acids solution (100x) 10 ml insulin (5mg/ml), sterile 10 ml 2-Mercapto-ethanol (50mM) 30 ml Primatone RL 10% solution, sterile Fill up with triple-distilled H2O to 10 l total volume Set pH to 7 with NaOH 10 M Filtrate with 1 l sterile filter-units (0.22 µm) into 1 l sterile flasks

APPENDIX 1.3: Reagents

0.1 M DTT	*Invitrogen*
1 kb Plus DNA Ladder	*Invitrogen*

10 mM dNTP Mix	*Invitrogen*
10% Pluronic F127	*Invitrogen*
10 mM dNTP set	*Invitrogen*
2-Propanol	*Carl Roth*
2x Fast SybrGreen PCR Master Mix	*Applied Biosystems*
2x SybrGreen PCR Master Mix	*Applied Biosystems*
5x First-Strand Buffer	*Invitrogen*
7-AAD	*BD Pharmingen*
αCD40 [4.49µg/µl]	*DRFZ*
AffiniPure F(ab')$_2$ Fragment Goat Anti-Mouse IgM	*Jackson ImmunoResearch*
Agarose (NEEO)	*Carl Roth*
Ampicillin	*Sigma Aldrich*
Bio-Rad Protein Assay	*Bio-Rad*
BrefeldinA	*Sigma-Aldrich*
CellTrace CFSE	*Invitrogen*
Chloroform, 99%	*Sigma-Aldrich*
CpG ODN 1826	*invivoGen*
Cyclohexamide	*Sigma-Aldrich*
Dimethyl Sulfoxide	*Sigma-Aldrich*
Distilled water, DNase, RNase free	*Gibco*
EDTA	*Carl Roth*
Ethanol	*Carl Roth*
Ethanol absolut	*Merck*
Ethidium bromide solution	*Carl Roth*
Glycerol	*Sigma-Aldrich*
GM-CSF (5x10^5 U/ml)	*Active Bioscience*
HCL	*Sigma-Aldrich*
HEPES Solution	*Sigma-Aldrich*
IL-4 (mouse)	*Active Bioscience*
Indo-1, AM, 1 mM solution in anhydrous DMSO	*Invitrogen/Molecular Probes*
Ionomycin	*Invitrogen*
Isopropanol	*Merck*
Kanamycin Sulphate (100x)	*Sigma-Aldrich*
KCl	*Sigma-Aldrich*
Ketamin	*Bayer*
KH_2PO_4	*Sigma-Aldrich, Seelze*
LPS (Salmonella typhimurium SL1344) (1 mg/ml)	*invivoGen*
mAb CD28 (1,15 mg/ml)	*ATCC*
mAb CD3 (2,2 mg/ml)	*ATCC*
Na_2HPO_4	*Sigma-Aldrich*

NaCl	*Sigma-Aldrich*
$NaHCO_3$	*Sigma-Aldrich*
NaOH	*Sigma-Aldrich*
PAM3CSK4 (1 mg/ml)	*invivoGen*
Paraformaldehyd (PFA)	*Sigma*
Percoll	*Biochrom*
Poly (I:C) (10 µg/µl)	*invivoGen*
p-Nitrophenyl Phosphate Tablets, SIGMA FAST™	*Sigma-Aldrich*
Saponine	*Carl Roth*
SDS Solution 20%	*Fluka*
Streptavidine	*Jackson ImmunoResearch*
TRIS	*Carl Roth*
Triton X-100	*Sigma-Aldrich C*
TRIzol Reagent	*Invitrogen*
Trypan blue	*Sigma-Aldrich*
Tween20	*Sigma-Aldrich*

APPENDIX 1.4 Plastic ware

0.2-ml Thermo Strip	*Thermo Fischer*
14-ml tube, round bottom	*BD Pharmingen*
15-ml, 50-ml tube, conical bottom	*Sarstedt*
24 well cell culture cluster	*Nunc*
48 well cell culture plate, flat bottom	*Corning*
70-µm Filters	*BD Pharmingen*
96 MicroWell™ Plate Nunclon Delta - 96x0,36 cm^2	*Nunc, Roskilde*
96 well cell culture plate, U bottom	*Cellstar*
BD Falcon™ Polysterene Round-Bottom Tube 5ml	*BD Pharmingen*
BD Microtrainer (serum seperator)	*BD Pharmingen*
BD PlastipakTM 1-ml Sub-Q	*BD Pharmingen*
Cap Lock 0.2-ml Thermo Strip	*Thermo Fischer*
Cell strainer, nylon 40-µm	*BD Pharmingen*
CFU-bags (Whirl Pak)	*Nasco*
Costar®Stripette 50-ml, 25-ml, 10-ml, 5-ml	*Corning Life Scienes*
Hypodermic needle (1.20x40 mm; 0.7x 30 mm)	*B. Braun*
MACS Separation Columns (MS; LS Columns)	*Miltenyi*
MACS® Pre-Separation Filters 30-µm	*Miltenyi*
Maxisorp Plate for ELISA 96 well	*Nunc*
MicorAmp™ Optical 96-Well Reaction Plate	*Applied Biosystems*

MicroAmp™ Fast Optical 96-Well Reaction Plate	*Applied Biosystems*
Microtube 0.5-ml, 1.5-ml, 2.0-ml	*Sarstedt*
Omnifix syringe (5-ml, 10-ml, 20-ml)	*B. Braun*
Petri dish 92 x 16 mm	*Sarstedt*
Pipet tips	*Fischer Scientific*
Rotilabo® - cassettes for biopsies	*Carl Roth*
Surgical disposable scalpel	*Carl Roth*
Tissue culture flasks (75 cm^2 and 150 cm^2)	*TPP*
Vacuum Filter (0.22 µm GP Express Plus Membrane)	*Millipore*

APPENDIX 1.5: Antibodies

Abbreaviations used in application section; IVR: *in vitro* restimulation, FC: flow cytometry surface staining, FC-ICS: flow cytomertry intracellulary cytokine staining, FC-INS: flow cytometry intranuclear staining, B: blocking antibody, ELISA: enzyme linked immuno sorbent assay.

Specificity	**Clone**	**Fluorochrome /Enzyme**	**Application**	**Source**
AA4.1 (CD93)	AA4.1	APC	FC	*ebioscience*
B220	RA3-6B2	PE-Cy7	FC	*ebioscience*
B220	RA3-6B2	PacificBlue	FC	*ebioscience*
B220	RA3-6B2	eFluor™ 450	FC	*ebioscience*
B7RP-1 (ICOS-L)	MIL-5733	AlexaFluor647	FC	*RKI*
CCR7	4B12	APC	FC	*ebioscience*
CD103	2E7	FITC	FC	*ebioscience*
CD11b	5C6	Cy5	FC	*ATCC*
CD11b	M1/70	PE-Cy7	FC	*BD Pharmingen*
CD11b	M1/70	APC-Cy7	FC	*BD Pharmingen*
CD11c	N418	Cy5	FC	*ATCC*
CD11c	N418	FITC	FC	*ATCC*
CD11c	N418	Pacific Blue	FC	*eBioscience*
CD127	A7R34	PE-Cy7	FC	*eBioscience*
CD19	ID3	PerCP-Cy5.5	FC	*BD Pharmingen*
CD19	1D3	PE	FC	*BD Pharmingen*
CD19	ID3	APC-Cy7	FC	*ebioscience*
CD19	ID3	PE-Cy7	FC	*ebioscience*
CD21/CD35	eBio8D9	FITC	FC	*ebioscience*
CD23	B3B4	PE	FC	*ebioscience*
CD25	PC61	PerCP-Cy5.5	FC	*eBioscience*

CD25	PC61.5	PE-Cy7	FC	*eBioscience*
CD27	LG.3A10	FITC	FC	*eBioscience*
CD27	LG.7F9	APC	FC	*eBioscience*
CD28	37.51		IVR	*ATCC*
CD3	145-2C11		IVR	*ATCC*
CD4	RM4-5	PerCP	FC	*BD Pharmingen*
CD4	RM4-5	PacificBlue	FC	*BD Pharmingen*
CD4	FITC	RM4-5	FC	*ebioscience*
CD4	RM4-5	FITC	FC	*eBioscience*
CD40L	MR1	FITC	FC-ICS	*ATCC*
CD40L	MR1	PE	FC	*eBioscience*
CD43	1B11	FITC	FC	*BioLegend*
CD43	eBioR2/60	FITC	FC	*ebioscience*
CD44	IM7	Pacific Blue	FC	*eBioscience*
CD5	53-7.3	APC	FC	*ebioscience*
CD62L	MEL-14	APC	FC	*ATCC*
CD62L	MEL-14	APC-APCAlexa750	FC	*ATCC*
CD69	H1.2F3	PE-Cy7	FC	*BD Pharmingen*
CD8α	53-6.7	PerCP	FC	*BD Pharmingen*
c-Kit	ACK4	biotin	FC	*ATCC*
c-Kit	ACK4	Cy5	FC	*ATCC*
$F(ab')_2$ αIgM			IVR	*Jackson*
Fas (CD95)	Jo2	PE	FC	*ebioscience*
Fc Receptor*	24G2		B	*ATCC*
FoxP3	FJK/16S	PE	FC-INS	*eBioscience*
GL7	GL7	FITC	FC	*ebioscience*
GR1	RB6-8C5	PacificBlue	FC	*ATCC*
GR1	RB6-8C5	PE-Cy7	FC	*ebioscience*
ICOS	7E.17G9	AlexaFluor647	FC	*eBioscience*
ICOS	MIC280	Cy5	FC	*RKI*
IFN-γ	XMG1.2	PE-Cy7	FC-ICS	*ATCC*
IgD	11.26C	PacificBlue	FC	*ATCC*
IgD	11-26C	PE	FC	*ebioscience*
IgG3	LO-MG3	AP	ELISA	*Southern Biotech*
IgM	M41	Cy5	FC	*ATCC*
IgM	M41	biotin	FC	*ATCC*
IgM	1B4B1	AP	ELISA	*Southern Biotech*
IL-10	JES5-16E3	PE	FC-ICS	*BD Pharmingen*
IL-17	TC11-18H10.1	PE	FC-ICS	*BD Pharmingen*

IL-2	JES6-5H4	APC	FC-ICS	*BD Pharmingen*
MHCII	T1B120	FITC	FC	*ATCC*
MHCII	M5/114.15.2	APC	FC	*ebioscience*
NK1.1	PK136	PE-Cy7	FC	*BD Pharmingen*
NK1.1	PK136	FITC	FC	*eBioscience*
NKp46	29A1.4	PE	FC	*eBioscience*
Rat serum	αRat.-Ktr.		B	*ATCC*
TNF-α	XT-22	FITC	FC-ICS	*ATCC*

APPENDIX 1.6: Primers

Primer for qRT-PCR or tail DNA PCR were synthesized by Metabion and delivered at a concentration of 100 pg/mol.

name	**sequence 5' to 3'**	**application**
Random Primer (3µg/ml)	NNN NNN	cDNA-Synthese
b-actin fwd	TGG AAT CCT GTG GCA TCC ATG AAA C	qRT-PCR
b-actin rev	TAA AAC GCA GCT CAG TAA CAG TCC G	qRT-PCR
GAPDH fwd	GCA ACT CCC ACT CTT CCA CCT TC	qRT-PCR
GAPDH rev	CCT CTC TTG CTC AGT GTC CTT GCT	qRT-PCR
treml6 EEJ5 L	TGAGGAAAGCTCGAAGAAAG	qRT-PCR
treml6 EEJ5 R	TGC TGA TTG AAG CTA GTG GT	qRT-PCR
cxcl13 F	CTC TCC AGG CCA CGG TAT T	qRT-PCR
cxcl13 R	TAA CCA TTT GGC ACG AGG AT	qRT-PCR
cxcr5 F	TGC AGA ACC GTG AAG ACA CCT G	qRT-PCR
cxcr5 R	TTC CCA GCT GGT TGT TGG ATG C	qRT-PCR
ccr7 F	AGG CCA TCA AGG TGA TCA TTG C	qRT-PCR
ccr7 R	TGT AGG GCA GCT GGA AGA CTA TG	qRT-PCR
il-5 F	AGC ACA GTG GTG AAA GAG ACC TT	qRT-PCR
il-5 R	TCC AAT GCA TAG CTG GTG ATT T	qRT-PCR
B4 Tail WT fw1 (P11)	GTG CTA GGA TTT TGG CTC ATA TAC	PCR
B4-Tail WT rev1 (P12)	TTG CTA CTT TGT ATT TTC TGA CCT ATA	PCR
TP_B4_KO-sHA_ fw (P9)	GAC TCT GTC ACC TGC CTT CTG T	PCR
TP_B4_KO-lacZ-rv (P10)	TGG GGT CTT CTA CCT TTC TCT TC	PCR

APPENDIX 1.7: Enzymes

Collagenas Type VIII from *Clostridium histolyticum*	*Sigma-Aldrich*

Collagenase D from *Clostridium histolyticum*	*Roche*
SuperScript III Reverse Transcriptase (200 U/µl)	*Invitrogen*
GenTherm DNA- Polymerase	*Rapidozym*

APPENDIX 1.8: Kits

B Cell Isolation Kit	*Miltenyi Biotech*
Bio-Plex Cytokine Assay	*Bio-Rad*
BrdU Flow Kit (APC)	*BD Pharmingen*
Mouse Immunoglobulin Isotyping Kit	*Millipore*
Mouse Regulatory T cell Staining Kit	*eBioscience*

APPENDIX 1.9: Machines

7900 HAT Fast Real-Time PCR System	*AB Applied Biosystems*
Bio-Rad Bio-Plex HTF System	*Bio-Rad Laboratories GmbH*
Centrifuge 5417 R	*eppendorf AG*
CO_2-incubator Nuaire Autoflow	*Zapf, Sarstedt*
FACS-Sorter, FACSAria Cell Sorting System	*Becton Dickinson GmbH*
Haemocytometer	*LO Labor Optik GmbH*
Homogenizer, ULTRA-TURRAX T8	*IKA Labortechnik*
Hood, LaminAir HB 2448	*Heraeus-Instruments*
Incubator, Modell 800	*Memmert*
Lab-Shaker, KS 250basic	*IKA Labortechnik*
Light microscope, LEICA DMLB	*Leica Microsystems AG*
LSR II	*Becton Dickinson*
Megafuge 2.0R	*Heraeus Instruments*
MS1 Minishaker	*IKA Labortechnik*
NanoDrop ND-1000 Spectrophotometer	*peqLab Biotechnologie GmbH*
Pipetboy acu comfort	*IBS Integra Bioscience GmbH*
Pipettes, FINNPIPETTE (0-10 µl, 0.3-3 µl, 3-300 µl, 100-1000 µl)	*Thermo Electron GmbH*
SpectraMAX 190 Microplate Reader with PatchCheck	*Molecular Devices*
Thermomixer 5431	*eppendorf AG*
Vacuumfiltrationsystem, MultiScreen vacuum manifold	*Millipore GmbH*

APPENDIX 1.10: Software

Tables, calculations, statistics	GraphPad Prism (*GraphPad Software*) Excel (*Microsoft*)
Graphics	GraphPad Prism (*GraphPad Software*) PowerPoint (*Microsoft*)
Flow cytometric analysis	BD FACSDiva software (*BD*) FACS Data Analyser (V0.9.9) (*Köberle, MPIIB*) FlowJo (*TreeStar*)
DNA/RNA quantification	ND-1000 (*peqLab Biotechnologie*)
RT-PCR analysis	SDS 2.2.2 (*AB*) REST-MCS© beta (*Pfaffl &Horgan*)
Proteinanalysis	Bio-Plex Manager (*Bio-Rad*)
ELISA	SoftMax Pro v3 and v5
Text	Word (*Microsoft*) and SciWriter

APPENDIX 1.11: Online programs and databases

Program Signal P	http://www.cbs.dtu.dk/services/SignalP/
TMHMM v2.0 software	http://www.cbs.dtu.dk/services/TMHMM/
SMART domain database	http://smart.embl-heidelberg.de/
ScanProsite software	http://www.expasy.ch/tools/scanprosite/
Pfam 24.0	http://pfam.sanger.ac.uk/
CLUSTAL multiple sequence alignment program	http://www.ebi.ac.uk/Tools/clustalw2/index.html
boxshade program	http://www.ch.embnet.org/software/BOX_form.html

APPENDIX 1.12: Suppliers

Supplier	**Location**	**web address**
AB Applied Biosystems	Darmstadt, Germany	www.appliedbiosystems.com
Active Bioscience	Hamburg, Germany	www.activebioscience.com
ATCC	Manassas, VA, USA	www.atcc.org
B. Braun	Melsungen, Germany	www.bbraun.de
Bayer AG	Leverkusen, Germany	www.bayer.com
Becton Dickinson GmbH	Heidelberg, Germany	www.bdbiosciences.com
(BD Biosciences): comprising products from Pharmingen and Clontech		
Biochrom	Berlin, Germany	www.biochrom.com

BioLegend	Uithoorn, The Netherlands	www.biolegend.com
Bio-Rad Laboratories GmbH	München, Germany	www.bio-rad.com
Carl Roth	Karlsruhe, Germany	www.carl-roth.de
Cellstar/Greiner Bio-One	Solingen, Germany	www.greinerbioone.com
Charles River Laboratories	Wilmington, MA, USA	www.criver.com
Corning Life Scienes	Amsterdam, The Netherlands	www.corning.com/lifesciences/
ebioscience	Kranenburg, Germany	www.ebioscience.com
eppendorf AG	Hamburg, Germany	www.eppendorf.de
Fermentas	St. Leon-Rot, Germany	www.fermentas.de
Fischer Scientific	Schwerte, Germany	www.de.fishersci.com
Fluka	Basel, Switzerland	www.sigmaaldrich.com
Gibco	Karlsruhe, Germany	www.Invitrogen.com
GraphPad Software	San Diego, CA, USA	www.graphpad.com
Heraeus-Instruments	Hanau, Germany	www.heraeus-instruments.de
IBS Integra Bioscience GmbH	Fernwald, Germany	www.integra-biosciences.de
IKA Labortechnik	Staufen, Germany	www.ika.de
Invitrogen/Molecular Probes	Karlsruhe, Germany	www.Invitrogen.com
invivoGen	Toulouse, France	www.invivogen.com
Jackson ImmunoResearch	Suffolk, UK	www.jacksonimmuno.com
Leica Microsystems AG	Bensheim, Germany	www.leica-microstystems.com
LO Labor Optik GmbH	Friedrichsdorf, Germany	www.lo-laboroptik.de
Memmert	Büchenbach, Germany	www.memmert.com
Merck	Darmstadt, Germany	www.merck.de
Metabion	Martinsried, Germany	www.metabion.com
Microsoft Deutschland	Berlin, Germany	www.microsoft.de
Millipore GmbH	Schwalbach, Germany	www.millipore.de
Miltenyi Biotech	Bergisch Gladbach, Germany	www.miltenyibiotec.com
Molecular Devices	Ismaning, Germany	www.moleculardevices.com
Nasco	Fort Atkinson, WI, USA	www.enasco.com
Nunc	Wiesbaden, Germany	www.nuncbrand.com
PAA	Pasching, Austria	www.paa.com
peqLab Biotechnologie GmbH	Erlangen, Germany	www.peqlab.de
Quest	Almere, The Netherlands	www.sheffield-products.com
Rapidozym	Berlin, Germany	www.rapidozym.de
Roche Diagnostics	Mannheim, Germany	www.roche-applied-science.com
Sarstedt	Nuembrecht, Germany	www.sarstedt.com
Sigma-Aldrich	München, Germany	www.sigmaaldrich.com
Southern Biotech	Birmingham, AL, USA	www.southernbiotech.com
Thermo Fischer/Electron GmbH	Dreieich, Germany	www.thermo.com
TPP	Trasadingen, Switzerland	www.tpp.ch
TreeStar	Olten, Switzerland	www.treestar.com